Solar Energy 287 (2025) 113205

Contents lists available at ScienceDirect

Solar Energy

journal homepage: www.elsevier.com/locate/solener

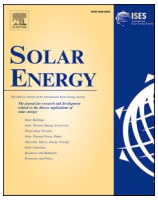

Perovskite solar cells: Progress, challenges, and future avenues to clean energy

Mohsin Afroz [a], Ratneshwar Kumar Ratnesh [a,*], Swapnil Srivastava [a], Jay Singh [b]

[a] Department of Electronics and Communication Engineering, Meerut Institute of Engineering and Technology, Meerut, UP 250005, India
[b] Department of Chemistry, Institute of Science, Banaras Hindu University, Varanasi, UP 221005, India

ARTICLE INFO

Keywords:
Power conversion efficiency
Band gap tuning
Efficiency
Stability
Fabrication techniques
Interfacial engineering

ABSTRACT

Perovskite solar cells (PSCs) have emerged as a viable photovoltaic technology, with significant improvements in power conversion efficiency (PCE) over the past decade. This review provides a comprehensive overview of the progress, challenges, and future prospects of PSCs. Historical milestones, including unique properties of perovskite materials, device design advancements and perovskite composition optimization, are discussed. The paper explores the fundamental aspects of perovskites, such as their crystal structures, fabrication techniques, from solution-based methods to vapor deposition methods and strategies like band gap tuning and tandem solar cell designs to overcome the Shockley-Queisser limit. Challenges related to stability, scalability, and degradation mechanisms are critically analyzed, with emphasis on intrinsic and extrinsic instability factors and mitigation strategies, considering the effects of environmental stressors and encapsulation techniques. Finally, the review concludes by outlining future research directions and the potential of PSCs to revolutionize the photovoltaic industry.

1. Introduction

The amplification of global energy demand has created a significant paradox in the 21st century, driven by population growth, industrialization, and technological advancement. This ever-increasing demand on energy sources has greatly affected traditional sources of energy especially fossil fuels, which have for a longer period been considered the main and the most popular source of energy [1]. However, over reliance on fossil fuels has been associated with the problems of air pollution, global warming, and resource depletion among other adverse environmental impacts. In order to address these challenges, it is vital that we move towards clean derivate energies as it is the only practical means of overcoming surging demand for energy. Additionally, it is also essential from the perspective of global energy security [2]. As an alternative to the existing limited energy structure, solar energy has been one of the most persuasive answers to the global energy crisis in its abundant and almost inexhaustible energy sources of the sun. It is estimated that in one hour, the Earth receives sufficient solar energy to meet the total annual energy requirements of the world, stimulating enormous scientific research, engineering activities and progress related to the photovoltaics [3]. Over the past several decades, the photovoltaic industry has experienced rapid progress, with silicon-based solar cells emerging as the dominant market leader due to their high efficiency and reliability. The evolution of photovoltaic technologies (Fig. 1) has spanned multiple generations, each characterized by distinct materials, fabrication processes, and efficiency levels.

A. **First generation: Conventional crystalline silicon solar cells:** These are the most mature and widely commercialized solar cells, dominating the current market. They are based on wafers of highly purified crystalline silicon and are known for their high efficiency (around 20–25 %) and long lifespan [4]. However, their production is energy-intensive and relatively expensive.
B. **Second generation: Thin-film solar cells:** This generation features technologies like amorphous silicon, cadmium telluride, and copper indium gallium selenide. They require significantly less material than crystalline silicon solar cells, making them cheaper to manufacture [5]. However, the efficiency of second generation is generally lower than first generation cells.
C. **Third generation:** The third generation of photovoltaic technologies, characterized by broad spectrum of advancements, seeks to overcome the shortcomings and limitation present in the previous

* Corresponding author.
E-mail address: ratnes123@gmail.com (R.K. Ratnesh).

https://doi.org/10.1016/j.solener.2024.113205
Received 30 September 2024; Received in revised form 11 December 2024; Accepted 15 December 2024
Available online 25 December 2024

generations of technologies. Among these are Quantum Dot Solar Cells (QDSCs), Perovskite Solar Cells (PSCs), Organic Photovoltaics (OPV), and Dye-Sensitized Solar Cells (DSSCs). The light harvesting elements in OPV technology are organic polymers. While, DSSCs contains a photosensitive dye which helps in absorbing sunlight, they possess properties of being light weight, flexible and potential for inexpensive manufacture. Nevertheless, their efficiencies still lag behind from other photovoltaic technologies [6]. Generally, third generation cells are known to deliver good performance in low-light conditions and options to various configurations. On the other hand, a light-absorbing material called perovskite is used in PSCs. They are very popular due to their rapid increase in efficiencies which exceeds 25 % within a short period of research in laboratory conditions and is ideal for mass production at low cost [7]. In QDSCs quantum dots are used as a light-absorbing components. These are nanocrystals of semiconductors. They provide the possibility of tunable bandgaps and therefore better efficiency [8].

D. **Fourth generation:** This generation represents the cutting edge of photovoltaic research, focusing on novel concepts and materials to further enhance efficiency, reduce costs, and broaden the applications of solar energy. This generations include technologies like Multi-junction solar cells which combine multiple semiconductor materials with different bandgaps to capture a wider range of solar spectrum, potentially exceeding the theoretical efficiency limits of single-junction cells [9], hot carrier solar cells that aims to capture the excess energy of photogenerated charge carriers before it's lost as heat, and offer potential for much greater efficiencies [10], and plasmonic solar cells which utilizes plasmonic nanoparticles to enhance light absorption and improve the performance of thin-film solar cells [11].

While the first and second generations is well-established, the third and fourth generations hold immense potential for the future of solar energy. PSCs have emerged as one of the most promising options in the third generation of solar technologies. Since their introduction in 2009, PSCs have seen a significant improvement in power conversion efficiency (PCE), exceeding 25 % within just over a decade of research [12]. This rapid improvement in efficiency is competitive compared with traditional silicon photocells which have dominated the market for decades.

PSCs are appealing not only for their higher efficiencies but also for their low-cost manufacturing using low-cost fabrication techniques such as solution-based methods and vacuum deposition methods. They can be fabricated at lower temperatures compared to silicon cells, which involve more complex and expensive manufacturing processes, including high-temperature crystallization and purification of silicon. These technologies enable mass production of PSCs, thus permitting their potential for commercial use. Besides, PSCs have their own interesting features such as the ability to tune the bandgap, high absorption coefficient and long charge carrier diffusion lengths, making them applicable to several novel applications including but not limited to flexible electronics and building integrated photovoltaics (BIPV) [13,14].

The flexibility of the PSCs extends further, given that they can be manufactured on flexible substrates, which makes it possible to fit them into curved surfaces or wear it or have it in places other than traditional solar energy systems. Furthermore, PSCs provide opportunities for tandem solar cells, which combines the perovskite absorber layer with other materials like silicon to exceed the efficiency limits of single-junction solar cells. In comparison, silicon solar cells are predominantly used in large-scale solar farms and residential installations due to their proven track record and reliability in various environmental conditions. Even with the remarkable advancements that have been made in PSC technology, there are still a number of key issues that have to be resolved before the technology can go into mass production. One of the major restraints is stability, as the PSC tend to deteriorate due to exposure to external factors, for example, humidity, heat, and UV exposure for long durations. Recent research has focused on improving their stability through various encapsulation techniques and material modifications. On the other hand, silicon solar cells are known for their durability and longevity, often exceeding 25 years with minimal degradation [15,16]. Their performance is well-understood, making

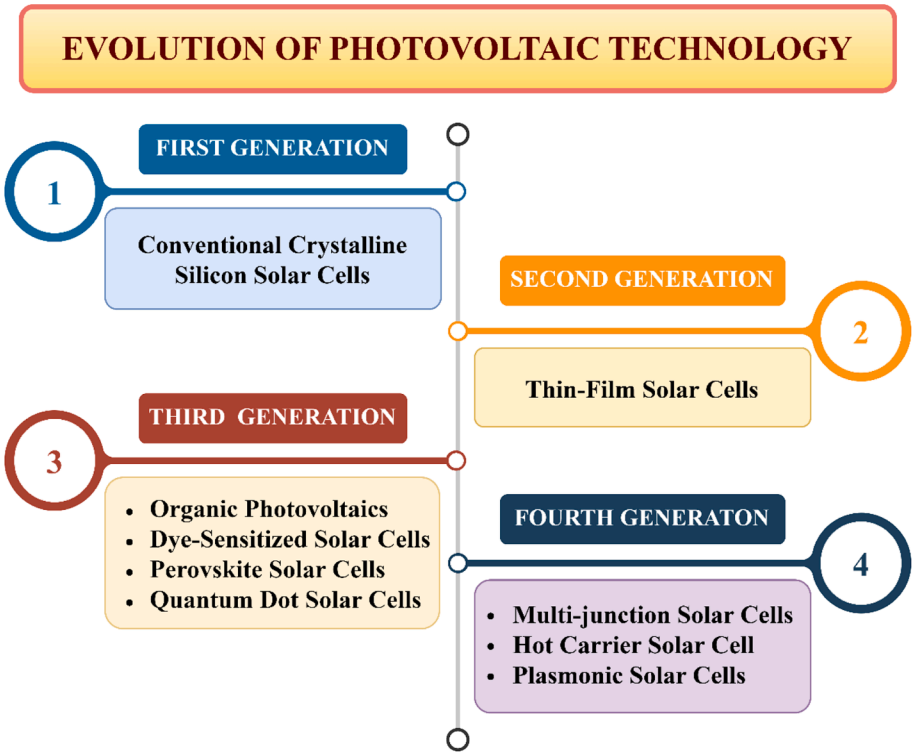

Fig. 1. Different generations of photovoltaic technologies.

them a reliable choice for long-term energy generation. The presence of lead in PSC composites is also a significant issue since it raises safety and health concerns, and therefore there is more emphasis in trying to develop lead-free alternatives that could mitigate these issues while maintaining efficiency levels. Also, great attention should be paid to the fact that even though PSCs can be efficiently manufactured in laboratory settings, the currently available scalable manufacturing techniques appropriate for industrial production are still under research. The current fabrication techniques employed in making high efficiency PSCs tend to be used in relatively small areas and hence not possible for mass production. Additionally, the potential for flexible PSCs opens avenues for innovative applications but also poses challenges regarding recycling and disposal [17]. Silicon cells have a well-established recycling process, although the extraction of raw materials can have environmental impacts. The lifecycle emissions are comparatively lower than fossil fuels but still significant when considering mining and manufacturing processes.

Recent advancements in material science and device physics and architecture have provided effective solutions to these issues. The stability of the PSCs and their operational lifetimes have improved due to various advancements in compositional engineering, improvements of the interfaces and encapsulation strategies. There are still quite inefficient lead-free solar cells, but the research for the development towards an eco-friendly PSC technology is clearly evident.

This review therefore aims at presenting an extensive overview of the current state of the development of the perovskite solar cell technology. It will review the evolution of PSCs and the recent development and advancement in efficiency and stability over time. The review will deal with the basic concepts of perovskite materials and will analyze the physics and chemistry that drive their extraordinary performance. It will also discuss about different device topologies, the manufacturing processes, and the strategies of tackling difficulties related to scalability, stability and ecological impact.

Moreover, the analysis will focus on the application of PSCs in tandem configurations, in particular the use of them together with silicon cells whose efficiency could exceed the Shockley-Queisser limit. Lastly, the assessment will provide an assessment of the role advanced PSCs will play in resolving the global energy crisis, and their potential to change the photovoltaic industry.

2. History and development of perovskite solar cells

The origin of PSC technology can be traced back to the 19th century with the discovery of naturally occurring perovskite minerals. Gustav Rose discovered the mineral calcium titanate ($CaTiO_3$) in 1839, giving rise to the perovskite structure named after Russian mineralogist Lev A. Perovski [18,19]. Over time, many inorganic metal oxides such as $BaTiO_3$, $PbTiO_3$ and $SrTiO_3$ showed that they also have the perovskite structure. These materials were of great scientific interest due to their interesting electrical and physical characteristics including ferroelectricity and piezoelectricity which enabled their use in dielectric and pyroelectric devices among other uses. Nevertheless, they were not appropriate for photovoltaic (PV) applications due to their low semiconducting characteristics [17].

The next milestone in the history of perovskites was in 1893, when Wells and 15 co-workers synthesized lead halide compound of type $CsPbX_3$ (X = Cl, Br, I) [20]. C. K. Moller carried out further research in 1957 concerning perovskites and stated that this type of structure is also exhibited by compounds such as $CsPbCl_3$ and $CsPbBr_3$ which stirred the attention of researchers towards the chemistry of the perovskites [21]. In 1978 came the breakthrough of D. Weber who showed for the first time that the organic cation methylammonium ($CH_3NH_3^+$) could be incorporated into these halide compounds structure in place of Cs^+ resulting into methylammonium lead halide compounds ($CH_3NH_3MX_3$, M = Pb, Sn; X = I, Br) [22]. This marked the beginning of interest in organic–inorganic hybrid perovskites. In the late 1990s, David Mitzi designed other halides perovskites containing small and large functional organic cations, promoting the research and development of two dimensional (2-D) and three dimensional (3-D) perovskite structures [23,24].

However, it wasn't until the early 21st century that the potential of perovskites for solar energy conversion came to light. In 2005, exploratory research on perovskite materials for solar applications began in the Miyasaka laboratory in Toin University, Japan. The name "perovskite" at the time mostly referred to metal oxides recognised for their ferroelectric and piezoelectric capabilities [25]. The breakthrough moment came in 2009 when Tsutomu Miyasaka and his colleagues at Toin University reached a major milestone by using organic lead-halide perovskites specifically, methylammonium lead iodide ($CH_3NH_3PbI_3$) as the light-absorbing material in a dye-sensitized solar cell. Although this early effort generated a small power conversion efficiency of 3.8 %, it attracted significant research interest, marking the beginning of the rapid evolution of perovskite-based photovoltaics [25].

3. Milestones: A decade of unprecedented progress

The development of perovskite solar cells (PSCs) has seen rapid progress since their inception, marked by significant breakthroughs in power conversion efficiency (PCE) and material optimization as illustrated in Fig. 2.

In 2006, the first reported PCE of 2.2 % was achieved using methylammonium lead bromide ($MAPbBr_3$) as a sensitizer in dye-sensitized solar cells (DSSCs), setting the foundation for further research in perovskite-based photovoltaics [26].

By 2009, Kojima and coworkers described for the first time the application of organic lead halide perovskites $CH_3NH_3PbBr_3$ and $CH_3NH_3PbI_3$ in photoelectrochemical cells achieving PCE of 3.81 % and 3.13 % respectively. This work set the framework for PSC research [27].

In 2011, an improved PCE of 6.5 % was reported for $CH_3NH_3PbI_3$ based iodide liquid electrolyte systems, while rapid breakdown of the perovskite nanocrystals in the electrolyte created substantial stability problems [28].

Great progress was noted in 2012 when after the development of solid-state DSSCs, the PCE for the first time reached 9.7 %. This significant improvement in efficiency was obtained by employing spiro-OMeTAD as the hole transport material (HTM), which enhanced the stability of the devices compared to their liquid electrolytes equivalents [29].

The year 2013 saw important advancements in PSC technology. The sequential deposition technique was incorporated, as a result raised the PCE to 15 % by proper shaping of the film growth of the perovskite layer coated on the porous metal oxide film. Also, thanks to the introduction of mixed halide perovskites such as $CH_3NH_3Pb(I_{1-x}Br_x)_3$, the performance of devices was improved remarkably [30].

In 2014, the Korean Research Institute of Chemical Technology (KRICT) obtained a validated PCE of 20.1 % using formamidinium lead iodide ($FAPbI_3$) as the active layer, a significant milestone in the development of high-efficiency PSCs. This achievement was recognized by the National Renewable Energy Laboratory (NREL) [31].

In 2016, KRICT along with Ulsan National Institute of Science and Technology (UNIST) jointly achieved a record PCE of 22.1 % pushing the limit of efficiency in PSC even more [32]. The next year, 2017, the certified PCE was at its peak at 22.7 % achieved with a mixed-perovskite $(FAPbI_3)_{0.85}$ $(MAPbBr_3)_{0.15}$ composition that integrated unique dopant free hole transporting materials that enabled vertical charge transport [33].

The highest certified efficiency for the year 2018 was 23.7 %, and the drivers behind this were advanced materials science and new PSC fabrication technologies, like cesium doping, which enhanced PSC stability and performance. This trend continued in 2019, when the record PCE jumped to 25.2 %, thanks to advancements in mixed-perovskite compositions that boosted light absorption and charge mobility [34].

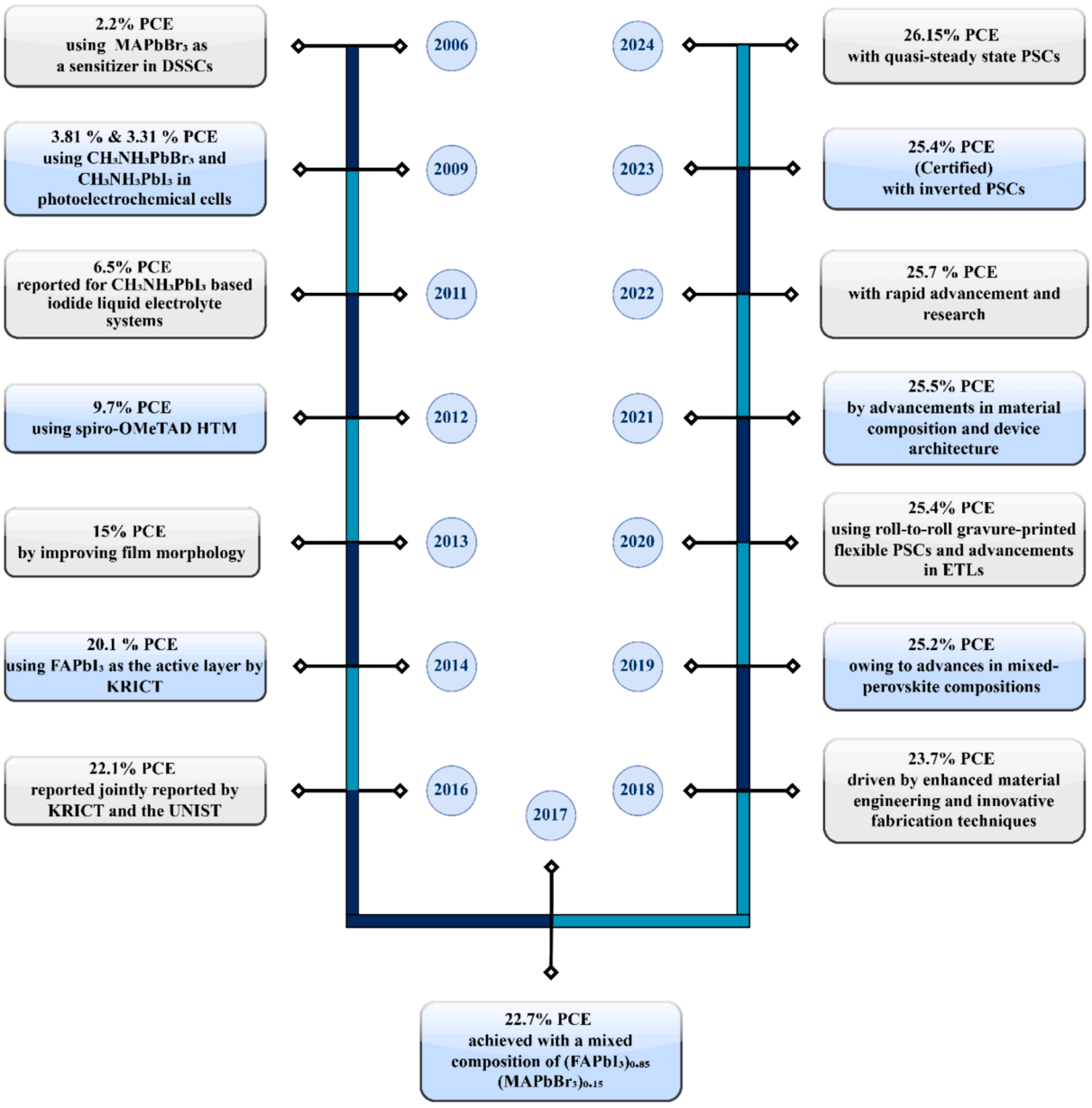

Fig. 2. Timeline showing the advances in PCE of PSC from 2006 to 2024.

By 2020, research on roll-to-roll gravure-printed flexible PSCs and developments in electron transport layers led to a new milestone, with the highest recorded PCE reaching 25.4 %. This marked a milestone in the commercial feasibility of flexible PSCs [35].

In 2021, the maximum approved PCE of 25.5 % was attained, a sign of the continual developments in material composition and device architecture. The development of heterojunction arrangements and other improvements have pushed the efficiency of PSCs closer to the theoretical limitations [36].

The journey of PSCs culminated in 2023, with inverted PSCs achieving a certified PCE of 25.4 % and further improvements seen in minimodules and large-area devices [37].

By 2024, the quasi-steady state PSC's PCE reached 26.15 %, with devices retaining 95 % of their initial efficiency after 1200 h of operation, highlighting both the progress in efficiency and stability [38].

This series of milestones demonstrates the extraordinary progress made in PSC research over the past decade. The continuous improvement in PCE reflects advancement in perovskite composition, material science, interface engineering, and fabrication techniques. A pivotal change occurred with the transition to solid-state devices. The advancements in charge transport layers (electron transport layer and hole transport layer) significantly enhanced both efficiency and stability. Innovations in mixed perovskite compositions, dopant-free transport layer, device architecture, fabrication techniques and interface engineering pushed PCE above 25 %, emphasizing scalability and device optimization.

4. Fundamental properties of perovskite solar cells

The high PCE and open circuit voltage (Voc) are attributed to several unusual properties of perovskites (Fig. 3) such as high absorption coefficient ($> 10^5$ cm^{-1}), long carrier diffusion lengths, moderate carrier mobility, high defect tolerance, and slow carrier recombination. Studies suggest that these remarkable properties could be due to various factors like intrinsic ferroelectricity, bulk photovoltaic effects, surface fields and diffusion, carrier-lattice interactions, large polaron formation [39].

To gain deeper understanding of the exceptional performance of PSCs, it is essential to explore the fundamental structure, chemical

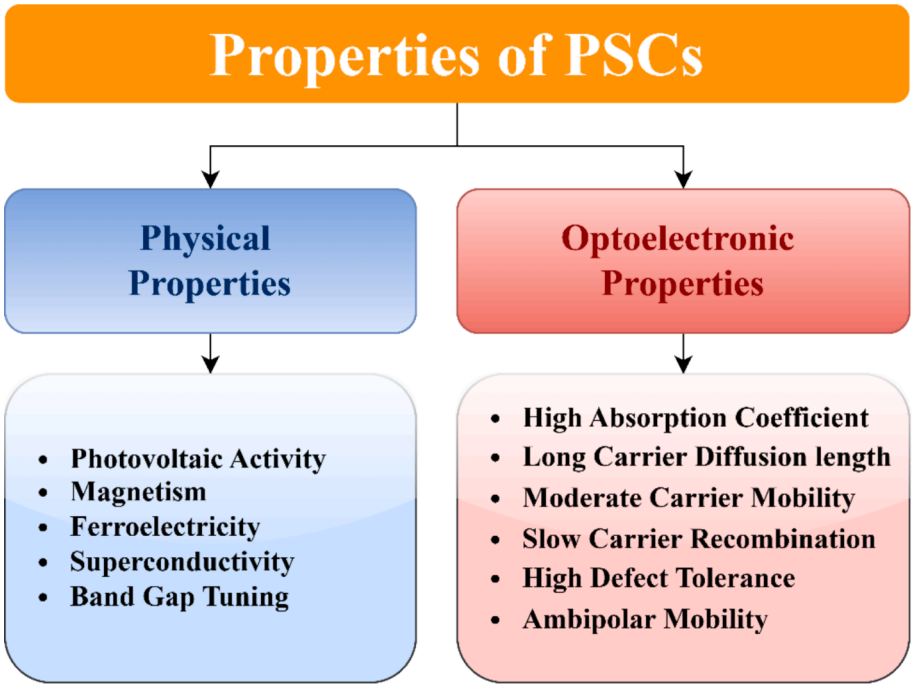

Fig. 3. Fundamental properties of PSC.

composition and material properties of the perovskite materials that underpin their unique behavior. The discussion begins with an examination of the structural aspects of perovskite materials and their relevance to photovoltaic applications which are analyzed in the accompanying sections of this study.

4.1. Structure of perovskite materials

Perovskite materials have garnered significant interest due to their exceptional physical properties, including photovoltaic activity, magnetism, ferroelectricity, and superconductivity. These materials typically adopt the general chemical formula ABX_3, where A represent organic or inorganic monovalent cation, B represent divalent heavy metal cation and X denotes an anion [40]. The ideal perovskite structure is cubic as shown in Fig. 4, characterized by A cations positioned at the corners of the unit cell, B cations at the center, and X anions at the face centers. The stability of this cubic structure depends on the coordination of 12 X anions around the A cation and an octahedral arrangement of X anions surrounding the B cation [41]. Deviations from the ideal cubic structure result in various lower symmetries, such as tetragonal, orthorhombic, rhombohedral, or monoclinic forms.

The structural stability of perovskites is quantitatively described by the Goldschmidt tolerance factor (τ) and the octahedral factor (μ) which are expressed as:

$$\tau = \frac{r_A + r_x}{\sqrt{2}(r_B + r_x)} \quad (1)$$

$$\mu = \frac{r_B}{r_x} \quad (2)$$

where r_A, r_B *and* r_x represent the ionic radii of the A, B, and X ions respectively. A τ value between 0.8 and 1.0 typically correlates with robust perovskite structures, whereas μ evaluates the stability of the B–X octahedron, with values greater than 0.41 signifying a stable structure.

Different structural phases of perovskites emerge based on the tolerance factor and temperature. At room temperature, a cubic phase (α phase) is observed when τ is between 0.89 and 1.0. Lower τ values lead to tetragonal (β phase) or orthorhombic (γ phase) formations.

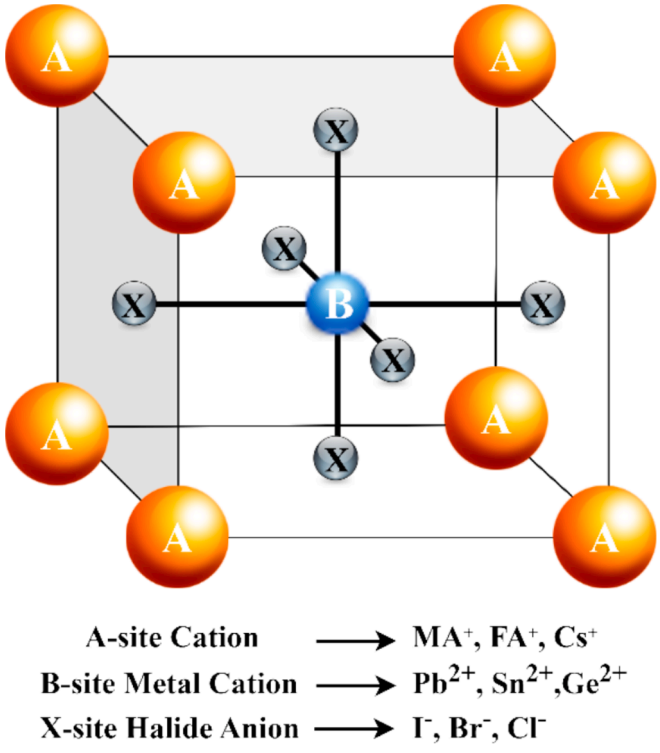

Fig. 4. Crystal structure of PSC.

Additionally, 2D layered perovskite structures can emerge when greater τ values disrupt the three-dimensional B–X network. Density functional theory (DFT) simulations and experimental approaches such as X-ray diffraction and high-resolution transmission electron microscopy have been used to examine phase transitions. DFT investigations reveal that the γ phase is the most stable near absolute zero, whereas the cubic α phase becomes the least stable [42,43].

4.2. Temperature dependent phase transition of perovskite materials

Perovskite materials experience unique phase transitions that are critical to their structural and photovoltaic characteristics. These materials are typically produced through a reaction between AX and BX_2, resulting in the creation of ABX_3.

$$AX + BX_2 \rightarrow ABX_3$$

The reaction kinetics are characterized by the rapid production of the perovskite phase, followed by temperature-dependent structural changes [44].

The essential phase transitions (Fig. 5) occur over a range of temperatures, with reversible transformations between tetragonal and cubic symmetry reported between 300 K and 400 K. At lower temperatures, often below 200 K, the material changes from the tetragonal phase to an orthorhombic phase [45]. The change from tetragonal to cubic symmetry has no significant effect in the photovoltaic performance, while the orthorhombic phase leads to a significant decrease in power conversion efficiency. These structural variations will be associated with the changes in the band structure of the material as well its optoelectronic properties. X-ray diffraction (XRD) gives a clear evidence of these phase changes [46]. In particular ordering of iodine ions is responsible for transition from cubic to tetragonal symmetry about 300 K temperature. Due to its large unit cell volume, the cubic phase state facilitates this transition. Further studies position that the transition from tetragonal to cubic is linked with the PbI_2 separation from $CH_3NH_3PbI_3$ which eventually leads to a decrease in the unit cell dimensions of the cubic perovskite.

However, a progressive analysis of several methyl ammonium lead halide perovskites shows that they have varied transition temperatures. In the case of $CH_3NH_3PbCl_3$, the cubic phase is present at 177 degrees Celsius and the tetragonal phase is recorded at 172 degrees Celsius. However, for this halide perovskite no orthorhombic transition has been reported [42]. $CH_3NH_3PbBr_3$ transitions to the cubic phase at 236 °C and undergoes a tetragonal phase transition between 149 °C and 154 °C, although no orthorhombic phase transition is found. In the instance of $CH_3NH_3PbI_3$, the cubic phase exists at 330 °C, with a transition to the tetragonal phase at 161 °C, albeit again, no orthorhombic transition is found for this material [48]. These findings underline the temperature induced character of the perovskite phase transitions and how they affect its functionality in solar applications.

Several notable perovskite materials exhibit distinct structural and physical characteristics. For example, barium titanate ($BaTiO_3$) undergoes phase transitions from cubic to tetragonal, orthorhombic, and rhombohedral phases as temperature decreases, a property that is integral to its ferroelectric behavior [49]. Strontium titanate ($SrTiO_3$) retains its cubic structure at room temperature but exhibits superconductivity at low temperatures. These structural and functional properties underpin the growing interest in perovskite materials, particularly in the development of perovskite solar cells.

4.3. Band gap tuning and halide variation

The most significant feature of perovskites is the ability to tune their band gap which is of great importance for the enhancement of such materials for solar cell usage. By altering or tuning the halide content (I^-, Br^-, Cl^-), it has been found to enable tuning the band gap over a wide range (1.5 eV to 2.3 eV) making perovskite materials versatile for various light-absorption requirements [50]. In the case of $CH_3NH_3PbX_3$ (X = Cl, Br, I), the band gap narrows from chlorine to iodide because of difference in electronegativity and ionic radii. The detailed analysis of bandgap tuning in PSC is performed in section 9 of this review article.

4.4. Optical absorption and defect tolerance

Perovskites offer exceptional optical absorption, particularly in the visible range. Methylammonium lead iodide ($CH_3NH_3PbI_3$ or $MAPbI_3$) is a prime example, with a high optical absorption coefficient due to strong Pb-I orbital interaction. This material's band structure, typified by a well-defined conduction band (CB) and valence band (VB), permits effective light absorption and charge carrier production [51]. As in other materials, the perovskites in this regard do not follow normal semiconductor trends but show inherent fault tolerance. Defects like vacancies; I^- or Pb^{2+}, normally create shallow trap states rather than deep trap states that would otherwise limit the mobility of charge carriers. Thus, it is possible to have rapid transfer and collection of carriers regardless structural imperfections are present. Consequently, large carrier diffusion lengths, up to 100 μm in single crystals, have been observed, significantly improving the effectiveness of PSCs [41].

4.5. Carrier transport, mobility, and recombination

Another significant characteristic of perovskites is their ambipolar carrier mobility, with both electrons and holes having equal effective masses. This results in efficient charge transport and minimum recombination losses. $MAPbI_3$, in particular, displays long photoluminescence (PL) lifetimes and low recombination rates, further adding to its strong photovoltaic performance. The suppression of electron-hole recombination is due to the high ionic density in the material, which promotes

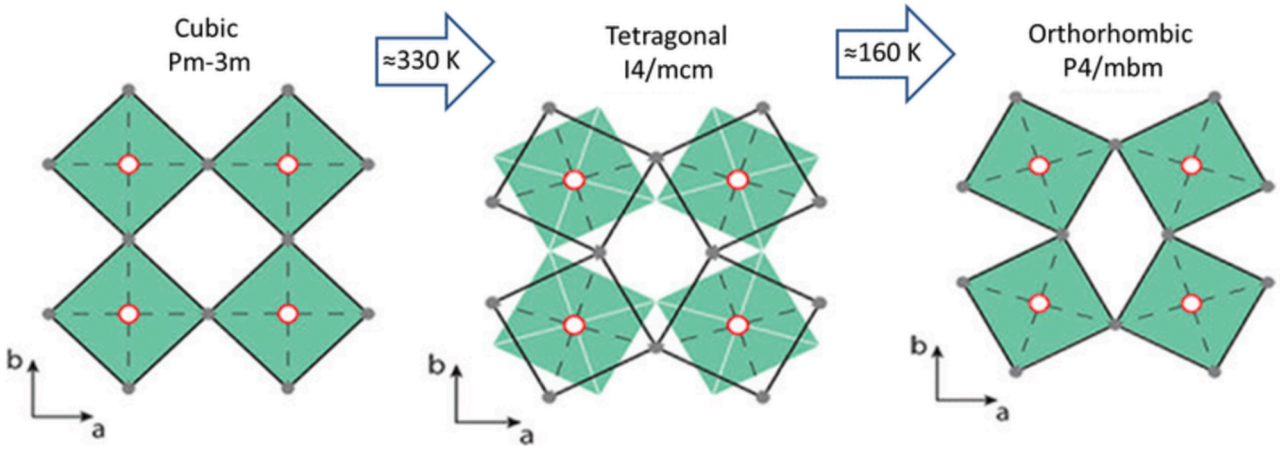

Fig. 5. Phase transition in $MAPbI_3$. Neighboring layers of PbI_6 octahedra are shown as filled green squares and black squares. Adapted with permission from reference [47] under the Creative Common license CC BY. (For interpretation of the references to colour in this figure legend, the reader is referred to the web version of this article.)

charge screening and lowers recombination via shallow defects [52].

4.6. Photovoltaic efficiency and voltage loss

The combination of high optical absorption, defect tolerance, and ambipolar mobility results in perovskites achieving outstanding solar efficiencies. PSCs frequently exhibit high Voc, often exceeding 1.1 V, even under low light conditions. This high Voc, along with a well-balanced charge transfer process, contributes to the outstanding PCE exhibited in perovskite-based solar cells [53]. Despite these advancements, PSCs still suffer from voltage loss due to the presence of defects and trap states, particularly in polycrystalline films, where the trap density can range from 10^{16} cm^{-3}. By comparison, single-crystal perovskites have lower trap densities (~10^{10} cm^{-3}), indicating the opportunity for further optimization in device construction and material processing [36].

4.7. Electronic structure and phase transitions

The electronic structure of perovskites is principally dictated by the B cations and X anions, which dictate the material's conduction and valence band properties. For example, in $CH_3NH_3PbI_3$, the Pb-I bond angle and lattice constant influence the band gap, which can vary between 1.5 eV and 1.6 eV depending on whether the material is in its cubic or tetragonal phase. Similarly, modifications in the halide composition (e.g., substituting iodide with chloride) impact the band gap, allowing for more control over the material's optoelectronic capabilities [54]. The temperature-dependent phase transitions in perovskites also play a crucial role in their performance as shown in Fig. 5. For instance, the shift from cubic to tetragonal or orthorhombic phases impacts both the optical characteristics and carrier mobility, albeit these changes are frequently reversible with temperature [55].

5. Working of PSCs

When PSCs were first explored, their behavior was initially believed to mimic that of DSSCs. Early experiments involved PSCs paired with a TiO_2 mesoporous photoanode within liquid electrolyte-based cells, where it was assumed that photoexcited electrons from the perovskite layer would inject into the TiO_2 conduction band and flow through an external circuit, similar to the mechanism observed in DSSCs [56]. This assumption stemmed from a limited understanding of perovskites during the early stages of research. However, while PSCs share certain operational principles with DSSCs and organic solar cells (OSCs), the transport mechanisms in PSCs differ significantly [57]. Instead of relying on an external scaffold, charge carrier transport in PSCs occurs directly within the perovskite film itself, reflecting a distinct underlying physics compared to DSSCs. The basic working of PSCs is depicted in Fig. 6.

Further research revealed that PSCs do not require a semiconducting scaffold such as TiO_2 for efficient electron transport. Instead, electron and hole transport can occur directly within the perovskite film itself, even in planar architectures [25]. This led to a paradigm shift in understanding, where PSCs were realized to behave more like solid-state p-n junction solar cells rather than following the sensitization mechanism seen in DSSCs. This breakthrough allowed researchers to focus on optimizing the perovskite material itself, paving the way for higher PCEs.

One intriguing aspect of PSCs is their Voc. Unlike conventional solar cells, where Voc typically shows a clear dependence on the work function difference between the selective contacts [58], PSCs exhibit unusual carrier behavior. Despite this, they achieve high Voc and PCEs due to the material's intrinsic properties, such as high optical absorption, long carrier diffusion lengths, and low recombination rates. These attributes highlight the unique physics governing PSC performance, distinguishing them from other solar cell technologies.

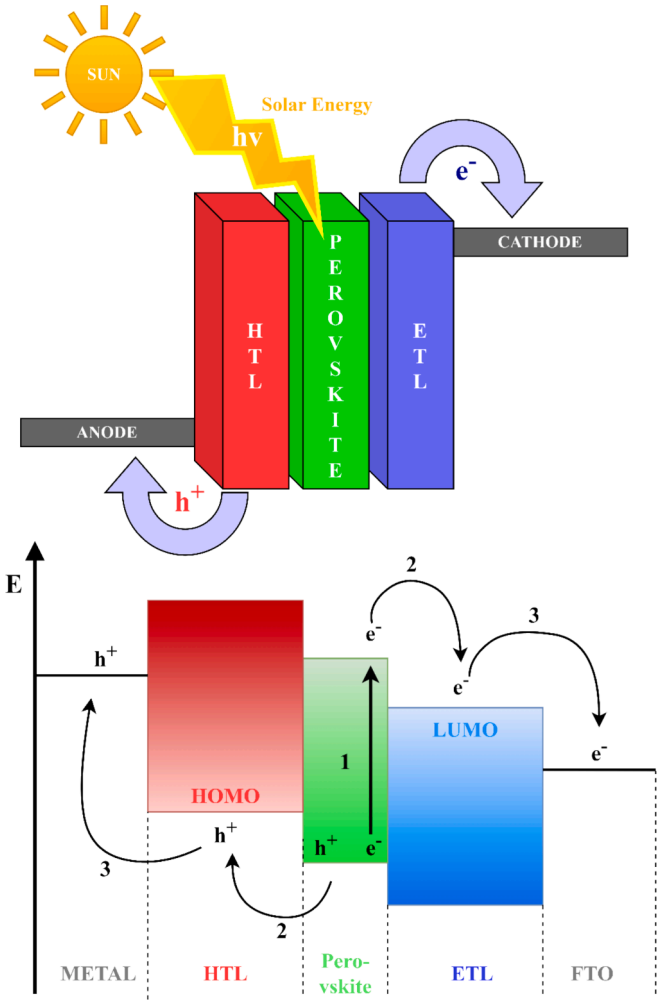

Fig. 6. Basic working of perovskite solar cell. Hole transport layer (HTL). Electron transport layer (ETL). Fluorene doped tin oxide (FTO). Highest occupied molecular orbital (HOMO). Lowest unoccupied molecular orbital (LUMO).

6. Device structure of PSCs

The typical structure of a PSC involves a perovskite photoactive film sandwiched between two electrodes, with interfacial buffer layers facilitating charge transport. A PSC consists of five key layers (Fig. 7), each performing a specific role in converting sunlight into energy. The

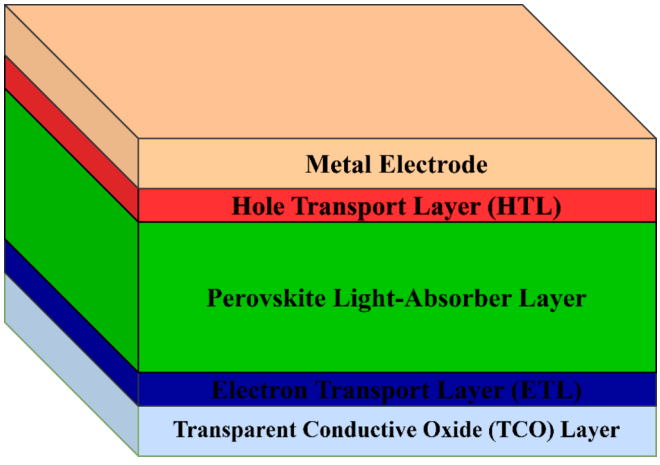

Fig. 7. Basic structure of perovskite solar cell.

analysis of these layers is done in the following sections.

1. Conducting substrate (Transparent conductive oxide – TCO Layer)

The TCO layer transmits light to the adjacent layers and facilitates the extraction of charge carriers to the external circuit. The most common materials used are indium-doped tin oxide (ITO) and fluorine-doped tin oxide (FTO), known for their high conductivity and good transparency. Aluminum-doped zinc oxide (AZO) is another alternative.

2. Hole transport layer (HTL)

The HTL collects photogenerated holes from the perovskite layer and transfers them to the back electrode while inhibiting electron flow. This prevents charge recombination and boosts efficiency. Common HTL materials include spiro-OMeTAD, albeit it suffers from instability. Alternatives like copper oxide (CuO), copper iodide (CuI), nickel oxide (NiO), PEDOT(poly(3,4-ethylenedioxythiophene)sulfonate), and PTAA (poly[bis(4-phenyl)(2,4,6-trimethylphenyl)amine) have been researched for greater stability and performance [59].

3. Perovskite light-absorber layer

The perovskite layer is responsible for absorbing sunlight and creating electron-hole pairs (excitons) when exposed to photons. Common perovskite materials include methylammonium lead iodide ($MAPbI_3$), formamidinium lead iodide ($FAPbI_3$), methylammonium germanium iodide ($MAGeI_3$), and methylammonium tin iodide ($MASnI_3$). Mixed cation perovskites such as $CsPbIBr_2$, $CsPbI_2Br$, and versions of $MAPbI_{3-x}Cl_x$ or $MAPbI_{3-x}Br_x$ are being researched for better characteristics, tunable bandgaps, and improved stability [60].

4. Electron transport layer (ETL)

The ETL collects photogenerated electrons from the perovskite layer and transmits them to the external circuit while inhibiting the transit of holes. This minimises recombination and boosts overall device efficiency. Titanium dioxide (TiO_2) is the most extensively used ETL, but it requires high-temperature processing. Alternatives like tin dioxide (SnO_2), indium gallium zinc oxide (IGZO), and zinc oxide (ZnO) are also exploited, offering advantages such as lower processing temperatures and cost-effective manufacturing [32].

5. Metal electrode

The metal electrode captures the electrons and enables their flow through the external circuit. Common materials include gold (Au), silver (Ag), and aluminum (Al), chosen for their superior conductivity. Silver and aluminum are typically used to cut expenses compared to gold [61].

6.1. *Structural classifications of PSCs*

Perovskite solar cells (PSCs) are primarily classified into two main architectures: mesoporous (mesoscopic) and planar (planar heterojunction) structures [62]. Both architectures have distinct designs, materials, and functional properties that influence the performance and efficiency of the PSC devices (Fig. 8). These architectures can be further classified into n-i-p and p-i-n configurations depending upon which of the charge transport layer (ETL or HTL) is met with the incident light first [62]. The major differences between mesoporous and planar structures are discussed in Table 1 while the differences between n-i-p and p-i-n configurations are discussed in Table 2.

6.1.1. *Mesoporous (Mesoscopic) structures*

The mesoporous structure often adheres to the standard n-i-p configuration, wherein electrons are extracted via the transparent conducting substrate. This architecture mirrors the configuration of DSSCs,

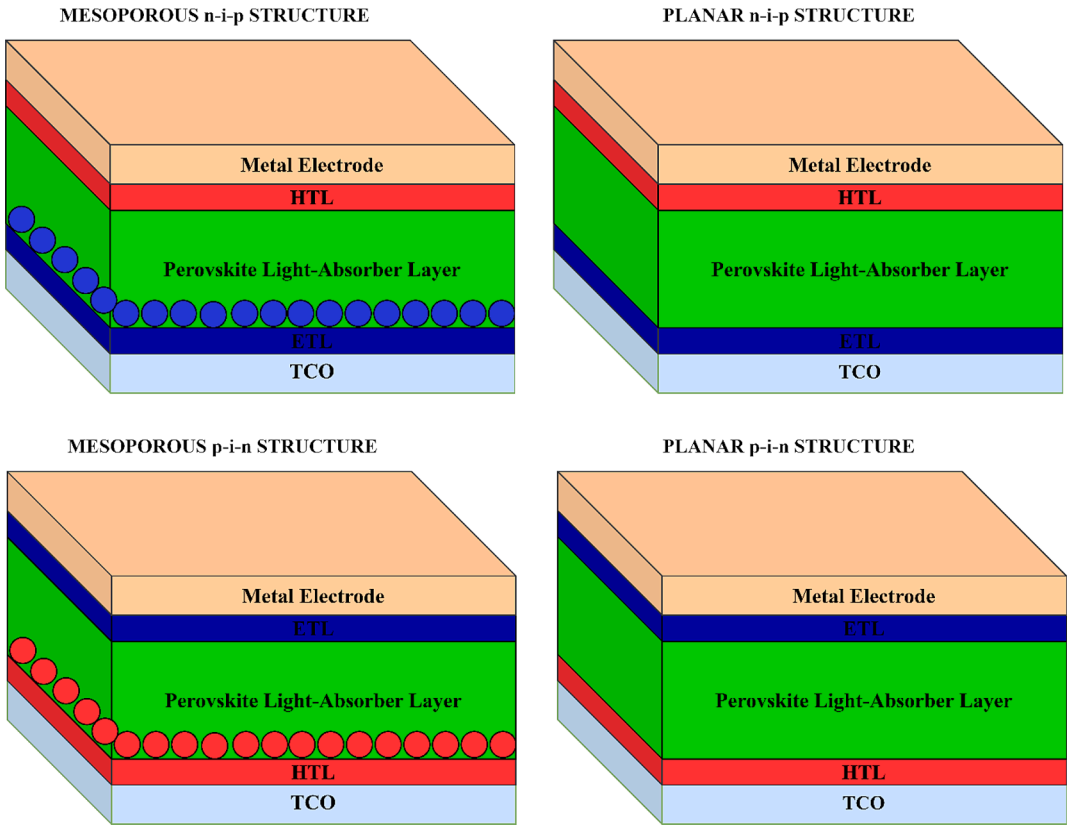

Fig. 8. Classification of different PSC architecture.

Table 1
Comparison between mesoporous architecture and planar heterojunction architecture.

Aspect	Mesoporous Architecture	Planar Architecture
Design	Consists of a scaffold made of mesoporous metal oxides (e.g., TiO_2, Al_2O_3, ZrO_2), with the perovskite filling the pores. Uses the conventional n-i-p configuration.	Features a flat, layered structure without a scaffold, where the perovskite is deposited between the ETL and HTL. Often uses the p-i-n configuration.
Electron Transport Layer (ETL)	Typically uses mesoporous TiO_2, Al_2O_3, or ZnO, which serve as a scaffold for the perovskite.	Organic or inorganic ETLs such as C60, PCBM, ZnO, or SnO_2 are employed in planar structures.
Hole Transport Layer (HTL)	Typically uses spiro-OMeTAD or other organic HTLs, placed on top of the perovskite layer.	Can use PEDOT, PTAA, or spiro-OMeTAD as the HTL, which directly interfaces with the perovskite layer.
Charge Collection	The mesoporous scaffold extends into the photoactive layer, reducing the distance for electron transport and improving collection efficiency.	Planar structures rely on the interface between the perovskite and the ETL/HTL for charge collection, with no additional scaffold.
Processing Temperature	Requires high-temperature sintering (450–500 °C), especially for TiO_2. This makes it less suitable for flexible substrates and roll-to-roll manufacturing.	Can be processed at lower temperatures (typically below 150 °C), making it more compatible with flexible substrates and scalable production.
Power Conversion Efficiency (PCE)	Historically associated with high PCEs due to better electron transport and reduced recombination in the scaffold. Often performs better with halide perovskites.	Planar structures have shown higher PCEs in recent years, particularly with mixed halide perovskites and organic ETLs. Holds the record for the highest PCE.
J-V Hysteresis	Mesoporous structures exhibit less hysteresis compared to planar designs, due to more efficient charge transport.	More prone to J-V hysteresis, especially when using certain ETLs and HTLs. Requires careful optimization to reduce hysteresis.
Film Formation	The mesoporous scaffold helps in forming uniform films by providing a structural template for the perovskite.	Planar structures are more sensitive to film uniformity, and defects in the perovskite film can reduce efficiency and stability.
Stability	Stable under high temperatures and environmental conditions, especially on glass substrates. Stability can be compromised by moisture and light exposure if not properly encapsulated.	Historically less stable, but recent advancements in materials and interface engineering have improved stability. Planar devices are more sensitive to degradation.
Flexibility	Due to the high-temperature processing and rigid scaffold, mesoporous structures are not well-suited for flexible substrates.	Well-suited for flexible substrates due to low-temperature processing. Ideal for flexible solar cells and wearable technologies.
Applications	Primarily used in rigid solar panels where high efficiency and stability are prioritized over flexibility.	Widely used in flexible, large-area, and roll-to-roll manufactured solar panels. Also preferred for wearable and portable devices.
Light Absorption and Scattering	The mesoporous scaffold enhances light scattering, increasing photon absorption and improving device performance.	Planar structures rely entirely on the properties of the perovskite film for light absorption, without the added benefit of light scattering.
Fabrication Complexity	More complex due to the need for a scaffold and high-temperature sintering. The fabrication process involves multiple steps, including the creation of a mesoporous layer.	Simpler fabrication process, with fewer steps. Planar PSCs do not require a scaffold, making them easier to produce, particularly at scale.
Current Research Focus	Ongoing research aims to reduce processing temperatures and improve stability, particularly in environmental conditions.	Research focuses on improving film uniformity, reducing hysteresis, and enhancing long-term stability while maintaining flexibility and scalability.

with a slender mesoporous charge-transport layer composed of metal oxide nanoparticles, including TiO_2, Al_2O_3, or ZrO_2 [63]. The perovskite material permeates the mesoporous scaffold, with the complete structure positioned between two electrodes—typically fluorine-doped tin oxide (FTO) or indium-doped tin oxide (ITO) serving as the cathode, and a metallic anode such as gold (Au) or silver (Ag). The mesoporous metal oxide layer, generally 150–300 nm in thickness, functions as a scaffold for selective charge transport and extends into the optical path of the photoactive perovskite layer [64]. This configuration improves electron collection and minimises charge recombination by shortening the carrier travel distance. The structure efficiently facilitates light absorption via scattering, resulting in enhanced photon capture and improved charge separation. The thickness of the perovskite light-absorbing layer is normally up to 300 nm. Mesoporous structures are known to offer improved PCE due to their ability to reduce charge carrier recombination and improve charge collection [65]. TiO_2 scaffolds have notable efficacy in electron transport; nonetheless, they necessitate high-temperature sintering (450–500 °C), which may result in current–voltage (I-V) hysteresis. Devices utilising mesoporous TiO_2 or Al_2O_3 scaffolds have exhibited enhanced stability and efficiency on glass surfaces following high-temperature annealing. The elevated-temperature sintering necessary for TiO_2 can induce hysteresis, especially during the current–voltage sweep. Furthermore, while mesoporous structures are good for charge transfer, they are less appropriate for applications requiring flexible substrates because to the stiffness and high-temperature requirements of metal oxides. Despite these limitations, mesoporous devices have showed higher PCE compared to planar structures in certain perovskite compositions, particularly halide perovskites [66,67].

6.1.2. Planar structures

The planar structure is commonly related with the inverted p-i-n configuration, where holes are extracted through the transparent conductive oxide (TCO) substrate. This concept provides a simpler, stacked layer arrangement without the need for a mesoporous scaffold. The planar architecture consists of an electron transport layer (ETL), the perovskite absorber, a hole transport layer (HTL), and a metal back electrode. The ETL is commonly manufactured from organic electron transport materials (ETMs) such as C60 and its derivatives like PC61BM, PC71BM, and ICBA [68]. The HTL frequently uses materials like PEDOT (poly(3,4-ethylenedioxythiophene) sulfonate) or spiro-OMeTAD. In planar designs, the perovskite absorber layer is placed between the ETL and HTL, considerably improving the collection of photogenerated holes and electrons. The planar architecture provides for better control of layer thickness and uniformity, resulting to more effective charge extraction. The absence of a scaffold means that planar structures rely on the inherent properties of the perovskite material for light absorption and charge production. Planar PSCs can be produced at lower temperatures (usually around 150 °C), making them appropriate for flexible substrates and large-scale roll-to-roll fabrication [69]. This lower processing temperature also enables for compatibility with a larger range of materials, cutting production costs and making the technology more accessible for commercial applications. Planar designs now hold the record for the highest power conversion efficiency in perovskite solar cells [70]. Planar perovskite films offer excellent charge carrier mobility, frequently surpassing 20 cm^2/Vs, particularly in devices using mixed halide perovskites. These designs are more compatible with organic materials and are hence commonly used for flexible solar cells and heterojunction devices. Planar structures, however, are prone to J-V hysteresis, particularly when compared to mesoporous structures. The homogeneity of the perovskite film and its interactions with the ETL and HTL layers is critical for good performance. Planar devices are also more vulnerable to open-circuit voltage loss due to high trap densities in the perovskite layer [63]. Achieving uniform and defect-free film

Table 2
Comparison between n-i-p and p-i-n configurations.

Aspect	n-i-p Configuration	p-i-n Configuration
Current Flow Direction	Electrons flow from the n-type layer (ETL) through the perovskite to the p-type layer (HTL).	Holes flow from the p-type layer (HTL) through the perovskite to the n-type layer (ETL).
Electron/Hole Extraction	Electrons are extracted through TCO substrate, whereas holes are collected at the back electrode.	Holes are extracted through the TCO substrate, whereas electrons are collected at the back electrode.
Power Conversion Efficiency (PCE)	Historically associated with higher PCE, especially in the early development of PSCs, with PCEs exceeding 25 % in recent years.	Recently competitive PCE, matching and even exceeding n-i-p designs in some cases, particularly with better interface engineering.
Stability	Lower stability due to the use of certain ETL materials (e.g., TiO_2) and higher temperature processing, making the structure more susceptible to degradation from moisture, light, and oxygen.	Higher stability, especially in the long term, as this architecture uses lower-temperature fabrication techniques and materials with better resistance to environmental factors.
Processing Temperature	Requires high-temperature processing, especially for the ETL (e.g., TiO_2 sintering at 450–500 °C).	Processing temperatures are typically below 150 °C.
Electron Transport Layer (ETL)	Common ETL materials include mesoporous TiO_2, Al_2O_3, ZnO, which often require high-temperature sintering.	Uses organic ETLs (e.g., PCBM, C60) or low-temperature inorganic ETLs (e.g., SnO_2, ZnO) that are more compatible with flexible substrates.
Hole Transport Layer (HTL)	HTLs like spiro-OMeTAD are commonly used but suffer from stability issues. Other materials include PTAA.	Typically uses PEDOT, NiO, or other stable HTLs, contributing to the improved stability of the architecture.
J-V Hysteresis	Generally, shows less J-V hysteresis than p-i-n structures due to better alignment and charge collection through mesoporous ETLs.	More prone to J-V hysteresis, though advancements in interface engineering and material optimization have mitigated this issue in modern designs.
Device Stability and Degradation	Prone to degradation due to the high sensitivity of materials like TiO_2 to moisture and UV exposure. Requires robust encapsulation to enhance stability.	Generally, more stable against environmental degradation due to the use of more resilient materials in the ETL and HTL layers. Less reliant on encapsulation for stability.
Fabrication Complexity	More complex, with the need for high-temperature sintering and multiple processing steps, making it less compatible with low-cost, large-scale manufacturing.	Simpler fabrication, particularly with low-temperature processing and fewer steps, making it more scalable for industrial production. Ideal for roll-to-roll and flexible substrate applications.
Applications	Suited for rigid solar panels where high efficiency is prioritized over flexibility. Commonly used in laboratory-scale and commercial solar panel applications.	Ideal for flexible solar cells, wearable devices, and building-integrated photovoltaics (BIPV) due to the compatibility with flexible substrates and low-cost manufacturing.
Light Absorption and Scattering	Mesoporous structures in n-i-p devices enhance light absorption through scattering, improving overall device performance.	Relies on planar structures without scaffolds, which can limit light scattering but improve processing and scalability.
Interface Engineering	Focuses on optimizing the mesoporous scaffold and charge transport materials to improve electron extraction and reduce recombination.	Recent advancements in interface engineering have significantly reduced recombination and improved energy alignment, enabling p-i-n configurations to achieve competitive PCEs.
Trap States and Recombination	Mesoporous structures help reduce trap states, enhancing charge extraction and reducing recombination.	Prone to more trap states due to the planar structure, though advancements in interface engineering have mitigated these effects in modern devices.
Environmental Sensitivity	Sensitive to UV exposure, moisture, and oxygen, which can degrade materials like TiO_2 and reduce performance over time.	More environmentally resilient, with materials that offer better protection against moisture, light, and oxygen degradation.

production remains a challenge for planar topologies, which can lead to lower device stability and performance.

6.1.3. n-i-p structure (conventional architecture)

In the traditional n-i-p architecture, the current passes from the n-type layer (ETL) through the perovskite intrinsic layer to the p-type layer (HTL) (Fig. 8). Electrons are extracted through the substrate, typically a TCO like ITO or FTO, which serves as the front contact. The electrons are carried from the ETL via the perovskite and collected at the metal back electrode, commonly Au or Ag. The n-i-p arrangement has been traditionally linked with PCE because to its effective charge transport and collecting properties. However, it has experienced issues linked to long-term stability. The high PCEs reported in n-i-p structures are generally accomplished at the sacrifice of stability, as these devices tend to decay more quickly under environmental stressors including moisture and light [71–73].

6.1.4. p-i-n structure (inverted architecture)

In the p-i-n architecture, the current flows in the opposite direction compared to the standard n-i-p arrangement (Fig. 8). It passes from the p-type layer (HTL) through the perovskite intrinsic layer to the n-type layer (ETL) [62]. Holes are extracted through the TCO substrate (such as ITO or FTO), and the electrons are collected at the rear metal electrode. This inverted design commonly uses organic hole transport materials like PEDOT and electron transport materials like as PCBM derivatives (e.g., PC61BM, PC71BM). Historically, the p-i-n structure has been associated with greater stability compared to the n-i-p architecture [73]. The lower-temperature procedure, notably for the electron transport layer, decreases deterioration concerns. However, early p-i-n devices demonstrated lower PCEs than n-i-p counterparts due to less effective charge extraction methods and energy-level alignment problems. Modern p-i-n PSCs have attained both better stability and competitive PCEs, now rivaling those of n-i-p devices. This improvement is largely owing to superior material engineering and optimization of the interfaces between the perovskite, transport layers, and electrodes. Advances in manufacturing processes, particularly low-temperature processing procedures and improved deposition technologies, have enabled the manufacture of p-i-n PSCs with enhanced electronic characteristics [74]. These developments make the inverted design particularly ideal for flexible and scalable applications, including roll-to-roll manufacturing.

7. Materials for perovskite solar cells

A comprehensive understanding of the different type of materials used in PSCs is essential for unlocking their full potential. These materials not only influence the device's stability and efficiency but also dictate fabrication techniques, scalability, and cost effectiveness. By exploring each key layer of the PSC, we can assess how material selection impacts the overall performance and long-term reliability of the cell. A detailed analysis of various materials used for PSC is performed in the accompanying section.

7.1. Charge transport layers (CTLs)

CTLs play a vital role in the performance and stability of PSCs by extracting and moving photogenerated charge carriers from the perovskite active layer to the appropriate electrodes. The efficiency of PSCs is substantially determined by the characteristics and interfaces of CTLs, which need to demonstrate good electrical conductivity, optimal energy level alignment, high optical transparency, and compatibility with the perovskite layer [75]. Based on the type of charge carrier they facilitate The CTLs are categorized (Fig. 9) into two primary types: electron

transport layers (ETLs) and hole transport layers (HTLs).

7.1.1. Electron transport layer (ETL)

ETL is a critical component of PSCs, playing a vital role in electron extraction, energy level alignment, hole blocking, and decreasing recombination losses. By promoting effective charge transfer while inhibiting recombination, ETLs considerably influence the overall efficiency and stability of PSCs [32]. The conduction band minimum (CBM) of the ETL should align well with the perovskite layer for efficient transfer of electrons. The ETL must be stable against degradation by moisture, oxygen, light, and heat, as well as being insoluble in perovskite precursors to ensure device longevity. Some ETL materials help reduce J-V hysteresis, a known issue in PSCs, which can limit their performance. Uniform, thin, and compact ETLs promote efficient electron transport while minimizing recombination and short-circuit risks. Several materials, including organic and inorganic semiconductors, have been researched for their usefulness as ETLs, each presenting various advantages and challenges. The energy level representation of some most common ETLs used in PSC is presented in Fig. 10.

7.1.1.1. Types of ETLs. ETLs can be broadly characterized into inorganic, organic which are depicted in Fig. 8 respectively.

A. Inorganic ETLs

Inorganic materials, particularly metal oxides, have been widely employed as ETMs due to their high electron mobility and chemical stability. Table 3 summarizes the primary inorganic ETMs used in PSCs.

B. Organic ETLs

Organic electron transport materials (ETMs) have attracted attention due to their tunable properties and low-temperature processing. They are broadly divided into fullerene-based and non-fullerene-based materials [80].

i) Fullerene-based organic ETMs

Fullerene derivatives such as C60, C70, and [6,6]-phenyl-C61-butyric acid methyl ester (PCBM) are popular due to excellent electron extraction capabilities, high electron mobility, and appropriate energy levels but they suffer from poor stability, restricted solubility, and high costs [76].

ii) Non-fullerene organic ETMs

Non-fullerene organic ETMs provide greater flexibility in molecular design and offer alternatives to fullerenes. They are categorized as:

Small molecular organic ETMs: Characterized by simple, well-defined structures that allow easy purification and characterization. These form uniform, compact films on the perovskite layer, improving charge transport. Examples include pyrazine-azaacene, naphthalene-diimide, and perylene-diimide derivatives [81].

Polymer ETMs: These have more complex structures, offering better functionalization. Polymers such as PFN and PFNF create interpenetrating networks with perovskite layers, enhancing mechanical stability and reducing interface defects [82].

7.1.1.2. Film morphology and stability. The morphology of ETL films significantly impacts the performance and stability of PSCs. Both

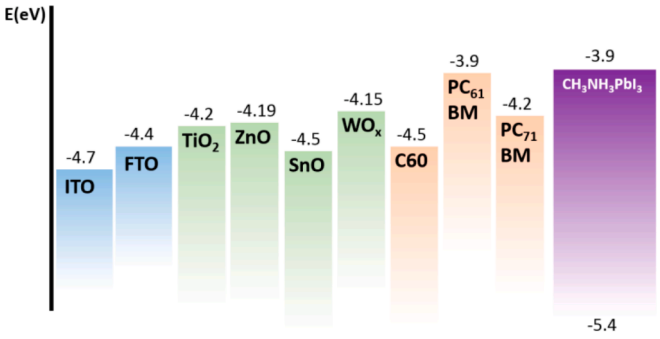

Fig. 10. Energy level representation of some most commonly used ETLs. Adapted from reference [76] under creative common license CC-BY.

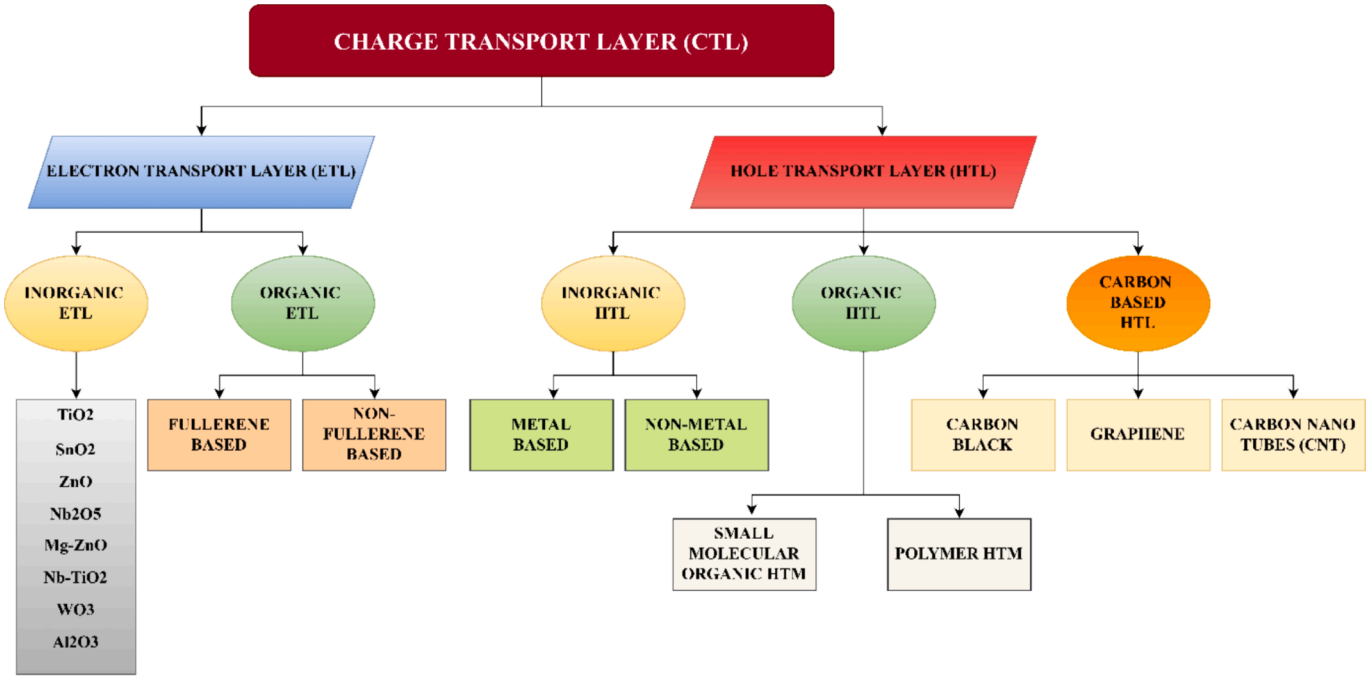

Fig. 9. Classification of charge transport layers of perovskite solar cell.

Table 3
Description of various inorganic ETLs used in PSCs.

Inorganic ETM	Description
Titanium Dioxide (TiO_2)	TiO2 is one of the most commonly used ETLs in PSCs due to its high electron mobility and wide bandgap (~3.2 eV), which provide good electron selectivity. Strong chemical stability, allowing it to function effectively as a front contact material in solar cells. Although TiO_2 is commonly used as ETL in PSC it suffers from significant surface trap states that can cause electron recombination and J-V hysteresis, impacting the stability and efficiency of the device [75].
Tin Oxide (SnO_2)	SnO_2 has gained popularity as an alternative to TiO2 due to its high electron mobility and wide bandgap (3.6 eV), making it highly transparent in the visible range. It offers lower recombination rates and reduced hysteresis compared to TiO2. SnO_2 requires low-temperature processing, making it compatible with flexible substrates and low-cost applications [77].
Zinc Oxide (ZnO)	ZnO offers high electron mobility and a wide bandgap (3.3 eV), making it efficient for electron transport. ZnO's instability in acidic perovskite precursor solutions leads to degradation over time, necessitating surface treatments to improve its long-term stability [77].
Niobium Pentoxide (Nb_2O_5)	Nb_2O_5 is less commonly used but shows promise due to its wide bandgap (3.4–3.6 eV) and good electron mobility. It offers high chemical stability and ability to reduce recombination losses in some PSC architectures [78].
Magnesium-Doped Zinc Oxide (Mg-ZnO)	Mg-doped ZnO enhances the properties of ZnO by increasing the bandgap and electron mobility, which improves stability and reduces recombination rates [78].
Niobium-Doped Titanium Dioxide (Nb-TiO_2)	Nb-TiO_2 improves upon pure TiO_2 by enhancing electron mobility and reducing the defect density at the interface with the perovskite, leading to higher performance in terms of Voc and Jsc [79].
Tungsten Trioxide (WO_3)	WO_3 is less commonly used but exhibits a wide bandgap (2.6–3 eV) and good electron mobility. Chemical stability, positioning it as a potential alternative ETL for specialized PSC architectures [79].
Aluminum Oxide (Al_2O_3)	Al_2O_3 is not a typical electron-transporting material, but its insulating properties allow it to serve as a mesoporous scaffold. It enhances mechanical stability while demonstrating long carrier transport distances in perovskite layers. It offers higher Voc, though lower fill factors due to increased impedance [78].

organic and inorganic ETLs need to form uniform, compact films on the perovskite layer to promote efficient charge transfer and prevent moisture or oxygen diffusion. Materials like SnO_2 and Nb-TiO_2 display better film-forming capabilities, contributing to improved stability and performance over time [81]. While substantial breakthroughs have been made in the construction of both organic and inorganic ETLs, significant challenges still remain. The synthesis of new ETMs is often time-consuming and resource-intensive. The development of computational methods to guide molecular design could streamline this procedure. Ensuring long-term stability under real-world circumstances is important for PSC commercialization. Continued research into materials that resist degradation from moisture, oxygen, and light is crucial. Low-cost, scalable synthesis methods are required for large-scale production of ETLs for commercial applications [83].

7.1.2. Hole transport materials (HTMs)

HTMs serve as a critical interface between the perovskite layer and the anode in PSCs. Their principal job is to harvest holes created in the perovskite layer and deliver them to the anode, while limiting electron-hole recombination.

7.1.2.1. Types of HTMs. HTMs are divided into three major classes (Fig. 8): organic, inorganic, and carbon-based materials, each with specific features that effect the performance of PSCs.

A. Organic HTMs

Organic HTMs are frequently employed in PSCs due to their tunable molecular architectures, adjustable energy levels, compatibility with the perovskite layer, and solution-processable features at low temperatures [84]. Organic HTMs are further classified into small molecular organic HTMs and polymer HTMs each offering their merits and demerits.

i) Small molecular organic HTMs

Small molecular HTMs have well-defined structures, which permit better purification and characterization (Fig. 11). They tend to form compact and homogeneous films on the perovskite layer, hence increasing charge transfer and extraction efficiency. Examples of regularly utilised small molecule HTMs include Spiro-OMeTAD and PTAA. These materials are selected for their potential to improve film morphology and device stability [63].

ii) Polymer HTMs

Polymeric HTMs, such as P3HT and PEDOT:PSS, exhibit more complicated structures, enabling them to create interpenetrating networks with the perovskite layer. This structural advantage promotes mechanical stability and eliminates interface flaws, contributing to increased device performance. Polymer HTMs are also noted for their capacity to be chemically changed, enabling versatility in increasing device efficiency and longevity.

In general, the molecular structure of organic HTMs controls their electronic characteristics, including ionization potential and highest occupied molecular orbital (HOMO) levels. A good HTM must have a high-lying HOMO level to match the valence band (VB) of the perovskite layer and the work function of the anode, minimizing energy losses and recombination [87].

B. Inorganic HTMs

Inorganic HTMs have received interest due to their greater thermal stability and ability to operate as a protective barrier, sheltering the perovskite layer from environmental elements such as heat, light, moisture, and oxygen. However, their integration into PSCs has been hampered by issues in film formation and energy level alignment. Metal-Based and Non-Metal based HTMs are the two types of inorganic HTMs which are discussed in the following section. The energy level representation of some most common inorganic HTMs is presented in Fig. 12.

i) Metal-based inorganic HTMs

Metal-based HTMs, such as NiOx, CuSCN, CuI, and $CuCrO_2$, offer strong electrical conductivity, suitable energy levels, and effective hole extraction capabilities. These materials are particularly appealing due to their toughness and high-performance stability [79]. Despite these advantages, several metal-based HTMs suffer from limitations such as high processing temperatures and inadequate solubility, which might hinder large-scale manufacturing.

ii) Non-metal-based inorganic HTMs

Non-metal-based HTMs, including materials like MoOx, WOx, and

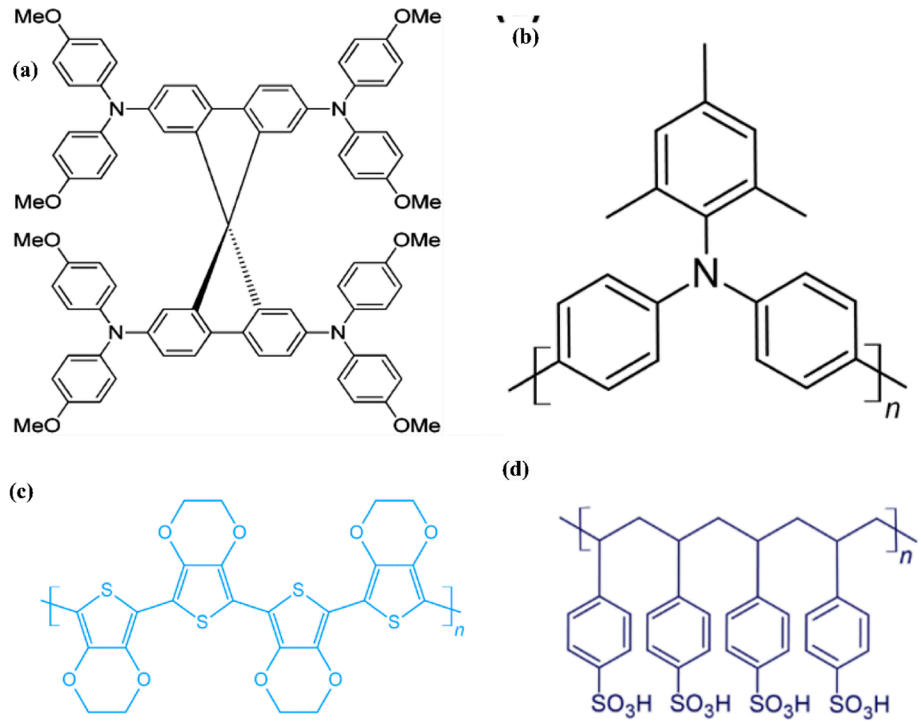

Fig. 11. Molecular structure of some most common organic HTMs. (a) Spiro-OMeTAD, (b) PTAA, (c) PEDOT, (d) PSS. (a) Adapted from reference [85] under creative common license CC BY-NC 3.0, whereas (b), (c), and (d) are adapted from reference [86] under creative common license CC BY.

V_2Ox, present an alternative to metal-based compounds. These chemicals often offer lower optical absorbance and better solubility, making them easier to process. However, non-metal HTMs may display inferior hole mobility and larger trap densities, which can negatively affect the device performance [59].

C. Carbon-based HTMs

Carbon-based materials have attracted interest as HTMs because to their strong electrical conductivity, broad surface area, and good compatibility with the perovskite layer [89]. These materials are commonly employed in three forms: carbon black, graphene, and carbon nanotubes (CNTs). Table 4 summarizes the main discussion about these three forms of carbon-based HTMs.

7.1.2.2. Energy levels and hole mobility. To optimize the performance of PSCs, inorganic HTMs must align their energy levels with those of the perovskite layer and the anode. A high ionization potential and a well-matched valence band maximum (VBM) are necessary to reduce recombination losses [92]. In addition, increased hole mobility is important for efficient charge transport and extraction, hence boosting the fill factor (FF) and short-circuit current of the solar cells. Improving the resilience of inorganic HTMs to environmental deterioration remains an important focus of continuing study.

7.1.2.3. Film morphology and stability. The shape of HTMs plays a vital role in defining the overall stability and performance of PSCs. A compact and homogeneous film is important to promote efficient charge transmission and minimize recombination losses. For inorganic and carbon-based HTMs, establishing a smooth, dense layer on the perovskite surface can boost the contact quality between the layers, further improving device longevity and stability [93]. Developing successful HTMs remains a problem due to the necessity for a compromise between high hole mobility, stability, and energy level alignment. Organic HTMs, while straightforward to process, often confront difficulties relating to heat and chemical deterioration. Inorganic and carbon-based HTMs, on

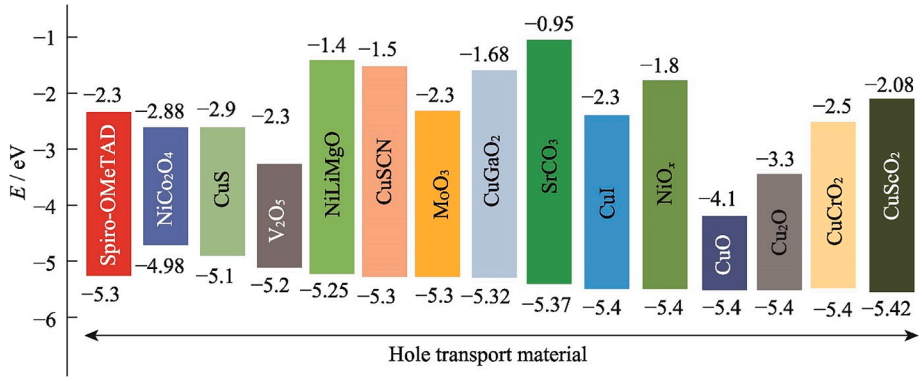

Fig. 12. Energy level representation of some most common inorganic HTMs used in PSCs. Adapted from reference [88].

Table 4
Description of various carbon based HTMs used in PSCs.

Carbon-based HTMs	Description
Carbon Black	Carbon black is formed of nanometer-sized graphite particles, offering strong conductivity and a huge surface area. Despite these advantages, carbon black suffers from obstacles such as poor film formation and strong optical absorption, which can restrict its efficacy as an HTM [90].
Graphene	Graphene, a two-dimensional sheet of sp^2-hybridized carbon atoms organised in a honeycomb lattice, is widely coveted for its exceptional hole mobility, transparency, and mechanical stability [91]. However, the exorbitant cost of graphene and its high sheet resistance remain impediments to its broad implementation.
Carbon Nanotubes (CNTs)	CNTs, which are cylindrical graphene structures, feature great electrical conductivity, transparency, and flexibility. Like graphene, CNTs confront hurdles in terms of cost and solubility, which limit their application in commercial-scale PSCs [91]. Improving the solubility and sheet resistance of these materials through chemical modification and hybridization processes is an ongoing topic of research.

the other hand, offer higher stability but suffer from high processing costs, poor solubility, and film forming problems. A crucial answer in enhancing HTM performance is the use of interfacial engineering [69]. Techniques such as the deposition of ultrathin compact layers (e.g., Al_2O_3) have been demonstrated to boost stability and minimise series resistance, hence increasing the power conversion efficiency (PCE) of PSCs.

7.1.3. Self-assembled monolayers (SAMs)

SAMs have become a crucial invention in PSCs, particularly as CTLs. Their exact molecular arrangement offers distinct advantages, including dopant-free operation, surface energy modulation, and increased stability. SAMs, serving as dopant-free hole-selective contacts, present a streamlined approach compared to conventional HTLs. It attained a PCE of up to 17.8 % [93]. These SAMs contributed to perovskite nucleation control and surface passivation, both of which are crucial for device efficiency and lifetime. Table 5 summarizes the major discussion about the main types of SAMs used in PSCs. SAMs offer regulated molecule architectures that allow fine-tuning of surface energy and interface characteristics, increasing charge transport. They can be applied using multiple deposition methods, including solution-based processes and vacuum techniques, making them amenable to different device architectures [94]. SAMs have greatly enhanced device lifetime, making PSCs more trustworthy for long-term applications.

7.2. Transparent electrodes (front electrodes)

Transparent conductive oxides (TCOs) such as indium tin oxide (ITO) and fluorine-doped tin oxide (FTO) are frequently employed as bottom electrodes in PSCs [98]. Their balanced combination of transparency and conductivity makes them important to the efficiency and functionality of these devices.

7.2.1. ITO vs. FTO

ITO is a versatile transparent conductor with outstanding transparency and resistance control. It can be deposited via several processes on diverse substrates, offering a smoother surface and higher transparency compared to FTO [99]. However, ITO's conductivity considerably diminishes when subjected to high-temperature heat treatments, restricting its applicability in operations that need increased temperatures. ITO is often employed in inverted p-i-n or n-i-p planar PSCs with low-temperature-processed transport layers. FTO, on the other hand, demands greater deposition temperatures and the handling of toxic gases during manufacture. Despite this, FTO is more compatible with mesoporous PSCs and is a regularly utilized substrate in such arrangements [100].

Table 5
Description of various SAM used as CTL in PSCs.

Types of SAMs	Description
Carbazole-Based SAM–HTLs	Common SAM materials include 2PACz, MeO–2PACz, and Me–4PACz, which are applied via vacuum evaporation processes [95]. These SAMs either equalled or enhanced device performance, displaying superior perovskite wetting and coating uniformity on both flat and textured surfaces.
Phenothiazine-Based SAMs for p–i–n PSCs	A well-aligned energetic contact between the SAM and perovskite absorber decreases charge recombination losses. It has yielded a high PCE of up to 22.44 %, exhibiting exceptional stability over long-term operation [96].
MeO–2PACz SAM with NiOx Layer	This SAM enhanced layer coverage, optimized energy-level alignment, and led to defect passivation. it produced nearly 22 % PCE with a fill factor (FF) of 83.9 %. The cell preserved 82 % of its initial efficiency after 800 h in ambient air [97].
NiOx:Cu + SAM in Tandem PSCs	It achieved a PCE of 23.4 %, a high open-circuit voltage (V_{OC}) of 1.72 V, and a 71 % FF in tandem devices integrating copper indium gallium selenide (CIGSe) and perovskite [97].

7.2.2. Alternative transparent conductors

Due to the brittleness, high costs, and production constraints associated with standard TCO electrodes, research has expanded into finding low-cost and flexible alternatives. These include:

i) **Cd_2SnO_4 TCO substrate:** This substrate offers greater electrical conductivity, enhanced optical transmission throughout the visible spectrum, and decreased surface roughness compared to FTO. Its performance has been proved with a greater power conversion efficiency (PCE) of 15.58 % [101].
ii) **Silver nanowire (AgNW) composite electrode:** Developed using an antioxidant-acid-modified chitosan polymer via a low-temperature solution process, this electrode exhibits a PCE of 7.9 % and offers remarkable long-term stability, highlighting its potential for sustainable and low-cost PSC manufacturing [102].
iii) **1D-2D AgNWs-graphene (AgNWs-G) transparent electrode:** This transparent electrode combines silver nanowires with graphene, achieving high transmittance (~86 %) and superior stability under air exposure, high temperatures, and continuous illumination. It has demonstrated a PCE of 15.31 %, making it a strong candidate for replacing traditional TCOs [102].
iv) **Biodegradable bamboo-derived transparent conductive electrode:** This eco-friendly electrode is extremely flexible and lightweight, achieving a PCE of 11.68 % for biomass-based PSCs. Notably, it maintained over 70 % of its original efficiency after 1000 bending cycles, making it an excellent choice for applications in flexible solar cells [103].

7.3. Metal electrode (back electrode)

The high cost and scarcity of noble metals like gold (Au) and silver (Ag) have driven research into lower-cost alternatives such as aluminum (Al), copper (Cu), nickel (Ni), molybdenum (Mo), and tungsten (W). These metals have been explored as rear electrode materials in perovskite solar cells (PSCs), aiming to maintain high efficiency while significantly reducing production costs.

i) **Aluminum (Al):** Aluminum offers high electrical conductivity at a very low cost. It is particularly suitable for inverted PSC structures due to its lower work function, making it compatible with electron transport layers. Early studies reported a PCE of 11.5 % on rigid substrates and 9.2 % on flexible substrates [98]. Subsequent improvements in film quality and carrier mobility led to an increased PCE of 17.1 %, with a fill factor (FF) of 0.80. The

addition of a polystyrene tunneling layer further enhanced the PCE to 20.3 %, along with stable performance under humid conditions [104].

ii) **Copper (Cu):** Copper is abundant, inexpensive, and offers good electrical conductivity and oxidation resistance. It is commercially available in the form of inks and pastes, making it ideal for scalable fabrication processes. Copper electrodes have shown excellent stability, with no significant Cu diffusion observed under mild thermal aging. PSCs with Cu electrodes retained their performance with minimal PCE loss over 20–30 days in environments with varying humidity levels [105].

iii) **Nickel (Ni):** Nickel's work function is well-matched with PSCs, and it is an economical option for electrode material. Sputtering-coated Ni films have achieved a PCE of 10.4 %, comparable to devices using Au electrodes [106]. Printable mesoporous Ni films exhibited a PCE of 13.6 % and demonstrated the potential for reuse with minimal performance degradation. Semi-transparent Ni-based electrodes have also been developed, achieving a PCE of 15.5 %, which is close to the 16.7 % PCE observed with Au-based electrodes [107].

iv) **Molybdenum (Mo) and Tungsten (W):** These metals are being investigated for their potential as low-cost, non-precious metal back electrodes in PSCs. Magnetron-sputtered Mo and W films have shown promise as replacements for Ag films, offering good performance at a fraction of the cost [108].

7.4. Carbon electrodes for PSCs

Carbon-based materials have gained significant attention in PSCs due to their tunability, abundant availability, low cost, and exceptional properties such as high electrical conductivity, chemical stability, and carrier mobility [98]. Unlike traditional organic HTMs and metal electrodes, which can compromise the stability of PSCs, carbon electrodes offer greater chemical resistance to halides and are moisture-tolerant, leading to improved device longevity [117]. Carbon materials are less expensive and more stable compared to conventional metal electrodes (such as gold and silver), making them attractive for large-scale, cost-sensitive applications. Carbon electrodes are generally classified into three main categories: conductive graphite/carbon black, graphene, and carbon nanotubes (CNTs). Grancini et al. Developed HTM-free perovskite solar modules (10 × 10 cm^2) using an industrial-scale, fully printable process [109]. The modules, based on a 2D/3D perovskite junction and a hydrophobic carbon black/graphite composite electrode, achieved an efficiency of 11.2 %. These modules demonstrated remarkable stability, lasting for 410,000 h without performance degradation under controlled environmental conditions. Barichello et al., reported a fully printable carbon-based PSC (C-PSC) incorporating a homemade mesoporous alumina (Al_2O_3) insulating layer and a graphite/carbon black electrode [110]. By employing a water pre-treatment step, the average V_{OC} was enhanced by 7 %, and the average power conversion efficiency (PCE) improved by 16 %, resulting in a maximum PCE of 12.3 %.

8. Fabrication methods for PSCs

PSCs have garnered significant attention due to their remarkable PCEs and relatively low manufacturing costs. The fabrication of PSCs involves various deposition techniques to form high-quality perovskite layers. These techniques can be broadly divided into solution-based methods and vapor-based methods, each offering distinct advantages and challenges while some other techniques like sol–gel method, electrodeposition and laser ablation are also employed for efficient and cost-effective manufacturing of PSCs. The choice of technique influences the morphology, crystallinity, and uniformity of the perovskite film, which directly impacts the efficiency, stability, and scalability of PSCs. The classification of various types of fabrication techniques for PSCs is depicted in Fig. 13.

8.1. Solution-based deposition techniques

Solution-processed methods have garnered significant attention due to their low cost, simplicity, and potential for scaling up. Among the various deposition technique some are popular and commonly known as spin coating, doctor blading, screen printing, slot-die coating, spray coating, and inkjet printing [111]. The various solution-based deposition techniques are illustrated in Fig. 14.

8.1.1. Spin coating

Spin coating is the most widely used deposition technique for small-area PSCs in lab-scale research. This method involves depositing a precursor solution onto a substrate, which is then rotated at high speed to spread the solution uniformly across the surface [101]. After spin coating, films are typically baked to produce a well-crystallized perovskite layer, enhancing adhesion and bonding between metal cations and halogen anions. Film thickness and quality can be optimized by adjusting spin speed, acceleration, and spin coating time. There are chiefly two techniques by which spin coating can be performed: One-step spin coating: A single precursor solution is used. A solution of lead halide (PbI_2) and methylammonium halide (MAI) is directly applied to the substrate and spun to form the perovskite layer. After deposition, the film undergoes thermal annealing to form a crystalline perovskite layer. Uniformity control is difficult, often resulting in inhomogeneous films with pinholes or large grain boundaries, limiting the PCE [108]. Two-step spin coating: In this process, PbI_2 is first spin-coated, followed by the deposition of an organic halide (e.g., MAI). This process offers more control over the film morphology compared to the one-step method. The difficulty lies in fully converting PbI_2 to the perovskite phase. Sometimes unreacted PbI_2 remains, impacting the film quality and device performance [101]. PSCs fabricated via spin coating have achieved efficiencies over 22 %, though this technique is limited in its scalability due to material wastage, the requirement for high precision, and low throughput.

8.1.2. Doctor blading

Doctor blading, also known as blade coating, is a scalable technique ideal for large-area film deposition. The method involves spreading the precursor solution onto the substrate using a blade. Only a small amount of solution is required to cover large areas, with minimal wastage. This technique is suitable for roll-to-roll production, making it a promising method for industrial-scale PSC fabrication [112]. Yang et al. demonstrated that adding additives like 1,8-diiodooctane (DIO) improves the uniformity and grain size of perovskite films. The introduction of ambient blade coating further optimized film crystallinity and PCEs [113]. Although doctor blading offers advantages for large-area PSC production, controlling film uniformity, especially over large substrates, remains a challenge.

8.1.3. Screen printing

Screen printing is a well-established film deposition technique frequently utilized in large-scale manufacturing, including in the production of PSCs. The process involves transferring a paste (or ink) through a mesh screen onto a flat substrate. The open mesh apertures determine the printed pattern, while areas that should remain unprinted are blocked by a stencil. A squeegee is used to push the paste through the mesh and deposit it onto the substrate, forming the desired film. This method is particularly attractive for large-scale PSC production due to its simplicity, low cost, and compatibility with continuous processes. It offers a scalable solution for manufacturing perovskite layers, electrode components, and other device layers in PSC modules. One of the most significant advancements in screen printing for PSCs is the development of fabricated large scale (A4 size) modules using commercially available screen printable pastes and only 1.6 mL of perovskite solution per

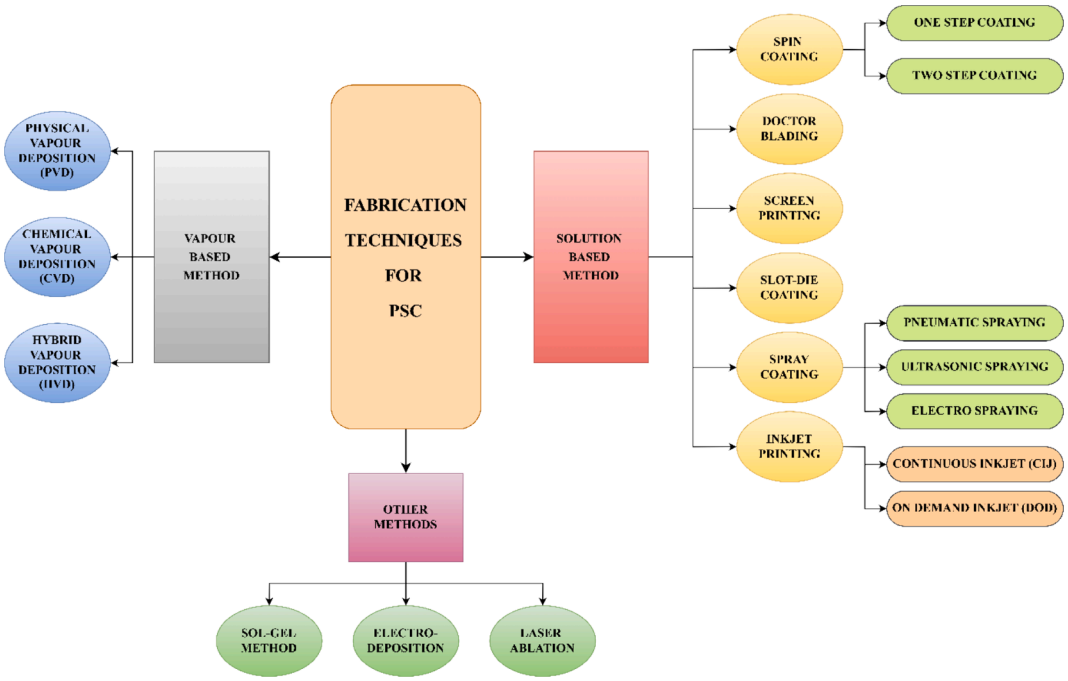

Fig. 13. Classification of different fabrication methods for PSCs.

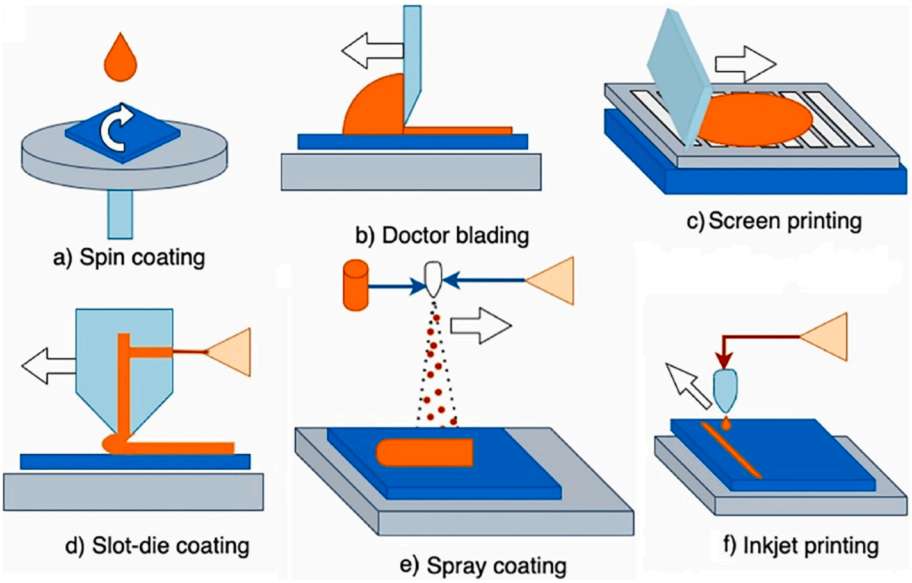

Fig. 14. Different solution based techniques. Adapted from reference [111] under the creative common license CC BY.

module. Patterning the TiO_2 blocking layer (BL) improved both Voc and FF due to reduced contact resistance. The best module with patterned BL achieved a PCE of 6.6 % (6.3 % stabilized) after two months of production, with no deterioration observed after hundreds of hours at 70 % RH [114].

8.1.4. *Slot-die coating*

Slot-die coating, a roll-to-roll compatible method, allows for continuous film deposition. It involves feeding the precursor solution through a narrow gap to create uniform films. The precursor solution is isolated within the system, reducing contamination. It is suitable for large-scale production [115]. This technique allows for fine-tuning of film thickness and uniformity by adjusting solution concentration and flow rates. Hwang et al. reported a two-step slot-die coating method where the drying process was optimized using high-pressure nitrogen, producing uniform films and achieving a PCE of 11.96 % [116]. Further work by Di Giacomo et al. showed PSC modules with an active area of 12.5×13.5 cm^2 and achieved an impressive PCE of 16.4 %, comparable to spin coating [117]. Controlling solvent evaporation and film crystallization during the coating process remains critical to ensure high-quality films.

8.1.5. *Spray coating*

Spray coating is an efficient technique for producing large-area perovskite films. A precursor solution is atomized into small droplets and sprayed onto a heated substrate. Suitable for mass production due to its high throughput and reproducibility. This method is simple and can produce films over large areas with minimal material wastage. Spray

equipment typically consists of three main parts: an atomizing nozzle, an injection pumping system, and a heating plate. Depending on the nozzle's operating mode, spray equipment can be classified into: pneumatic spraying, ultrasonic spraying, electro spraying [74]. Barrows et al. were among the first to apply spray coating for PSCs, achieving a PCE of 11.1 % [118]. They showed that substrate temperature plays a critical role in determining the film morphology and crystallinity. Heo et al. introduced a two-step spray coating method and improved film quality by using γ-Butyrolactone (γ-GBL) as an additive, achieving a PCE of 18.3 % [119]. Controlling the spray parameters such as flow rate, nozzle distance, and crystallization conditions is crucial for producing high-quality films.

8.1.6. Inkjet printing

Inkjet printing is a non-contact, digital printing method that allows for precise deposition of perovskite precursors onto the substrate. It uses very little precursor material, with minimal wastage. Specific patterns can be printed directly, reducing the need for masks or additional patterning steps. Wei et al. used inkjet printing for PSC fabrication, showing that adding carbon to the precursor solution can enhance the mechanical stability and lifetime of PSCs [120]. Li et al. demonstrated the effects of printing table temperature on film morphology, improving the quality of the inkjet-printed PSCs [121]. Controlling droplet formation and coalescence to produce uniform films with consistent thickness remains a key challenge. Inkjet printing can be divided into two categories based on the solution delivery method: Continuous Inkjet (CIJ) and On-Demand Inkjet (DOD). DOD is widely used for printing electronic and optoelectronic materials, such as metal nanoparticles, polymers, and PSCs [122]. It is reliable and cost-effective.

8.2. Vapor based deposition techniques

Various deposition techniques have been employed to fabricate the active perovskite layer, each have their unique advantages and challenges. Physical vapor deposition (PVD), chemical vapor deposition (CVD), and hybrid vapor deposition are the most common film deposition techniques used in PSC fabrication.

8.2.1. Physical vapor deposition (PVD)

PVD is a versatile technique that involves the physical removal of individual atoms or small clusters from a solid or liquid source, which are then deposited as a thin film on a solid substrate (Fig. 15). Common PVD techniques include evaporation, laser ablation, vacuum arc deposition, and sputtering [123]. PVD operates in an evacuated chamber, where material is vaporized from a source and condensed onto a substrate, forming a thin film. The study conducted by Liu et al. pioneered the fabrication of perovskite films using PVD [124]. The scientists adopted a dual-source co-evaporation approach, utilizing methylammonium iodide (MAI) as the organic source and lead chloride ($PbCl_2$) as the inorganic source to manufacture $MAPbI_{3-x}Cl_x$ perovskite films. X-ray diffraction (XRD) research indicated that the resultant films had an orthorhombic crystal structure, identical to films generated via spin coating. However, PVD-produced films were denser and more uniform, achieving a PCE of 15.4 %. Ono et al. focused on large-area (5 × 5 cm^2) semi-transparent perovskite films manufactured using PVD [125]. The procedure allows the deposition of ultra-thin perovskite layers (~50 nm), which is problematic with spin-coating technologies. These thin films obtained a PCE of 9.9 %, illustrating the promise of PVD for large-scale commercial applications in PSC technology.

8.2.2. Chemical vapor deposition (CVD)

CVD is commonly use for producing thin films of semiconducting materials, including perovskites (Fig. 16). In CVD, vapor-phase precursors are delivered into a reaction chamber, where they undergo a chemical reaction to generate a solid coating on the substrate. The process often requires the evaporation of reactants, which are delivered into the reactor by gas flow [127]. The reactants undergo surface diffusion, nucleation, and chemical reactions on the substrate to form a thin film, while any unreacted material is removed from the chamber. Fan et al., disclosed a one-step CVD approach for depositing $MAPbI_3$ and $MAPbI_{3-x}Cl_x$ perovskites [128]. Inorganic precursors (PbI_2 or $PbCl_2$) and organic precursors (MAI) were placed in distinct temperature zones according to their sublimation temperatures. A carrier gas, often argon, assisted the chemical reaction. The resultant films exhibited large grain sizes (>1 μm) and long carrier lifetimes, achieving PCEs in the range of 9–11 %. This work proved the potential of CVD for manufacturing high-quality films with controlled grain growth.

8.2.3. PVD vs CVD

PVD differs greatly from CVD in terms of its source material and operating circumstances. While PVD relies on solid or liquid sources, CVD utilizes gaseous precursors. Additionally, PVD operations occur at substantially lower vapor pressures compared to the normally greater working pressures observed in CVD systems.

8.2.4. Hybrid vapor deposition

Hybrid vapor deposition is a two-step process created to overcome the limitations of both PVD and CVD. It involves the sequential deposition of a lead halide precursor, followed by a reaction with an organic halide vapor to generate the perovskite film. This approach provides for

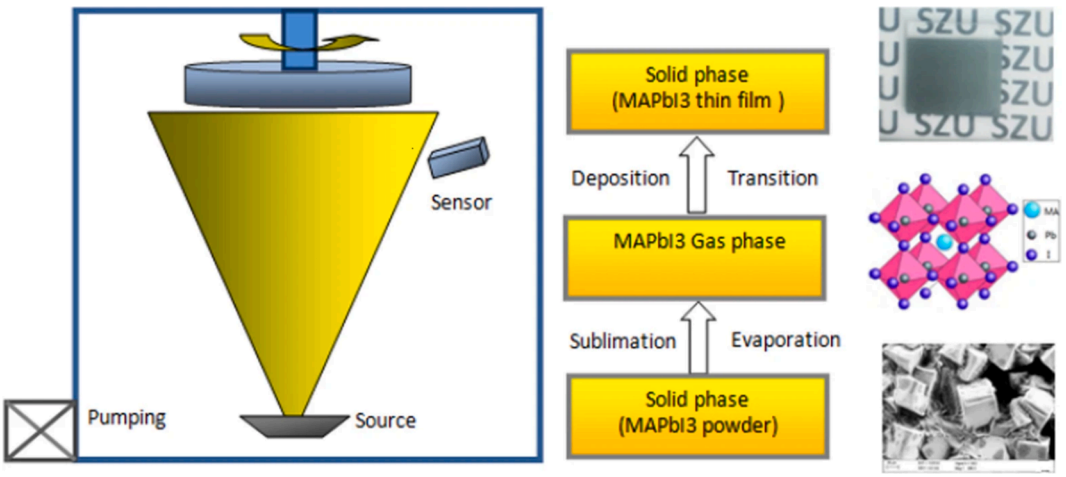

Fig. 15. Single-source physical vapour-deposition process of the perovskite MAPbI3 thin film. Adapted from reference [126] under the creative common license CC BY 4.0.

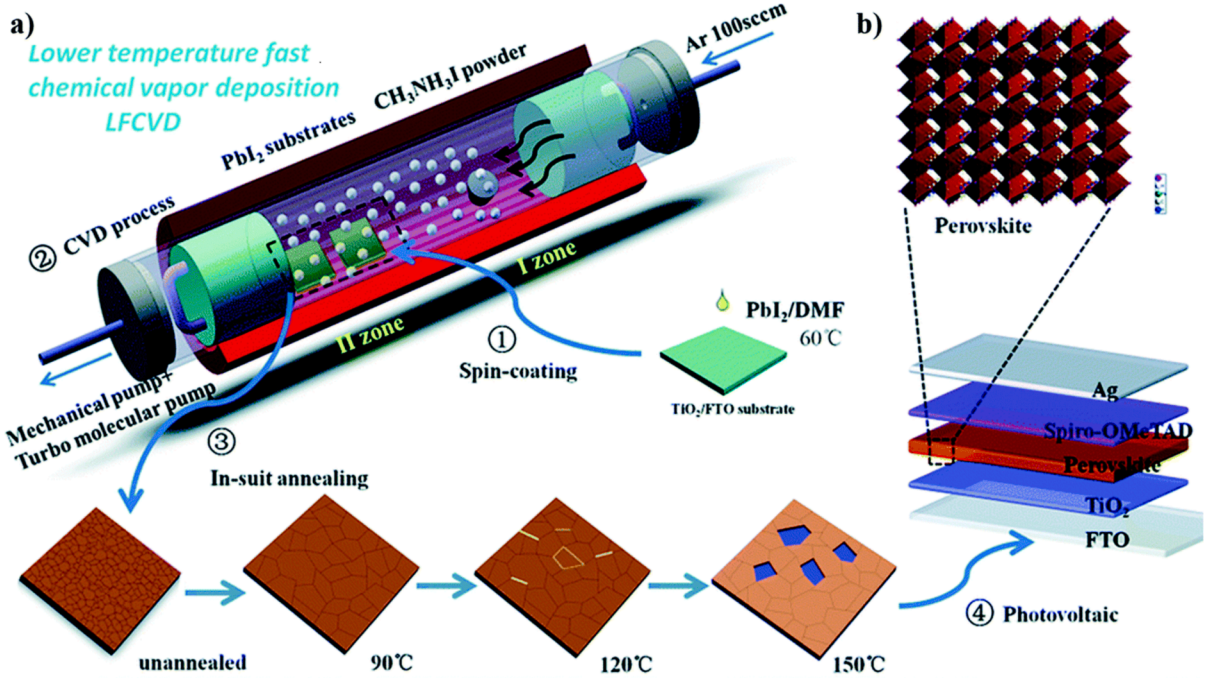

Fig. 16. Chemical vapour deposition process for perovskite solar cell. Adapted from reference [129] under the creative common license CC BY 3.0.

fine control over film composition and morphology, enabling enhanced surface coverage and film homogeneity. Yokoyama et al., this study reveals and demonstrates the advantages of kinetically regulated gas–solid interactions in synthesising $CH_3NH_3SnI_3$ perovskite sheets utilising a low-temperature vapor-assisted solution technique [130]. The films demonstrated great surface coverage and prevented short-circuit behavior frequently seen in conventional one-step methods. Although hybrid vapor deposition has been researched extensively for methylammonium lead iodide ($MAPbI_3$) films, research on inorganic perovskite materials like $CsPbBr_3$ remains limited.

A. Process overview

Stage 1: A lead halide layer (e.g., PbI_2, $PbCl_2$, or $PbBr_2$) is deposited using thermal evaporation or another vapor-based approach.

Stage 2: The lead halide film combines with an organic halide vapor in a controlled environment, generating the perovskite layer. This procedure can be carried out in a tube furnace under regulated pressure and temperature.

8.3. Other fabrication methods for PSCs

8.3.1. Sol-gel method

The sol–gel method is a bottom-up synthesis technique used to produce a wide range of materials, including inorganic membranes, monolithic glasses, ceramics, thin films, and ultra-fine powders. It involves producing a homogeneous sol from precursors, transforming it into a gel, and then removing the solvent from the gel structure [131] (Fig. 17). The properties of the dried gel depend on the drying method used.

8.3.2. Electrodeposition

Electrodeposition is a versatile, roll-to-roll compatible technique for manufacturing PSCs. It is cost-effective, rapid, and produces highly uniform thin films without the need for substrate heating, which can cause film rupture and island formation [133] (Fig. 18).

8.3.3. Laser ablation

Laser ablation is a subtractive method that fabricates micropatterns by removing a small fraction of substrate material using a focused pulsed laser beam [135] (Fig. 19).

9. Band gap tuning in PSCs

PSCs have showed amazing growth in recent years, driven mostly by their tunable optical and electrical features, particularly the band gap. Band gap tuning is an important parameter for maximising the efficiency of PSCs, as it effects the absorption range and eventually determines the PCE of the device [137]. In particular, effective band gap tuning plays a significant role in generating high-efficiency single-junction and tandem solar cells, where several perovskite layers absorb light throughout a broad spectrum [54]. The efficiency of a solar cell is strongly connected to the material's band gap, which regulates the fraction of the solar spectrum that can be absorbed and converted into electrical energy. The optimal band gap for increasing the efficiency of a single-junction PSC falls in the range of 1.48–1.62 eV [84]. Within this range, perovskite materials demonstrate excellent absorption of sunlight, leading to high PCEs. To further boost efficiency, especially in tandem solar cells, materials with narrower or wider band gaps are necessary to absorb light from different portions of the solar spectrum. Thus, band gap engineering becomes a vital tool in widening the range of light absorption and boosting overall device performance. Several famous instances highlight the usefulness of different band gap tuning strategies, as outlined below [138,139]:

$CsPbI_3$: A cubic 3D perovskite having a band gap of 1.73 eV. While this material is highly efficient, it suffers from thermal instability at ambient temperature [140].

$MAPbI_3$: A commonly used tetragonal perovskite having a band gap of 1.55 eV. This material has been thoroughly examined for its balance of efficiency and stability [141].

$FAPbI_3$: A hexagonal perovskite having a band gap of 1.48 eV, which is lower than $MAPbI_3$ and suited for usage in tandem solar cells [141].

$MASnI_3$: By substituting lead with tin, this orthorhombic perovskite reaches a band gap of 1.30 eV, making it a suitable option for the bottom cell in tandem setups [142].

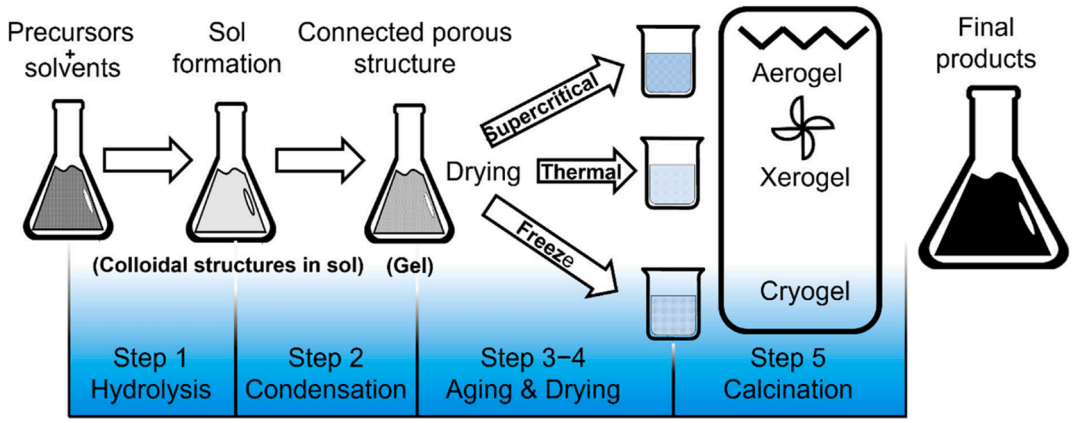

Fig. 17. Schematic representation of different steps involve in sol–gel method. Adapted from reference [132] under the creative common license CC BY.

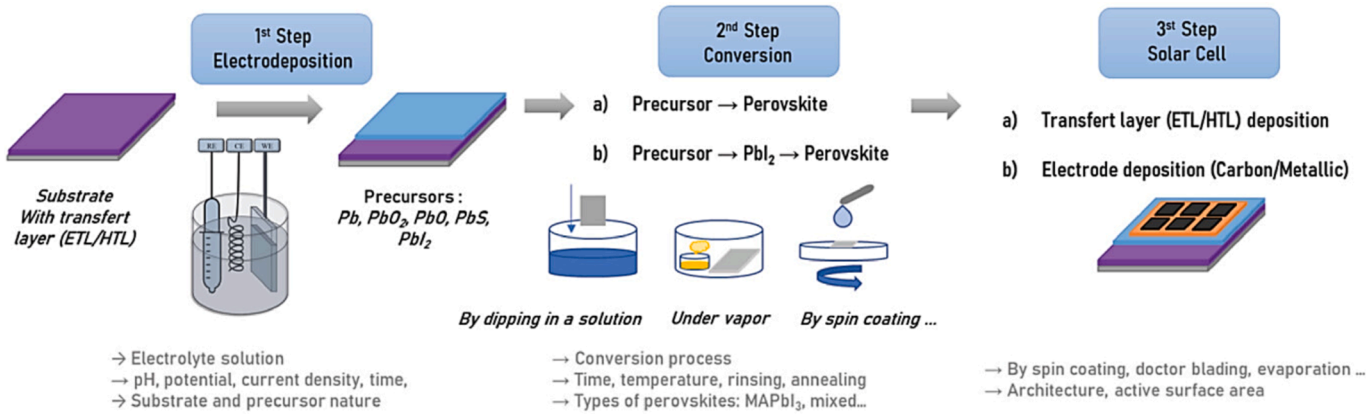

Fig. 18. Schematic representation of different steps involve in electrodeposition method. Adapted from reference [134] under the creative common license CC BY-NC-ND 4.0.

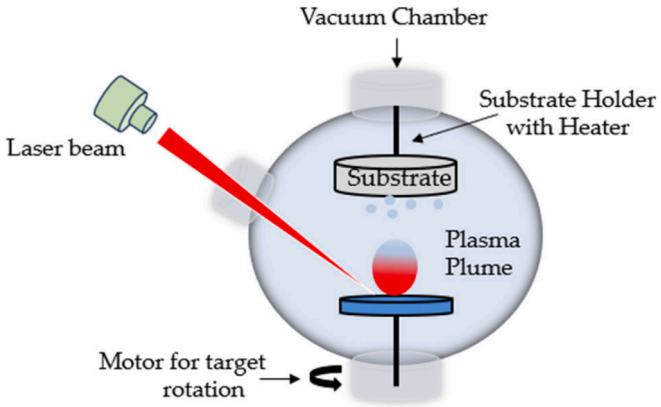

Fig. 19. Schematic representation of laser ablation method. Adapted from reference [136] under the creative common license CC BY 4.0.

9.1. *Tandem solar cells and band gap tuning*

Tandem solar cells are a potential architecture for breaking the Shockley-Queisser limit of single-junction solar cells, which imposes a theoretical maximum efficiency around 33 %. In tandem arrangements, two or more layers with distinct band gaps are layered to collect a greater range of the solar spectrum, hence enhancing total efficiency [143]. All-perovskite tandem solar cells, which combine layers of perovskite materials with variable band gaps, can be produced at low temperatures and are compatible with flexible, lightweight substrates. This makes them particularly appealing for commercial uses. For instance, a typical tandem structure would use a wide-band-gap perovskite (e.g., 1.7–1.8 eV) as the top cell to absorb high-energy photons and a narrow-band-gap material (e.g., ~1.2 eV) for the bottom cell to absorb lower-energy photons [144]. One of the more effective ways for constructing these tandem cells involves band gap adjustment of both the top and bottom perovskite layers, ensuring that each layer efficiently absorbs its own section of the solar spectrum [139].

9.2. *Challenges in band gap reduction*

While changing the perovskite band gap is a well-explored subject, reaching low band gaps (below 1.48 eV) offers substantial hurdles. Simple halide substitution, where iodide (I^-) is replaced with bromide (Br^-) or chloride (Cl^-) in the perovskite structure, cannot reduce the band gap below this threshold. To attain reduced band gaps, more advanced approaches, such as cation substitution, have been considered. For example, tin (Sn) substitution for lead (Pb) at the B-site of the perovskite structure has been found to successfully minimise the band gap. A major development in this area is the manufacture of tin–lead (Sn-Pb) perovskite absorbers, which can serve as the bottom cell in tandem solar cells [145]. These materials have band gaps in the range of 1.2–1.3 eV, making them perfect for absorbing the low-energy part of the solar spectrum. However, despite their potential, Sn-based perovskites suffer from stability difficulties, such as fast oxidation of Sn^{2+} to Sn^{4+}, leading to device deterioration [146].

9.3. Photostability issues and the Hoke effect

While band gap tuning using halide substitution can broaden the range accessible band gaps, this strategy brings problems relating to photostability. One of the most significant concerns is the Hoke effect, where a perovskite blend of halides (e.g., I^- and Br^-) tends to separate during continuous light exposure [147]. This segregation occurs in the creation of iodide-rich and bromide-rich domains, causing a reduction in the Voc and, subsequently, lower PCEs in PSCs. To counteract these consequences, alternate procedures for band gap tuning are needed, such as cation alloying or dimensionality control, which can reduce or eliminate halide segregation while keeping desirable optical characteristics [148].

9.4. Band gap tuning techniques

A variety of approaches have been developed to alter the band gap of perovskite materials. Each method offers a distinct way to manipulating the electrical structure and optical properties of the material, enabling fine-tuning of the band gap to match the requirements of different solar cell topologies [149]. The various band gap tuning strategies (Fig. 20) are detailed below.

i) Strain engineering

Mechanical strain can be applied to the perovskite lattice to alter its band structure. Strain engineering affects the interatomic distances, which can lead to variations in the band gap [148]. This approach is largely underexplored in PSCs but holds potential for fine-tuning the band gap without the requirement for chemical replacements.

ii) Cation alloying

Cation alloying includes swapping or mixing different A or B site cations within the perovskite structure to modify the band gap. For example, alloying the A-site with cesium (Cs), methylammonium (MA), or formamidinium (FA) leads in continuous or discontinuous alterations in the band gap. The band gap can be modified from 1.73 eV for $CsPbI_3$ to 1.55 eV for $MAPbI_3$ or 1.48 eV for $FAPbI_3$, allowing for customised absorption properties in PSCs [150].

iii) Halide mixing

Another typical way to band gap tuning is halide mixing, where halides such as iodide (I^-) and bromide (Br^-) are combined at the X-site of the perovskite structure. By altering the halide ratio, the band gap can be constantly controlled from 1.55 eV ($MAPbI_3$) to 2.30 eV ($MAPbBr_3$). This method is particularly effective for tuning the band gap of the top cell in tandem arrangements [151].

iv) Dimensionality control

Adjusting the dimensionality of the perovskite structure, such as shifting from 3D to 2D or quasi-2D, gives another option for band gap tailoring. Lower-dimensional perovskites frequently display bigger band gaps and better stability compared to their 3D counterparts [141]. These materials also demonstrate better resilience to environmental deterioration, making them desirable for long-term stability in PSCs.

10. Lead free PSCs

The amazing performance of lead-based PSCs in generating high PCEs has positioned them at the forefront of next-generation photovoltaic technology. However, the presence of poisonous lead in these devices creates major environmental and health problems. Lead's toxicity is well-documented, including detrimental effects on the brain system, kidneys, and reproductive organs [151]. Moreover, its inclination to leach into the environment creates issues of pollution and bioaccumulation, which could limit the large-scale commercialization and sustainable deployment of PSCs. Lead is also rather scarce and pricey, thus increasing concerns surrounding the long-term affordability and availability of Pb-based PSCs. As a result, the development of lead-free alternatives has become a major research emphasis to assure the safe and sustainable expansion of perovskite solar technology [152].

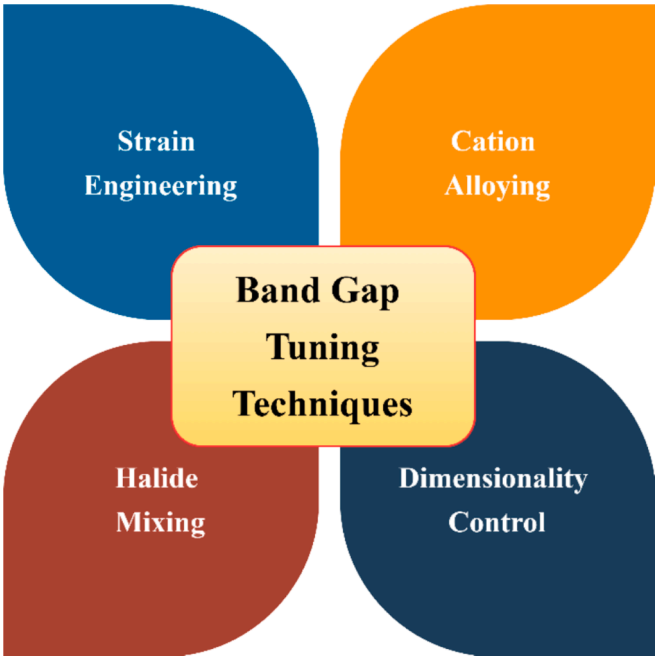

Fig. 20. Band gap tuning strategies.

10.1. Strategies for lead substitution in PSCs

To reduce the harmful consequences associated with lead, researchers have examined numerous ways for substituting lead (Fig. 21) with less toxic and more abundant elements. The goal is to preserve the beneficial optoelectronic features of PSCs while lowering their environmental impact. Several replacement procedures have been proposed, concentrating on substituting Pb with alternative cations, molecule complexes, or anions inside the perovskite crystal structure. The following strategies have showed promise in generating lead-free perovskites [153].

10.1.1. Metal cation substitution

Substituting Pb with other metal cations is the most direct technique for generating lead-free perovskites. Several metals have been examined, including tin (Sn), bismuth (Bi), and germanium (Ge). Each of these cations presents unique advantages and challenges in terms of electrical characteristics, stability, and environmental effect [151].

A. Tin (Sn)-based perovskites

Tin (Sn) is typically regarded the most promising alternative to lead due to its similar electrical arrangement and crystal structure. Tin-based perovskites, such as $MASnI_3$, have band gaps and absorption coefficients comparable to those of Pb-based perovskites, making them appropriate for solar applications. However, Sn-based perovskites confront substantial issues relating to stability. Sn^{2+} is very prone to oxidation, changing into Sn^{4+}, which significantly influences the charge carrier mobility and lifetime in the material. This leads to rapid device deterioration and poorer performance. To overcome these challenges,

Fig. 21. Strategies for lead (Pb) free PSCs.

researchers have developed numerous solutions, including the use of passivation agents, additives, and protective layers. Low-temperature processing has also been applied to lower the oxidation rate of Sn. The greatest recorded efficiency for Sn-based PSCs sits at 12.6 %, suggesting substantial development but still falling behind Pb-based counterparts [151].

B. Germanium (Ge)-based perovskites

Germanium (Ge) is another metal cation that has been examined as a lead alternative. Ge-based perovskites, such as $MAGeI_3$, tend to have bigger band gaps and lower absorption coefficients than Sn or Pb-based perovskites. As a result, these materials yield lower photocurrents and display poorer efficiency in solar systems. The best-performing Ge-based PSCs have reached efficiencies of up to 7.3 %, however these materials suffer limits in terms of both performance and stability. Their greater band gaps make them less effective in absorbing sunlight, which greatly limits their practical application in single-junction solar cells. Nevertheless, ongoing research into Ge-based perovskites attempts to improve both their efficiency and stability through materials engineering and device optimization [151].

C. Bismuth (Bi)-based perovskites

Bismuth (Bi) is considered a non-toxic and more stable alternative to lead. Bi-based perovskites, such as $Cs_3Bi_2I_9$, have shown potential stability and lower toxicity, making them environmentally favorable choices. However, the fundamental issue with Bi-based perovskites resides in their huge band gaps and low absorption coefficients. These features limit their efficiency as light-harvesting materials in single-junction PSCs, resulting in lower efficiencies[151,154]. Despite these limitations, Bi-based perovskites show potential in tandem solar cells, where they can serve as top cells with a broad band gap, complementing lower-band-gap bottom cells. The greatest recorded efficiency for Bi-based perovskites in tandem setups is 9.2 %. While this is smaller than that of Pb-based tandem cells, the promise of increased stability and lower environmental impact makes Bi-based perovskites an appealing area of research for future solar technology [155].

10.1.2. Substitution of metal clusters or molecular complexes

In addition to direct metal cation replacement, researchers have examined the use of molecular complexes and metal clusters as alternatives for Pb in the perovskite structure. These materials can bring novel optoelectronic characteristics, such as enhanced photostability and broader absorption spectra, and potentially increase stability, but they require further development to reach competitive efficiency levels compared to the conventional lead-based perovskites [154]. For instance, incorporating quadruple-decker Ru_6 molecular clusters into 2D Ruddlesden-Popper perovskite structures has demonstrated enhanced photostability and a broader absorption spectrum compared to their lead-based counterparts [155]. While these alternative molecular complexes offer promising avenues for lead-free PSCs, more research is needed to optimize their performance and address the challenges in terms of efficiency and stability.

10.1.3. Organic cation substitution

Organic cation substitution involves replacing lead cation in the perovskite structure with larger organic molecules. This change in the cation can significantly alter the crystal structure and electrical characteristics of the perovskite material. However, this method has shown limited success in PSCs due to the difficulties in maintaining high charge carrier mobility and efficient light absorption compared lead-based PSCs. The large organic cations can disrupt the optimal crystal packing and electronic characteristics, leading to lower photovoltaic performance [156]. As a result, more research is needed to further develop and optimize the organic cation-based PSCs to reach comparable efficiency levels.

10.1.4. Non-metal anion substitution

Another option involves the substitution of halide anions in the perovskite structure. This approach, although less prevalent than metal cation substitution, is still an active area of research. Researchers have been exploring different halide ions, such as fluoride, by incorporating them in the perovskite structure, as a mean of enhancing the stability and efficiency of PSCs. The goal is to improve the optoelectronic properties and reduce defects within the material [151]. However, the effectiveness of this approach has been shown to be variable and dependent on the particular perovskite composition and device architecture, demanding further investigation and optimization to fully realize its potential.

10.2. Challenges and future directions for lead-free PSCs

While lead-free perovskites offer a promising route toward safer and more sustainable solar technology, significant hurdles remain that must be overcome to bring these materials to commercial viability.

i) **Stability:** One of the most essential problems for lead-free perovskites is guaranteeing long-term stability under working conditions. Both Sn and Ge based perovskites suffer from oxidation, while Bi-based perovskites demonstrate restricted performance due to their structural and electrical features. Developing techniques to enhance the chemical and thermal stability of these materials is vital for their future success [157].
ii) **Efficiency**: Achieving PCEs comparable to or exceeding those of lead-based PSCs remains a significant hurdle. While substantial progress has been made, the efficiencies of lead-free perovskites are still far below the record efficiencies of Pb-based devices (exceeding 25 %). New materials and device architectures are needed to boost the efficiency of lead-free PSCs while maintaining their environmental and health benefits [158].
iii) **Scalability:** For lead-free perovskites to gain widespread adoption, scalable and cost-effective manufacturing processes must be developed. Many of the promising lead-free materials, such as Sn-based perovskites, require precise control over processing

conditions to prevent oxidation and ensure high performance. Scaling up these processes without compromising quality is a major challenge for the field.

iv) **Environmental impact:** While lead-free perovskites reduce the immediate environmental hazards associated with Pb, other materials, such as Sn, also pose environmental challenges. It is crucial to assess the full life cycle of lead-free perovskites, including material extraction, production, and disposal, to minimize their overall environmental footprint [159].

11. Efficiency controlling factors for PSCs

The efficiency of PSCs depends on the careful optimization of both material properties and device architecture. There are various factors on which efficiency of PSCs depends (Fig. 22) which are discussed in the following sections of this review paper.

11.1. Material properties and optoelectronic characteristics

One of the most essential aspects in determining the effectiveness of PSCs is the optoelectronic properties of the materials employed in various layers of the device, particularly the perovskite absorber layer. Theoretical techniques such as density functional theory (DFT) are crucial tools in researching the optoelectronic properties of perovskite materials [160]. DFT enables researchers to examine the electronic band structure, defect formation energetics, and the impact of various defects on the overall electronic behavior of PSCs. By offering insights into defect energetics and the distribution of electronic states, DFT can forecast the formation energy of defects and their influence on charge carrier mobility. This allows researchers to anticipate recombination dynamics and create techniques to limit recombination losses caused by trap states. DFT, along with molecular dynamics research, provides significant insights into the structural and compositional stability of perovskite materials [161]. These theoretical studies guide the selection of materials and production procedures, ensuring that the perovskite layers preserve their structural integrity and electronic properties throughout time, which is crucial for the long-term stability of PSCs.

11.1.1. Defects and impurities

The presence of defects and impurities considerably impacts the light absorption characteristics and charge carrier dynamics within PSCs. Defects, particularly in the form of vacancies or interstitials, introduce trap states that may contribute to recombination losses and a drop in device efficiency [161].

11.1.2. Energy bandgap

The energy bandgap of perovskite materials plays a vital role in determining their light-harvesting capabilities. By utilising chemical engineering approaches and compositional adjustments, researchers may tailor the bandgap of perovskites between 1.5 eV and 2.3 eV. This tunability allows adjustment of PSC performance by matching the absorption properties with the solar spectrum, enhancing the generation of photocurrent [162].

11.1.3. Carrier properties

Ideal perovskite absorbers feature low effective mass, strong charge carrier mobility, long diffusion lengths, and outstanding absorption coefficients. These qualities are critical for effective charge generation and transmission, resulting to better photovoltaic performance. High-quality perovskites should also feature a direct and optimized bandgap, perfectly suited for solar energy conversion [163].

11.2. Carrier transport and extraction in PSCs

Optimizing charge carrier transit and extraction is crucial for boosting PSC performance. Several critical parameters and strategies are involved in establishing effective carrier dynamics:

11.2.1. Carrier diffusion coefficient

The diffusion coefficient of carriers, which determines how quickly electrons and holes can flow through the perovskite layer, is a significant metric. Various experimental techniques, such as terahertz (THz) frequency measurements and the Hall effect, are employed to estimate diffusion coefficients in perovskites. For common lead-based PSCs, diffusion coefficients range between 0.01 and 4 cm^2/s [164].

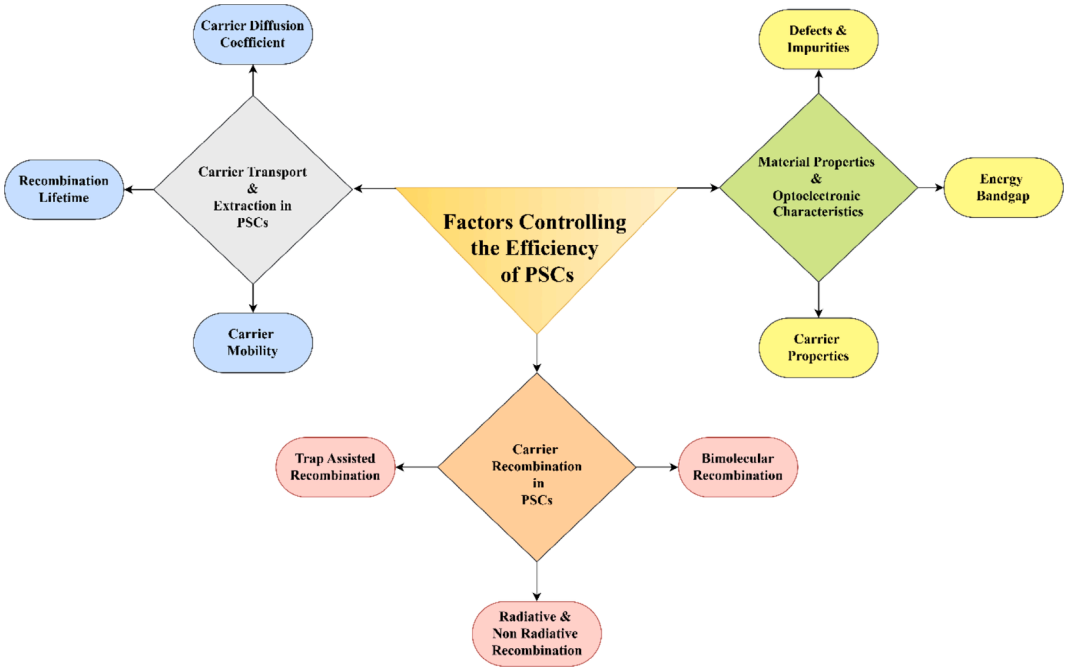

Fig. 22. Efficiency controlling factors for PSCs.

11.2.2. Recombination lifetime

The recombination lifespan is the average duration an electron-hole pair exists before recombining. Longer recombination lifetimes result into higher carrier diffusion lengths and overall better device performance. Efforts to prolong recombination lifetimes frequently involve passivation of surface and bulk defects, which operate as recombination centers [165].

11.2.3. Carrier mobility

The mobility of charge carrier directly effects the effectiveness of charge extraction in PSCs. Measurement techniques, including THz frequency approaches and space-charge-limited current (SCLC) techniques, are used to analyse electron and hole mobilities in perovskite materials. In high-quality lead-based perovskites, electron mobilities range from 1500 to 3100 $cm^2/V{\cdot}s$, whereas hole mobilities range from 500 to 800 $cm^2/V{\cdot}s$. Tin-based perovskites display comparable mobility values [163].

11.3. Carrier recombination in PSCs

Recombination is a primary loss mechanism in PSCs and severely impacts their efficiency. Understanding the various forms of recombination their dynamics and their impact on PSC efficiency demands advanced experimental and theoretical methodologies. Transient optoelectronic techniques, such as transient photovoltage and photoconductivity measurements, are utilised to analyse charge accumulation and recombination within the perovskite layer [51]. These methods provide real-time insights into the carrier dynamics and are critical for discovering recombination channels and optimizing device performance. Drift–diffusion models and transfer matrix approaches are commonly utilised to model the electrical and optical behavior of PSCs [166]. These theoretical models offer detailed insights into charge carrier transport and recombination processes, guiding the design of perovskite materials and device topologies for maximum performance.

11.3.1. Radiative recombination

Radiative recombination, however occurring, has a relatively minimal impact in the efficiency loss of PSCs. This process occurs when an electron and hole recombine, generating a photon. It is regarded a desirable kind of recombination in PSCs, as it shows acceptable material quality and minimum fault activity [51].

11.3.2. Non-radiative recombination

Non-radiative recombination, notably trap-assisted recombination, is the primary loss mechanism in PSCs. Deep trap states, frequently resulting from faults or impurities, enable non-radiative recombination, leading to large voltage and efficiency losses. In particular, Shockley–Read–Hall (SRH) recombination is one of the most prominent non-radiative processes [51].

11.3.3. Trap-assisted recombination

Trap-assisted recombination happens when charge carriers are trapped by trap states before they recombine. Shallow trap sites may allow for reversible charge trapping, while deep trap sites lead to irreversible trapping and enhanced recombination [166]. This mechanism is a key contributor to efficiency loss, particularly in PSCs with high defect density.

11.3.4. Bimolecular recombination

Bimolecular recombination happens when an electron and hole recombine without any intervening trap state. This mechanism is often observed at low energy and is often less prevalent than trap-assisted recombination. However, it can still affect the overall recombination dynamics and device efficiency, particularly in high-performance PSCs [163].

12. Challenges in attaining high efficiency in PSCs

Perovskite solar cells (PSCs) have drawn substantial attention due to their quick progress in achieving high power conversion efficiencies (PCE), reaching a record of greater than 25 % by 2023. However, various issues related to stability, material chemistry, processing processes, and device physics (Fig. 23) need to be overcome before PSCs may achieve full commercialization [167]. This analysis gives a complete overview of the problems impacting the efficiency and stability of PSCs and discusses the techniques being taken to address these hurdles.

12.1. Stability challenges

One of the biggest hurdles in commercializing PSCs is their intrinsic instability, which is impacted by environmental variables, material degradation, and device design.

12.1.1. Environmental sensitivity

Perovskite materials are particularly sensitive to humidity, temperature, and UV radiation. Exposure to these conditions can lead to structural breakdown, notably in organic–inorganic hybrid perovskites (OHPs), which are chemically unstable when exposed to moisture or oxygen. This degradation greatly affects the effectiveness and longevity of PSCs, rendering them unsuitable for long-term outdoor use [168].

12.1.2. Material degradation

In addition to environmental concerns, the perovskite structure itself is prone to internal breakdown over time. Weak hydrogen interaction between the A-site cation and the BX_6 octahedra makes these materials susceptible to thermal degradation at relatively low temperatures. As a result, perovskite-based solar cells tend to decay faster than typical silicon-based cells, providing a problem for maintaining efficiency over extended durations [169].

12.1.3. Structural stability

The stability of PSCs is also controlled by the structural features of perovskite materials. Specifically, the tolerance and octahedral factors of 3D ABX_3 perovskites can be used to determine their stability. However, hybrid perovskites present distinct issues due to the poor ionicity of massive iodide ions, making typical radius predictions less accurate [1]. Studies suggest that mixing low-dimensional perovskites with 3D perovskites boosts stability while maintaining high efficiency [170,171].

12.2. Defect structures and their impact on efficiency

Defects in perovskite materials significantly affect their efficiency by introducing nonradiative recombination centers that reduce the V_{OC} and fill factor of the cells [172]. Defects can be broadly categorized into intrinsic and extrinsic types.

12.2.1. Intrinsic defects

Intrinsic defects, such as vacancy, schottky, and frenkel defects, occur within the crystal lattice of the perovskite material. Delocalized defects, resulting from ion migration (e.g., the drift of I^- or Br^- ions), can also form, further impacting device performance [173].

12.2.2. Extrinsic defects

Extrinsic defects primarily occur at grain boundaries (GBs) and surfaces of polycrystalline films. These trap-state defects act as recombination centers, reducing the efficiency of charge carrier transport. Molecular defects, such as structural deformations in the polycrystalline film, further escalate these issues [173].

12.2.3. Strategies to address defects

To mitigate the impact of defects, several strategies have been

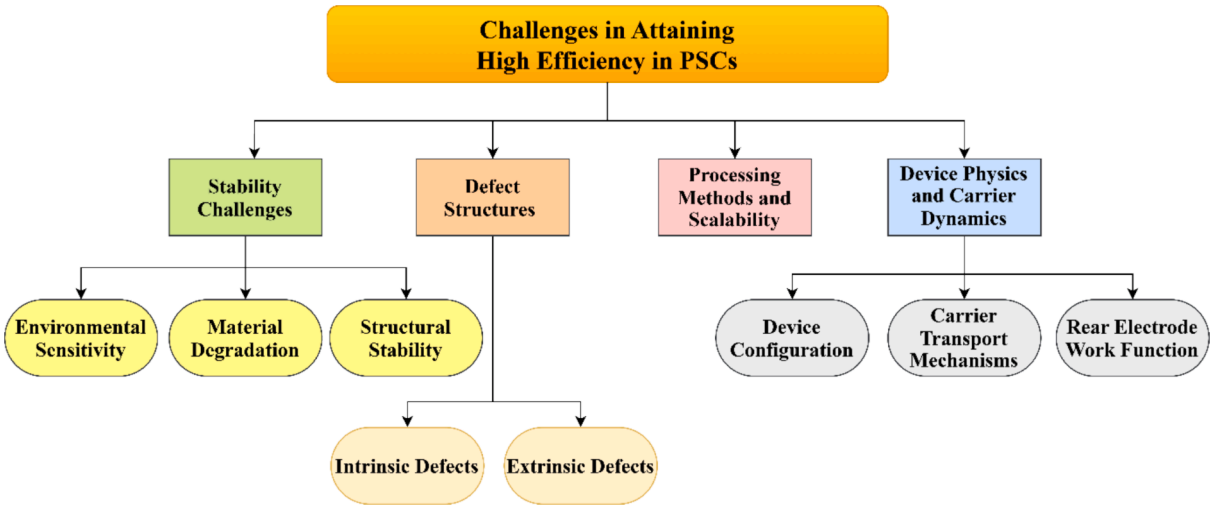

Fig. 23. Challenges in attaining high efficiency in PSCs.

employed. First principal calculations provide insights into the properties of point defects in materials like $MAPbI_3$. Additionally, the use of protective HTL materials that combine high hole mobility with protection against environmental factors helps mitigate instability. Moreover, compositional engineering and the use of additives have been shown to reduce defect densities and enhance the performance of PSCs [173].

12.3. Processing methods and scalability

The manufacture of high-efficiency PSCs demands precise control over the morphology and crystallinity of perovskite films, which are heavily influenced by the processing procedures applied [174]. Scaling up the production of PSCs for industrial applications brings new hurdles. Achieving homogeneous coatings across wide areas, maintaining repeatability, and assuring the compatibility of materials with varied substrates are significant concerns that need to be addressed. Continued research is centered on building scalable processing algorithms that maintain the great performance demonstrated in lab-scale systems [175]. Various types of efficient fabrication approaches are described before in this review article which can be applied for constructing highly efficient and cost-effective PSCs.

12.4. Device physics and carrier dynamics

Understanding the fundamental physics of PSC devices is key for enhancing their efficiency. The arrangement of layers, choice of materials, and carrier transport systems all play crucial roles in defining the overall performance of PSCs [176].

12.4.1. Device configuration

The configuration of PSCs, including the selection of ETLs and HTLs, is critical for effective charge carrier transport. Inorganic ETL materials like as TiO_2, SnO_2, and ZnO have been widely explored for their ability to enhance electron flow while inhibiting holes. Similarly, HTLs like PEDOT:PSS, Spiro-OMeTAD, and NiO play a crucial role in transporting holes and preventing electron leakage [177].

12.4.2. Carrier transport mechanisms

Optimizing carrier transport methods, such as charge extraction and recombination, is crucial to enhancing PSC performance. Trap-assisted recombination, which comes from flaws and impurities, results to non-radiative losses that degrade efficiency. Therefore, decreasing recombination losses by managing defect concentrations and increasing the transport characteristics of materials is critical for creating high-efficiency devices [178].

12.4.3. Rear electrode work function

The work function of the back electrode controls the electric field across the device, facilitating the efficient drift and diffusion of charge carriers. Adjusting the work function of electrodes can dramatically enhance carrier extraction, resulting to improved device performance [179].

13. Device ideas for targeted Shockley–Queisser (S-Q) limit

Different PSC designs aimed at overcoming the Shockley–Queisser (S-Q) limit, which restricts the maximum efficiency of single-junction solar cells to about 32.8 %, include advanced techniques such as tandem solar cells (TSCs), concentrator photovoltaics (CPVs), photon recycling, and hot carrier devices [10] (Fig. 24). These designs capitalize on the physics of light absorption, recombination, and energy loss mechanisms to boost PCE.

13.1. Tandem solar cells (TSCs)

TSCs use many absorber layers, each with a different bandgap, to catch a greater spectrum of sunlight. This design provides efficiency above the S-Q limit by avoiding energy losses. Monolithic 2-Tandem (2-T) architecture: uses sub cells with low and high bandgap absorbers coupled via a recombination layer [180]. This architecture ensures efficient exploitation of the full light spectrum, with notable configurations like perovskite-silicon tandems. Mechanically stacked 4-Tandem (4-T) architecture: uses independent cells for enhanced performance, while establishing long-term stability is a difficulty [181].

13.2. Concentrator solar cells (CPVs)

CPVs focus sunlight onto a smaller area using optical elements, achieving higher PCE in areas with high solar radiation. Features of this design include improved V_{OC} and recombination dynamics. Different recombination mechanisms dominate under varying light intensities, which can be optimized for higher PCEs [182]. For example, InGaP/InGaAs/Ge three-junction PV modules achieve PCEs of up to 41.6 %. Perovskite-based CPVs show promise, although further research is needed to enhance stability [181].

13.3. Photon recycling in PSCs

Photon recycling involves reabsorbing photons emitted through radiative recombination to boost efficiency. Nanostructures and plasmonics materials like $Ag@TiO_2$ and Au nanooctahedrons are utilised to

Fig. 24. Different device designs to overcome Sockley-Queisser (S-Q) limit.

trap light and promote photon recycling, enhancing PCE by 44 % [183].

13.4. Hot carrier devices

These devices exploit the kinetic energy of hot carriers created from high-energy photons before they lose their energy through thermalization [184]. Efficient collection of hot carriers and the minimisation of cooling losses are significant measures for enhancing PCE. Hemispherical core–shell AgOx@Ag nanoparticles and other materials have been found to boost PCE by regulating the energy dissipation of heated carriers [185].

14. Degradation mechanism for PSCs

PSCs encounter severe stability issues, which have been the focus of extensive research aimed at finding and reducing degradation mechanisms. These stability problems are often categorised into intrinsic and extrinsic instabilities [25] (Fig. 25). Intrinsic instabilities emerge from the inherent properties of the PSC materials and their interactions under operational settings, with elements like as temperature, humidity, and ultraviolet (UV) light being key contributors. Extrinsic instabilities, on the other hand, are induced by external environmental conditions, particularly the loss of protective layers and sealing systems, which allow exposure to degrading elements like moisture and oxygen. Key factors to the degradation of PSCs include exposure to atmospheric conditions, such as humidity, sunshine, and air, which can accelerate material degradation and create phase transitions that impact performance. To strengthen the stability of PSCs, numerous ways have been studied. Encapsulation procedures, which entail using chemically inert and strong materials to isolate the electronics from environmental conditions, are crucial [186]. Additionally, material engineering efforts aim to generate more stable perovskite compositions and increase the quality of interfacial layers by the addition of additives and dopants. Furthermore, modifying the device architecture, has shown potential in decreasing degradation risks. By incorporating material breakthroughs, architectural enhancements, and effective encapsulation, researchers intend to solve both intrinsic and extrinsic instabilities, thereby increasing the long-term durability and economic viability of PSCs. The accompanying part provides a complete explanation of the numerous forms of instabilities and degradation mechanisms for PSCs.

14.1. Extrinsic instability

Extrinsic instability occurs mostly from environmental stressors that directly alter the stability of PSCs. The main environmental elements contributing to degradation include moisture, oxygen, temperature impacts, and ultraviolet (UV) light exposure [186]. Additionally, degradation of encapsulation layers and mechanical damage during the packaging process led to extrinsic instability.

A. Environmental factors

i) Moisture and oxygen-induced degradation

Moisture and oxygen ingress constitute the most crucial environmental elements impacting the degradation of PSCs. Water molecules permeate the perovskite layer and interact with the perovskite substance, particularly methylammonium lead iodide ($MAPbI_3$) [103]. These interactions lead to hydrogen bond formation between water molecules and the methylammonium (MA^+) cation, which decreases the connection between the MA^+ ion and the $[PbI_6]4^-$ octahedral structure. This finally results in the destruction of the perovskite layer through hydrolysis. Additionally, moisture stimulates the dissolution of the perovskite structure, generating volatile by-products such as methylamine (CH_3NH_2) and hydroiodic acid (HI). Oxygen further exacerbates this process by oxidizing the reductive iodide (I^-) to iodine (I_2), causing flaws and secondary phases like lead iodide (PbI_2), which decrease the device's performance [187].

ii) Thermal degradation

Temperature variations and extreme temperatures also contribute considerably to PSC degradation. Organic-inorganic perovskites, such as

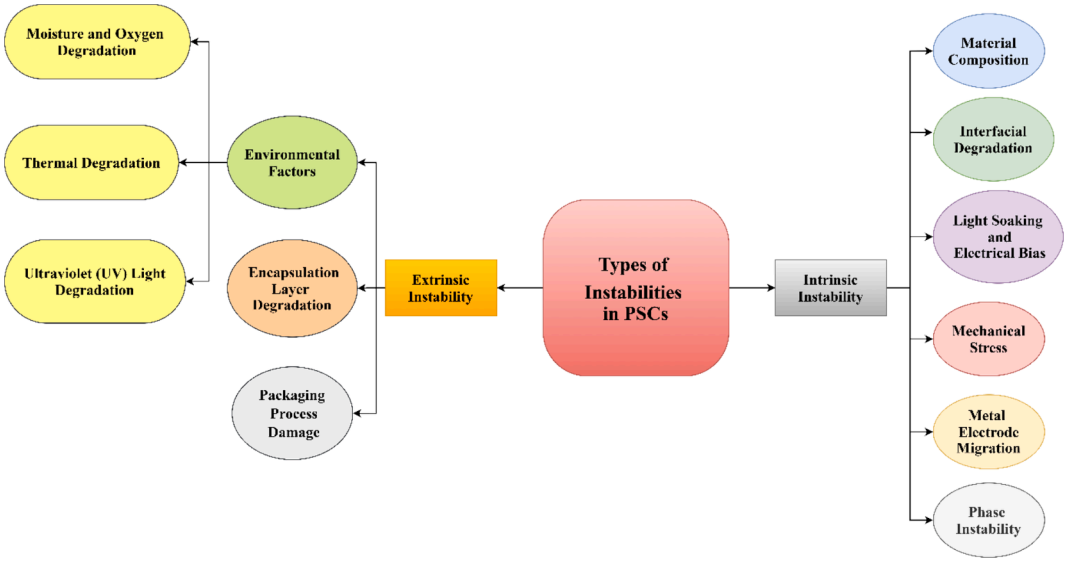

Fig. 25. Types of instabilities in perovskite solar cells.

$MAPbI_3$, are extremely sensitive to heat, while breakdown normally occurs at temperatures exceeding 250 °C, even moderate temperatures (~85 °C) commonly observed in terrestrial photovoltaic applications might cause partial degradation. Heat enhances the volatilization of organic components, such as methylammonium (MA^+) and formamidinium (FA^+), leading to the loss of these essential cations and resulting in phase instability. Over time, increased temperatures promote the generation of lead iodide (PbI_2) and other undesirable phases, drastically lowering device efficiency [187].

iii) Ultraviolet (UV) light degradation

Prolonged exposure to UV light also triggers deterioration in PSCs. UV photons have sufficient energy to disrupt chemical bonds inside the perovskite structure, notably in the organic components. This breakdown route involves photodissociation of the metal halide components, culminating in the creation of neutral iodine, chlorine, and bromine [188]. UV-induced decomposition is commonly accompanied by high temperatures, which further contribute the breakdown of the perovskite material.

B. Encapsulation layer degradation

The encapsulating layer, designed to protect PSCs from environmental stressors such as moisture and oxygen, can degrade over time, limiting their efficiency. Over lengthy operational durations, the encapsulant can experience mechanical or chemical breakdown, allowing ambient elements to infiltrate the device. As the encapsulation deteriorates, it becomes increasingly difficult to cover the perovskite layer from moisture and oxygen penetration, accelerating the deterioration process [189].

C. Packaging process damage

Mechanical damage incurred during the packaging process can generate micro-defects and pinholes in the device, giving paths for moisture and oxygen penetration. This physical degradation can also compromise the integrity of CTLs and the metal electrode, further limiting the device's performance. Defects produced during packing can aggravate ion migration and phase segregation within the perovskite layer, making the device more susceptible to failure.

14.2. Intrinsic instability

Intrinsic instability is induced by internal mechanisms within the PSCs, driven by their material composition and operational conditions. These influences include light soaking, electrical bias, interfacial deterioration, mechanical stress, metal electrode migration, and phase instability [190].

A. Material composition

The intrinsic instability of PSCs is very directly related to their material composition. Organic-inorganic hybrid perovskites, such as $MAPbI_3$ and $FAPbX_3$ ($X = I^-, Br^-$), are prone to disintegration due to the volatility of their organic components [190]. Under operating stress, these organic cations breakdown into volatile by-products such as CH_3NH_2, HI, and ammonia (NH_3), leaving behind lead iodide (PbI_2) and other secondary phases. This disintegration not only decreases the active perovskite material but also produces flaws and traps that degrade charge transport and overall device performance [191].

B. Interfacial degradation

The interfaces between distinct layers in PSCs, such as the perovskite layer and charge transport layers, are particularly prone to deterioration. Under operational settings, ion migration occurs largely at interfaces and grain boundaries, where faults are more concentrated. These flaws enhance phase segregation, notably in mixed-halide perovskites, resulting to performance loss. Additionally, the interaction between the perovskite layer and metal electrodes might lead to the creation of secondary phases that further damage the device [192].

C. Light soaking and electrical bias

Light soaking refers to the prolonged exposure of PSCs to continuous illumination, which induces photo-degradation of perovskite materials. Under light exposure, perovskites, particularly $MAPbI_3$, experience photodissociation of metal halides, producing neutral iodine and lead [192]. The photogenerated carriers (electrons and holes) interact with these halides and metals, initiating decomposition reactions. Light soaking also induces halide segregation in mixed-halide perovskites, creating iodine-rich and bromine-rich regions. This segregation, though reversible under certain conditions, weakens the lattice structure, facilitating ion migration and reducing carrier transport efficiency [193].

Electrical bias applied during PSC operation can induce ion migration, particularly for A-site cations and halide ions. The migration barriers for these ions are relatively low, leading to phase segregation and the accumulation of mobile ions at grain boundaries and interfaces. These localized charges create electric fields, promoting further ion migration and accelerating material degradation [192]. The continuous accumulation of charges under electrical bias also leads to the formation of electronic traps, which act as recombination centers, reducing the device's efficiency.

D. Mechanical stress

Mechanical stress, generated by thermal expansion, external forces, or operational cycling, can cause delamination at heterointerfaces. This delamination disturbs charge transport between the perovskite layer and the neighbouring charge transport layers, lowering the efficiency of the device. Repeated mechanical stress, such as during thermal cycling, weakens the bonding between layers, resulting to micro-cracks and increased vulnerability to environmental degradation [194].

E. Metal electrode migration

Metal electrode migration is another key degradation mechanism in PSCs. Under prolonged working conditions, metal ions from the electrodes, notably silver and gold, can migrate into the perovskite layer. These moving metal ions combine with halide ions, generating secondary phases that produce electronic traps and act as recombination sites. This behavior drastically decreases the efficiency of the PSC and promotes its degradation [195].

F. Phase instability

Phase instability, particularly in mixed-cation and mixed-halide perovskites, comes from ion migration and segregation under operational stress. Phase segregation leads to the creation of I-rich and Br-rich regions, creating an inhomogeneous material that exhibits poor charge transfer and enhanced recombination. Phase instability is often increased by light soaking and electrical bias, thus adding to the degradation of PSCs over time [192].

15. Factors influencing the PSCs device stability

PSCs devices have achieved significant stability and PCE due to extensive research and development over a short period of time. However, the long-term stability of these devices remains a critical challenge, limiting their commercial viability [196]. There are various factors

which influence the stability of these devices (Fig. 26) which are discussed in the subsequent section of this review paper.

15.1. Material structure and functional layers

The intrinsic material properties of perovskites, as well as the interfaces between functional layers in PSCs, play a pivotal role in determining device stability.

i) **Perovskite absorber materials:** $MAPbI_3$ (Methylammonium Lead Iodide) is one of the most widely used perovskite absorber materials, $MAPbI_3$ exhibits a bandgap of 1.55 eV. However, it undergoes an irreversible phase transition from a tetragonal to cubic structure at temperatures above 55 °C, which significantly impacts device performance [197]. Some reports suggest that it can retain its tetragonal phase up to 100 °C, but the material's inherent thermal instability remains a concern. $MAPbBr_3$ and $MAPbCl_3$ do not exhibit phase transitions within the typical operational temperature range of −40 °C to 85 °C, making them more thermally stable. However, their higher bandgaps result in lower efficiencies compared to $MAPbI_3$ [198].

ii) **Alternative perovskite materials:** Replacing the methylammonium (MA) cation with cesium (Cs) improves thermal stability, but $CsPbI_3$ struggles to crystallize at room temperature, limiting its application in ambient conditions. $CsSnI_3$ and $CsSnBr_3$ offer promising electronic properties but suffer from thermal and oxidative stability issues. For instance, $CsSnI_3$ undergoes a phase change at 152 °C, while $CsSnBr_3$ remains stable up to 450 °C but is prone to oxidation, leading to self-doping and reduced carrier lifetimes [199].

15.2. Hysteresis in perovskite solar cells

Hysteresis in the current–voltage (J–V) characteristics is a serious concern in PSCs, affecting both the correct assessment of device performance and overall stability [67]. The movement of ions within the perovskite layer affects the internal electric field, leading to performance discrepancies during forward and reverse voltage scans. Hysteresis is more prominent with high scan rates during J–V measurements and is minimized at slower scan rates, suggesting a time-dependent effect on charge transport. Slow transient capacitive currents and high dielectric permittivity in perovskite materials result in delayed charge responses, adding to hysteresis [67]. The presence of defects at grain boundaries and interfaces leads to charge trapping, lowering photocurrent extraction efficiency and aggravating hysteresis. Perovskite materials with ferroelectric domains display polarization features that change the band alignment at interfaces, generating variances in device performance depending on scan direction [200,201].

15.2.1. Mitigation strategies

Inverted PSCs are less prone to hysteresis compared to standard planar PSCs. Optimizing grain size and enhancing the quality of the perovskite layer, together with engineering interfaces to eliminate charge traps, can greatly mitigate hysteresis. Using slower scan rates during J–V measurements can provide more accurate performance assessments and avoid hysteresis artifacts. Incorporating new HTL materials like incorporating phenoxazine 9 (POZ9) and phenoxazine 10 (POZ10) as HTLs resulted in PCEs of 17.1 % and 19.4 %, respectively. POZ10, in instance, displayed improved hole carrying capabilities and minimised charge recombination [72]. Adding a minor concentration of potassium iodide to various perovskite compositions (e.g., MAPbI3, FAPbI3) considerably reduced J–V hysteresis. This reduction is related to the mitigation of iodide frenkel defects rather than iodide ion movement [202]. Using poly(1butyl3vinylimidazoliumbis (trifluoromethylsulfonl) imide) as a dopant for the HTL resulted in a PCE of 20.3 % without hysteresis losses. This configuration employed TiO2 as the ETL and Au as the back contact metal. Processing perovskite films at room temperature, as opposed to high temperature annealing, offers a simplified and cost-effective fabrication approach. It also enhances humidity stability and reduces hysteresis by promoting a more uniform and well organized perovskite film structure [197].

15.3. Environmental stressors and degradation pathways

Environmental factors, including ultraviolet (UV) radiation, humidity, and temperature, are major contributors to the degradation of PSCs.

15.3.1. Impact of ultraviolet (UV) radiation

Exposure to UV light, especially in the UV range (310–317 nm), has been shown to significantly degrade PSCs, reducing the PCE by up to 50 % over 1700 h. UV light (360–380 nm), by contrast, has a minimal impact on stability. Strategies to mitigate UV-induced degradation include the use of UV filters and luminescent downshifting layers, which convert harmful UV radiation into visible light, enhancing both stability and device efficiency. Material innovations, such as incorporating samarium-doped nanomaterials (Sr_2CeO_4:Sm^{3+}), can enhance the PCE by 16.2 % while maintaining 50 % of the initial PCE after 60 days of UV

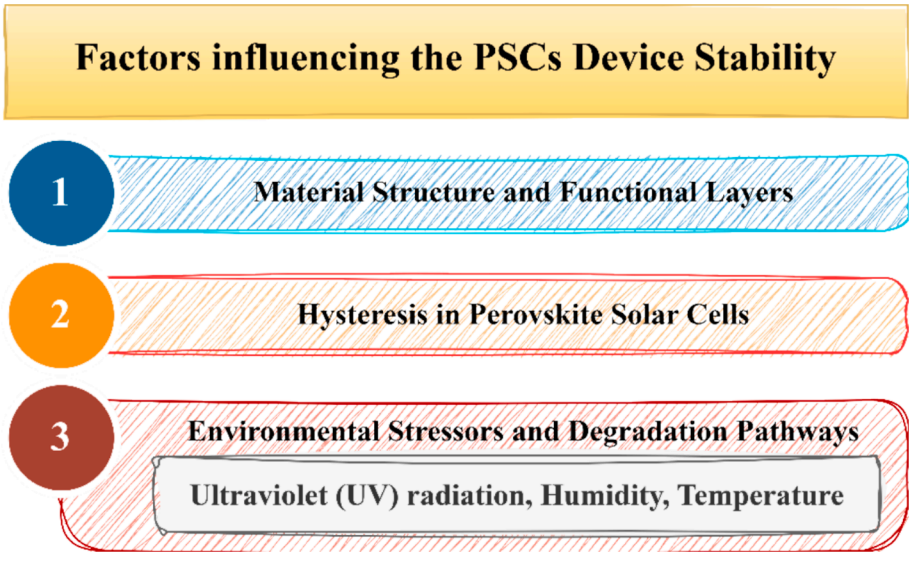

Fig. 26. Factors influencing the PSCs device stability.

exposure [203]. Additionally, surface fluorination of TiO_2 nanocrystals improves UV stability and boosts efficiency, achieving a PCE of 22.68 %. Other approaches include using dopant-free TiO_2 as the electron transport layer (ETL) and CuSCN as the hole transport layer (HTL), resulting in devices that retain 95 % of their initial PCE after 2000 h of exposure to the AM 1.5G spectrum [204].

15.3.2. Impact of humidity

Perovskite materials are highly sensitive to moisture, leading to rapid degradation. Humidity accelerates the decomposition of perovskites into lead iodide (PbI_2), resulting in reduced device performance. To enhance moisture resistance, strategies such as doping with rubidium (Rb) have been employed. For instance, Rb doping stabilizes $FAPbI_3$ by transforming it from a hexagonal to a trigonal phase, resulting in improved PCE and moisture stability [204]. Another efficient strategy involves the use of 2D/3D perovskite composites, where a 2D perovskite capping layer boosts charge transport and moisture resistance, leading to a PCE of 22.06 %. Protective coatings, such as atomic layer deposition (ALD) of Al_2O_3, create an ultrathin barrier that guards the perovskite layer from ambient moisture while ensuring efficient charge transmission [205].

15.3.3. Impact of temperature

Thermal deterioration is another important concern for PSCs. High temperatures raise series resistance and induce carrier recombination, lowering device efficiency. The intrinsic volatility of organic components in the ETL and HTL additionally exacerbates thermal instability. Efforts to increase thermal stability include the development of HTL-free devices, which substitute organic HTLs with carbon-based electrodes, giving devices with stable PCEs even after prolonged exposure to 80 °C [195]. Another new strategy involves the addition of caffeine to perovskite materials, which promotes crystallinity and thermal stability, enabling a PCE of 19.8 % with stability maintained for 1500 h at 85 °C. Sealing techniques, such as edge encapsulation to prevent the loss of volatile components, and additive engineering, such as the incorporation of reduced graphene oxide (rGO) or fullerene-based additives, have also demonstrated improvements in both PCE and thermal stability under elevated temperatures [189].

16. Key challenges in commercialization of PSCs

Despite their rapid development and impressive laboratory performance, several key challenges hinder the commercialization of PSCs. The subsequent section of this review paper discusses such critical issues which hinders the commercialization of PSCs.

16.1. Efficiency and scaling challenges

While small-area PSCs have achieved PCEs exceeding 25 %, scaling these efficiencies to large-area modules presents significant difficulties. Larger modules exhibit higher sheet and series resistance, which can lead to energy losses. Achieving uniform film quality across greater areas is difficult, resulting in variable performance. bigger carrier collection zones might worsen losses, thus diminishing overall efficiency [206].

16.2. Performance gap between small and large area cells

A substantial performance disparity occurs between small-area and large-area PSCs, with large-area modules frequently achieving only 10–14 % PCE. Enhancing electrode designs to maximise charge collection and minimize losses. Developing strategies to assure homogeneous film morphology throughout scale-up processes. Tailoring solution compositions and annealing conditions to obtain high-quality films consistently [58].

16.3. Operational stability

Operational stability is critical for the long-term success of PSCs. Moisture, oxygen, light, heat, and electrical bias can accelerate material breakdown. The inherent ionic characteristics of perovskites make them sensitive to disorder and phase separation under stress. Poor interface adhesion might cause to delamination and void formation during operation [207].

16.4. Industrialization considerations

For PSCs to be commercially successful, industrial-scale procedures must meet many considerations. Processes must be robust enough to perform under varied environmental circumstances. Efficient thermal processing technologies are needed for large-scale production. Ensuring consistent performance across batches is vital for commercial success [208].

The commercialization of perovskite solar cells holds tremendous potential but confronts considerable obstacles relating to efficiency scaling, operational stability, and industrialization. By solving these difficulties through sophisticated material processing techniques, scalable deposition processes, interface engineering, structural optimization, and robust encapsulation strategies, researchers can pave the path for the effective integration of PSCs into the renewable energy market. The numerous tactics and procedures which can be applied to solve these crucial concerns are explored in the ensuing section 17 of this review study.

17. Methods to enhance stability of PSCs

PSCs have emerged as a promising technology for renewable energy generation due to their high PCE and low manufacturing costs. However, to accelerate the commercialization of PSCs, it is crucial to enhance both their photovoltaic performance and stability. This review paper explores various strategies and techniques employed by researchers to improve the stability of PSCs (Fig. 27), including compositional engineering, interfacial engineering, device encapsulation, hole conductor free architectures, addressing hysteresis effects, enhancing light absorption, optimizing carrier transport and innovative cell structure design.

17.1. Compositional engineering

Composition engineering offers a versatile approach in advancing the performance and stability of PSCs by modifying the intrinsic properties of the material optimizing perovskite materials for solar cell applications. By carefully selecting and substituting ions, researchers can tailor the electronic properties, stability, and overall performance of PSCs [127]. Continued advancements in this field is crucial for overcoming current challenges and achieving higher efficiencies in perovskite solar cells.

A. Types of additives in compositional engineering

Additives employed in composition engineering can be broadly classified into inorganic and organic categories:

i) Inorganic additives: These often include metal cations and inorganic acids. Their primary function is to incorporate into the perovskite lattice, reducing the density of trap states in the bulk of the material, thus improving carrier mobility and reducing recombination [209].
ii) Organic additives: Polymers, small organic molecules, and fullerenes fall under this category. Unlike inorganic additives, organic additives typically deactivate surface defect states, which enhances surface passivation without fundamentally altering the bulk properties of the perovskite material [90].

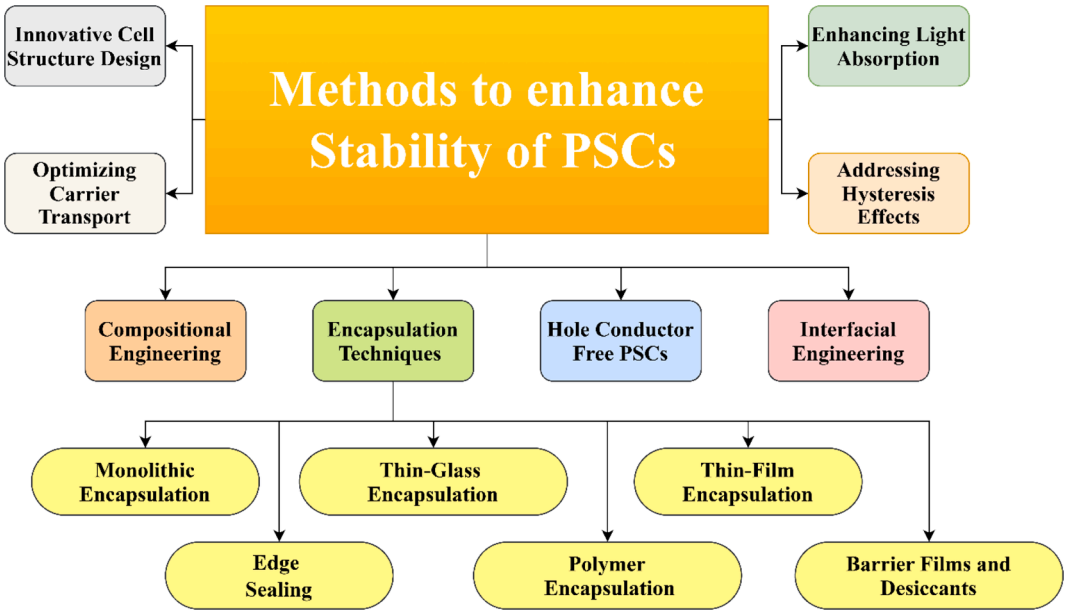

Fig. 27. Various methods to enhance stability of PSCs.

B. Ion substitutions, and their effects

The ability to substitute A, B, or X ions in the perovskite structure offers an effective method to tailor the material's band gap, stability, and overall performance. A site cation can be either organic (e.g., methylammonium [MA], formamidinium [FA], or guanidinium [GA]) or inorganic (e.g., Cs, Rb, K, Na). The choice of A site cations directly influences the structural stability of the material [210]. Lead (Pb) and tin (Sn) are the most commonly used B site cations. Lead based perovskites, such as $MAPbI_3$, have high efficiencies but face environmental concerns. Tin based perovskites offer a potential leadfree alternative but are prone to oxidation, making them less stable [210]. The halides (Cl, Br, I) serve as Xsite anions, and their substitution directly impacts the band gap. For instance, substituting iodine with bromine or chlorine can increase the band gap, making the material more suitable for tandem solar cells [211].

C. Perovskite dimensionality

The dimensionality of perovskites, dictated by the arrangement of the BX_6 octahedral network, profoundly influences their optoelectronic properties. Three Dimensional (3D) perovskites, like $MAPbI_3$, exhibit high carrier mobility and efficiency but suffer from long term instability [212]. Two Dimensional (2D) perovskites, with layered structures, have enhanced stability against moisture but often come with a tradeoff in performance [213]. Quasi2D and Zero Dimensional (0D) perovskites combine features from both 2D and 3D structures, offering intermediate properties in terms of stability and efficiency [214].

D. Notable examples of compositional engineering

i) Cs Doping in $FAPbI_3$: Adding a trace amount of Cs to $FAPbI_3$ perovskite enhances the PCE from 7.41 % to 11.47 %. The resulting $FA_{0.85}Cs_{0.15}PbI_3$ PSC is thermally stable at 150 °C and 90 % humidity [215].

ii) $FeCl_2$ in $CsPbI_2Br$: Incorporating $FeCl_2$ into $CsPbI_2Br$ perovskite results in a PCE of 17.1 % and thermal stability for 330 h with 95 % PCE retention [216].

iii) MA and Br in $FAPbI_3$: Adding 1 % MA ion and Br to $FAPbI_3$ improves stability and performance under high temperature and moisture [216].

iv) $MAGeI_3$ with Iodine and Bromine: Adding 10 % iodine and bromine to $MAGeI_3$ forms $MAGeI_{2.7}Br_{0.3}$, achieving a PCE of 0.57 % and good thermal stability [217].

v) Polymer Mixture in PbI_2 Precursor: Adding polyvinylpyrrolidone and polyethylene glycol to the PbI_2 precursor solution during fabrication improves PCE by 30 % and enhances air stability by preventing ion migration [215].

Despite the promising advances made through compositional engineering, several challenges remain to address. One of the primary challenges in PSC development is improving the thermal and chemical stability of perovskite materials. Many compositions, particularly lead based perovskites, degrade rapidly when exposed to environmental factors like moisture, heat, and UV light. The presence of defects, such as grain boundaries and surface traps, is a major source of recombination losses in PSCs. Future research needs to focus on strategies to reduce these defects. The use of lead in PSCs poses significant environmental risks. Developing leadfree alternatives, such as tin based perovskites, is critical for the widespread adoption of this technology.

17.2. Interfacial engineering

Improving the interfaces between different layers in PSCs can significantly enhance stability by reducing charge recombination and improving charge transport. Key strategies and examples of interfacial engineering include:

A. Buffer layers

i) BCP (2,9 Dimethy, l4,7 dipheny, l1,10 phenanthroline): Enhances stability by improving carrier dynamics in hybrid perovskite based PSCs [19].

ii) Poly (9,9bis(3(N, N dimethylamino)propyl)2,7 fluorene) alt 2,7 (9,9–dioctylfluorene): Used as a buffer layer material to enhance performance [90].

B. Surface passivation

CF_3PEABr (Trifluoromethylphenethylamine Hydrobromide): Passivates the perovskite film surface, coordinates with halide dangling bonds, and suppresses nonradiative carrier recombination, achieving a PCE of 21.3 % [218].

C. Physical Isolation

PMMA (Poly(methyl methacrylate)): Depositing PMMA in topographic depressions like grain and domain boundaries enhances shunt resistance and fill factor (FF) by physically isolating defects, preventing charge carriers from reaching these locations [218].

D. Interfacial layers

i) PCBA ([6,6]PhenylC61butyric Acid): Acts as a hole blocking material, reducing trapsite density and carrier recombination at the TiO_2/perovskite interface, resulting in a PCE of 17.76 % [205].
ii) PDINO (Perylene Diimide): Forms an interface layer between ETL (PCBM) and rear contact (Ag), providing proper band alignment, enhanced shunt resistance, and reduced series resistance, achieving a PCE of 14 % [205].

17.3. Encapsulation techniques for perovskite solar cells

Encapsulation is vital for safeguarding perovskite solar cells from environmental elements that cause degradation, such as moisture, oxygen, and UV radiation. Effective encapsulation strives to construct a barrier around the PSC, preventing the intrusion of these damaging substances while assuring long-term device stability and performance. Here are some typical encapsulation approaches for PSCs:

A. Thin-film encapsulation

This technique utilizes thin layers of materials deposited directly onto the PSC surface to create a barrier. This can be implemented by using atomic layer deposition, chemical vapor deposition and solution processed thin films.

i) **Atomic layer deposition:** ALD gives fine control over film thickness and homogeneity, enabling the deposition of dense and pinhole-free layers. Metal oxides like aluminum oxide (Al_2O_3) and zirconium oxide are extensively used [218].
ii) **Chemical vapor deposition:** CVD enables for conformal coating of complicated structures, making it suited for encapsulating flexible PSCs. Silicon nitride and silicon dioxide are widely employed as barrier layers [219].
iii) **Solution-processed thin films:** This cost-effective method involves depositing thin films from a solution, often utilising spin-coating or printing techniques. Materials including polymers, metal oxides, and hybrid composites are employed [220].

B. Edge sealing

While thin-film encapsulation covers the PSC's top surface, the margins remain exposed. Edge sealing approaches address this:

i) **UV-curable resins:** These resins are applied to the device edges and cured using UV light, establishing a durable seal. They give good adhesion and moisture resistance [214].
ii) **Glass frit sealing:** This approach includes utilising a glass frit paste that is applied to the edges and then heated to melt and seal the device. It provides good hermeticity but can be troublesome for flexible devices [221].
iii) **Laser sealing:** Lasers can be used to selectively melt and fuse materials at the device edges, forming a hermetic seal. This approach delivers excellent precision and is appropriate for diverse substrate materials [221].

C. Other encapsulation strategies

i) **Monolithic encapsulation:** This technology integrates the encapsulation layer directly into the device structure during fabrication process, simplifying the process and potentially reducing manufacturing costs [217]. By incorporating the encapsulation layer as an integral part of the device structure, the fabrication process becomes more streamlined, potentially leading to cost savings and improved production efficiency.
ii) **Thin glass encapsulation:** Similar to classic encapsulation method used for traditional silicon-based solar cells, this encapsulation approach uses thin sheets of glass to encase and protect the PSC. The glass layers form a durable and robust barrier, shielding the sensitive perovskite materials from environmental factors that could otherwise degrade the device's performance over time [217]. This encapsulation technique helps to improve the long-term stability and operational lifetime of PSCs.
iii) **Barrier films and desiccants:** Combining barrier films with desiccants within the encapsulating package can further enhance moisture protection, thereby significantly improving the long-term stability of PSCs. The barrier film act as a physical barrier to prevent moisture and other environmental contaminants from degrading the perovskite material, while the desiccants actively absorb any residual moisture that may penetrate the encapsulation, providing a multi-faceted approach to moisture protection [176].
iv) **Polymer encapsulation:** Polystyrenecopolyacrylonitrile (SAN) copolymer encapsulates the grain boundaries (GBs) of perovskite structures, limiting the migration of organic cations. This polymer-based encapsulation technique protects the PSCs by safeguarding the perovskite layer from environmental factors that could cause degradation over time. As a result device encapsulating using this method retain 85 % of their initial PCE after 1000 h of exposure to 1 solar light [72].

The choice of encapsulation technique depends on factors like the PSC architecture, desired lifetime, cost constraints, and scalability requirements. Often, a combination of techniques is employed to achieve optimal protection. For instance, thin-film encapsulation might be combined with edge sealing and the use of desiccants for comprehensive protection. Research continues to advance encapsulation technologies for PSCs, aiming for more robust, cost-effective, and scalable solutions to enable the widespread adoption of this promising solar energy technology.

17.4. Hole conductor free PSCs

Removing HTL and using alternative materials like carbon electrodes can enhance thermal stability and reduce costs. Several developments in hole conductor free PSCs are discussed:

i) Solution processed PSCs: A PSC fabricated without an HTL using a solution processing method achieved a PCE of 16 %, surpassing the performance of PSCs with NiOx as the HTL [222].
ii) Graphene based contacts: Used as schottky junctions, multilayered graphene facilitates faster carrier extraction, resulting in a PCE of 11.5 % [222].
iii) Single layered graphene: Employed as ohmic contacts, achieving a PCE of 6.7 % [223].
iv) Stacked perovskite layers: MAPbIxBr3x/MAPbI3 HTL free configuration achieved a PCE of 16.2 % and demonstrated excellent stability under both dark and illuminated conditions [219].
v) Carbon nanotube (CNT) electrodes: An HTL free MAPbI3/TiO2-based PSC with super aligned CNT electrodes exhibited a PCE of 8.65 %, which improved to 10.54 % with iodine doping [91].

17.5. Addressing hysteresis effects

Hysteresis in PSCs significantly affects their performance and stability, posing a challenge for their practical outdoor applications.

Several strategies have been employed to minimize J–V hysteresis effects which are discussed previously in section 15.2. of this review paper.

17.6. Enhancing light absorption

Enhancing light absorption is crucial for improving the efficiency of PSCs. Researchers have designed nanostructures, such as nanowires and nanoparticles, to increase the specific surface area of the perovskite layer, thereby improving light absorption efficiency. Additionally, photonic crystals and other structures have been used to regulate the propagation path of light, causing it to reflect and refract multiple times within the perovskite layer, thus increasing light absorption [224].

17.7. Optimizing carrier transport

Efficient carrier transport is critical to reduce energy loss and boost PSCs performance. Researchers have synthesized new high-performance transport materials, including organic–inorganic hybrid materials and low-dimensional materials, to boost carrier mobility and longevity. Fine-tuning the interface between the perovskite layer and the transport layer has also proved helpful in lowering interface recombination and energy loss [225].

17.8. Innovative cell structure design

Innovative cell structure designs have led to major advancements in PSC efficiency. Traditional structures have struggled to match increasing performance needs, forcing researchers to explore novel designs such as multi-layer and gradient structures. These designs not only boost light absorption and carrier transport but also efficiently prevent flaws and recombination centers, further improving PSC efficiency [226].

18. Applications of PSCs

Perovskite solar cells are adaptable and hold potential for a wide range of uses beyond typical solar panels. Their unique qualities, such as high efficiency, low-cost manufacture, and configurable bandgap, make them suited for several novel uses:

18.1. Traditional energy applications

PSCs can be integrated into rooftop solar panels for residential and commercial structures, offering sustainable electricity generation. Large-scale solar farms can utilize PSCs to harvest solar energy and feed it into the electrical grid. PSCs can be embedded into building facades, windows, and roofs, transforming buildings into energy-generating structures [17].

18.2. Flexible and portable applications

PSCs can be produced on flexible substrates, enabling their usage in wearable devices, curved surfaces, and other flexible electronics. Lightweight and flexible PSCs can power portable devices like cell-phones, laptops, and sensors, giving off-grid energy alternatives. Integrating PSCs into fabrics can make solar-powered garments and tents, supplying power for numerous applications.

18.3. Specialized and emerging applications

PSCs can be made transparent or semi-transparent, allowing their incorporation into windows, greenhouses, and displays without impeding natural light [100]. PSCs display good performance under low-light circumstances, making them appropriate for harvesting indoor light to power small devices and sensors. Combining PSCs with other solar cell materials like silicon in tandem topologies can transcend the efficiency constraints of single-junction cells, leading to even higher energy conversion rates [142]. PSCs' lightweight and high-efficiency potential make them appealing for space applications, delivering power for satellites and spacecraft [227].

19. Conclusion

PSCs have emerged as a promising technology in the field of photovoltaics, demonstrating tremendous breakthroughs in PCE during the past decade. This paper comprehensively examines the history, fundamental properties, working, device structure and architectures, manufacturing processes, challenges, and recent breakthroughs in PSC technology. The excellent optoelectronic features of perovskite materials, particularly high absorption coefficients, long carrier diffusion lengths, and fault tolerance, have permitted rapid increases in device performance. Through compositional engineering, interface optimization, and new device topologies, researchers have produced PCEs above 26 % in laboratory settings, comparable to typical silicon-based solar cells. Notwithstanding these improvements, some key obstacles exist. Stability concerns, particularly related to moisture sensitivity, thermal degradation, and UV induced degradation, continue to hamper the long-term stability of PSCs. The presence of harmful lead in high-performing electronics increases environmental concerns, encouraging development of lead-free alternatives. Scaling up from small area laboratory cells to large area module while maintaining high efficiency involves significant fabrication and technological challenges. Efforts to overcome these obstacles have led to encouraging advancements. Encapsulation techniques, including thin-film deposition and edge sealing, have proven an acceptable potential in enhancing the device stability. The study of both mixed cation and mixed halide perovskites has produced more stable materials with tunable bandgaps. Novel materials like the 2D/3D perovskite composites and using additives offered greater resistance to the environmental factors. PSCs versatility in applications extends beyond the simple solar panel applications. Their anticipated implementation in small, lightweight, and flexible electronic devices, building-integrated photovoltaics, and tandem solar cell architecture highlights the adaptability and potential for different energy harvesting situations.

20. Future scope

Moving forward, further focus should be shifted towards researching lead-free perovskites particularly tin-based and bismuth based to address toxicity concerns. It shall promote the efforts to focus on further major improvement in stability and efficiency of these alternative compositions. Improving encapsulation provides a good barrier for the intrusion of any moisture while developing passive methods and compositional techniques to address intrinsic instability will be crucial to extending the lifetime of these devices. This involves finding new compounds and novel passivation methods, which lead to the mitigation of defect density and ion migration. For the technology to be commercially viable, it is also very important to develop large area processes for deposition of films that are even and of high quality. This involves optimizing and enhancing solution processing techniques and developing vapor-based deposition strategies for industrial-scale production. Integrating perovskites with silicon and other solar technologies in tandem arrangements could boost efficiency beyond single junction limitations. This involves careful bandgap engineering and interface optimization. Expanding research on flexible PSCs for portable and wearable applications, focusing on mechanical robustness and low-temperature processing processes. Enhancing computational models to better understand degradation mechanisms, predict material properties, and guide experimental design would accelerate the development of high-performance, stable PSCs. Establishing industry-wide standards for stability testing and performance measurement is vital for reliable comparison of devices and assessment of commercial readiness.

Developing efficient recycling techniques for PSCs, particularly for lead-containing devices, to address environmental concerns and enhance sustainable lifecycle management. Exploring the potential of PSCs in integrated energy systems, particularly their use in building-integrated photovoltaics and off-grid applications. Investigating unorthodox applications of PSCs, including as indoor light harvesting and space-based solar power, to utilize their unique features in varied situations. By addressing these future prospects, the area of perovskite solar cells can continue its trajectory of rapid growth, potentially transforming the solar energy landscape and contributing considerably to global renewable energy aspirations. The adaptability of PSCs opens up intriguing prospects for the future of solar energy. As research and development continue to address difficulties relating to stability and scalability, we may anticipate to see PSCs playing a more significant role in numerous sectors, leading to a more sustainable and energy-efficient future.

CRediT authorship contribution statement

Mohsin Afroz: Writing – review & editing, Writing – original draft, Formal analysis, Conceptualization. **Ratneshwar Kumar Ratnesh:** Writing – review & editing, Supervision, Formal analysis, Conceptualization. **Swapnil Srivastava:** Writing – review & editing, Formal analysis, Data curation. **Jay Singh:** Conceptualization, Supervision, Validation, Writing – original draft, Formal analysis.

Funding

This work received no specific grant from public, commercial, or not-for-profit funding agencies.

Declaration of competing interest

The authors declare that they have no known competing financial interests or personal relationships that could have appeared to influence the work reported in this paper.

Acknowledgments

The authors would like to thanks the department of electronics and communication engineering, meerut institute of engineering and technology for providing useful infrastructure and support to carried out various experiment and work related to this paper. Author R. K. Ratnesh expresses gratitude to the Science and Engineering Research Board (SERB) (TAR/2022/000618), Department of Science and Technology (DST), Government of India for their financial assistance. Author J.S. acknowledges BHU for providing a seed grant and BRIDGE grant under MoE Govt. India, Institute of Eminence (IoE), under Dev. Scheme No. 6031 & 6031A respectively.

References

[1] G.M. Wilson, M. Al-Jassim, W.K. Metzger, S.W. Glunz, P. Verlinden, G. Xiong, L. M. Mansfield, B.J. Stanbery, K. Zhu, Y. Yan, J.J. Berry, A.J. Ptak, F. Dimroth, B. M. Kayes, A.C. Tamboli, R. Peibst, K. Catchpole, M.O. Reese, C.S. Klinga, P. Denholm, M. Morjaria, M.G. Deceglie, J.M. Freeman, M.A. Mikofski, D. C. Jordan, G. Tamizhmani, S.-K. The, photovoltaic technologies roadmap, J. Phys. Appl. Phys. 2020 (2020) 53, https://doi.org/10.1088/1361-6463/ab9c6a.

[2] D. Gielen, F. Boshell, D. Saygin, M.D. Bazilian, N. Wagner, R. Gorini, The role of renewable energy in the global energy transformation, Energy Strategy Rev. 24 (2019) 38–50, https://doi.org/10.1016/j.esr.2019.01.006.

[3] M.B. Hayat, D. Ali, K.C. Monyake, L. Alagha, N. Ahmed, Solar energy-a look into power generation, challenges, and a solar-powered future, Int. J. Energy Res. 43 (2019) 1049–1067, https://doi.org/10.1002/er.4252.

[4] N. Kant, P. Singh, Review of next generation photovoltaic solar cell technology and comparative materialistic development, Mater. Today Proc. 56 (2022) 3460–3470, https://doi.org/10.1016/j.matpr.2021.11.116.

[5] M.A. Iqbal, M. Malik, W. Shahid, S.Z.U. Din, N. Anwar, M. Ikram, F. Idrees, M. A. Iqbal, M. Malik, W. Shahid, S.Z.U. Din, N. Anwar, M. Ikram, F. Idrees, Materials for photovoltaics: overview, generations, recent advancements and future prospects. thin films photovolt, IntechOpen (2022), https://doi.org/10.5772/intechopen.101449.

[6] M. Giannouli, Current status of emerging PV technologies: a comparative study of dye-sensitized, organic, and perovskite solar cells, Int. J. Photoenergy 2021 (2021) 1–19, https://doi.org/10.1155/2021/6692858.

[7] A. Garg, R.K. Ratnesh, Solar cell trends and the future: a review, J Pharm. Negat. Results 2051 –60 (2022) 10.47750/pnr.2022.13.S06.268.

[8] A. Pandikumar, editor. Third Generation Photovoltaic Technology. vol. 165. 1st ed. Materials Research Forum LLC; 2024. 10.21741/9781644903032.

[9] M. Ebrahimi, Solar power plants, Power Gener. Technol., Elsevier (2023) 419–461, https://doi.org/10.1016/B978-0-323-95370-2.00010-7.

[10] G. Conibeer, S. Shrestha, S. Huang, R. Patterson, H. Xia, Y. Feng, P. Zhang, N. Gupta, M. Tayebjee, S. Smyth, Y. Liao, Z. Zhang, S. Chung, S. Lin, P. Wang, X. Dai, Hot carrier solar cell absorbers: materials, mechanisms and nanostructures. In: Sulima OV, Conibeer G, editors., San Diego, California, United States: 2014, p. 917802. 10.1117/12.2067926.

[11] X. Li, N.P. Hylton, V. Giannini, N.J. Ekins-Daukes, S.A. Maier, Design guidelines for efficient plasmonic solar cells exploiting the trade-off between scattering and metallic absorption 2014. 10.48550/ARXIV.1408.2603.

[12] N. Elumalai, M. Mahmud, D. Wang, A. Uddin, Perovskite solar cells: progress and advancements, Energies 9 (2016) 861, https://doi.org/10.3390/en9110861.

[13] A. Garg, R.K. Ratnesh, Design and Simulation of GaAs/InP and Si/SiC Heterojunction Solar Cells. In: Bindhu V, Tavares JMRS, Vuppalapati C, editors. Proc. Fourth Int. Conf. Commun. Comput. Electron. Syst., vol. 977, Singapore: Springer Nature Singapore; 2023, p. 867–75. 10.1007/978-981-19-7753-4_66.

[14] S. Kashyap, R. Pandey, J. Madan, Simulated bending test analysis of 23% efficient lead-free flexible perovskite solar cell with different bending states, Phys. Scr. 98 (2023) 114001, https://doi.org/10.1088/1402-4896/acff28.

[15] M. Kumar Yadav, R. Kumar, R. Kumar Ratnesh, J. Singh, R. Chandra, A. Kumar, V. Vishnoi, G. Singh, S.A. Kumar, Revolutionizing technology with spintronics: devices and their transformative applications, Mater. Sci. Eng. B 303 (2024) 117293, https://doi.org/10.1016/j.mseb.2024.117293.

[16] E. Berger, M. Bagheri, S. Asgari, J. Zhou, M. Kokkonen, P. Talebi, J. Luo, A. F. Nogueira, T. Watson, S.G. Hashmi, Recent developments in perovskite-based precursor inks for scalable architectures of perovskite solar cell technology, Sustain Energy Fuels 6 (2022) 2879–2900, https://doi.org/10.1039/D2SE00162D.

[17] J.P. Tiwari. Flexible Perovskite Solar Cells: A Futuristic IoTs Powering Solar Cell Technology, Short Review. Small Methods 2024:2400624. 10.1002/smtd.202400624.

[18] A.R. Chakhmouradian, P.M. Woodward, Celebrating 175 years of perovskite research: a tribute to Roger H, Mitchell. Phys Chem Miner 41 (2014) 387–391, https://doi.org/10.1007/s00269-014-0678-9.

[19] T.M. Brenner, D.A. Egger, L. Kronik, G. Hodes, D. Cahen, Hybrid organic—inorganic perovskites: low-cost semiconductors with intriguing charge-transport properties, Nat. Rev. Mater. 1 (2016) 15007, https://doi.org/10.1038/natrevmats.2015.7.

[20] H.L. Wells, Über die Cäsium- und Kalium-Bleihalogenide, Z Für Anorg Chem 3 (1893) 195–210, https://doi.org/10.1002/zaac.18930030124.

[21] M. ChrKn, A phase transition in cæsium plumbochloride, Nature 180 (1957) 981–982, https://doi.org/10.1038/180981a0.

[22] D. Weber, $CH_3NH_3SnBr_xI_{3-x}$ (x = 0-3), ein Sn(II)-system mit kubischer perowskitstruktur / $CH_3NH_3SnBr_xI_{3-x}$ (x = 0-3), a Sn(II)-system with cubic perovskite structure, Z Für Naturforschung B 33 (1978) 862–865, https://doi.org/10.1515/znb-1978-0809.

[23] S.R. Kothiyal, R. Kumar Ratnesh, A. Kumar, Field Effect Transistor (FET)-Sensor for Biological Applications. 2023 Int. Conf. Device Intell. Comput. Commun. Technol. DICCT, Dehradun, India: IEEE; 2023, p. 433–8. 10.1109/DICCT56244.2023.10110155.

[24] D.B. Mitzi, Organic−inorganic perovskites containing trivalent metal halide layers: the templating influence of the organic cation layer, Inorg. Chem. 39 (2000) 6107–6113, https://doi.org/10.1021/ic000794i.

[25] A.K. Jena, A. Kulkarni, T. Miyasaka, Halide perovskite photovoltaics: background, status, and future prospects, Chem. Rev. 119 (2019) 3036–3103, https://doi.org/10.1021/acs.chemrev.8b00539.

[26] K. Mahmood, B.S. Swain, A.R. Kirmani, A. Amassian, Highly efficient perovskite solar cells based on a nanostructured WO3–TiO2 core–shell electron transporting material, J. Mater. Chem. A 3 (2015) 9051–9057, https://doi.org/10.1039/C4TA04883K.

[27] J.-H. Im, C.-R. Lee, J.-W. Lee, S.-W. Park, N.-G. Park, 6.5% efficient perovskite quantum-dot-sensitized solar cell, Nanoscale 3 (2011) 4088–4093, https://doi.org/10.1039/C1NR10867K.

[28] G. Niu, X. Guo, L. Wang, Review of recent progress in chemical stability of perovskite solar cells, J. Mater. Chem. A 3 (2015) 8970–8980, https://doi.org/10.1039/C4TA04994B.

[29] P. Baraneedharan, S. Sekar, S. Murugesan, D. Ahamada, S.A.B. Mohamed, Y. Lee, S. Lee, Recent advances and remaining challenges in perovskite solar cell components for innovative photovoltaics, Nanomaterials 14 (2024) 1867, https://doi.org/10.3390/nano14231867.

[30] J.H. Noh, S.H. Im, J.H. Heo, T.N. Mandal, S.I. Seok, Chemical management for colorful, efficient, and stable inorganic–organic hybrid nanostructured solar cells, Nano Lett. 13 (2013) 1764–1769, https://doi.org/10.1021/nl400349b.

[31] X. Tong, F. Lin, J. Wu, Z.M. Wang, High performance perovskite solar cells, Adv. Sci. 3 (2016) 1500201, https://doi.org/10.1002/advs.201500201.

[32] H. Pan, X. Zhao, X. Gong, H. Li, N.H. Ladi, X.L. Zhang, W. Huang, S. Ahmad, L. Ding, Y. Shen, M. Wang, Y. Fu, Advances in design engineering and merits of

electron transporting layers in perovskite solar cells, Mater. Horiz. 7 (2020) 2276–2291, https://doi.org/10.1039/D0MH00586J.
[33] K. Rakstys, S. Paek, P. Gao, P. Gratia, T. Marszalek, G. Grancini, K.T. Cho, K. Genevicius, V. Jankauskas, W. Pisula, M.K. Nazeeruddin, Molecular engineering of face-on oriented dopant-free hole transporting material for perovskite solar cells with 19% PCE, J. Mater. Chem. A 5 (2017) 7811–7815, https://doi.org/10.1039/C7TA01718A.
[34] X. Yang, W. Wang, R. Ran, W. Zhou, Z. Shao, Recent advances in cs_2 $agbibr_6$ -based halide double perovskites as lead-free and inorganic light absorbers for perovskite solar cells, Energy Fuels 34 (2020) 10513–10528, https://doi.org/10.1021/acs.energyfuels.0c02236.
[35] Y.Y. Kim, T.-Y. Yang, R. Suhonen, A. Kemppainen, K. Hwang, N.J. Jeon, J. Seo, Roll-to-roll gravure-printed flexible perovskite solar cells using eco-friendly antisolvent bathing with wide processing window, Nat. Commun. 11 (2020) 5146, https://doi.org/10.1038/s41467-020-18940-5.
[36] M. Shao, T. Bie, L. Yang, Y. Gao, X. Jin, F. He, N. Zheng, Y. Yu, X. Zhang, Over 21% efficiency stable 2D perovskite solar cells, Adv. Mater. 34 (2022) 2107211, https://doi.org/10.1002/adma.202107211.
[37] S. Zhang, F. Ye, X. Wang, R. Chen, H. Zhang, L. Zhan, X. Jiang, Y. Li, X. Ji, S. Liu, M. Yu, F. Yu, Y. Zhang, R. Wu, Z. Liu, Z. Ning, D. Neher, L. Han, Y. Lin, H. Tian, W. Chen, M. Stolterfoht, L. Zhang, W.-H. Zhu, Y. Wu, Minimizing buried interfacial defects for efficient inverted perovskite solar cells, Science 380 (2023) 404–409, https://doi.org/10.1126/science.adg3755.
[38] H. Chen, C. Liu, J. Xu, A. Maxwell, W. Zhou, Y. Yang, Q. Zhou, A.S.R. Bati, H. Wan, Z. Wang, L. Zeng, J. Wang, P. Serles, Y. Liu, S. Teale, Y. Liu, M. I. Saidaminov, M. Li, N. Rolston, S. Hoogland, T. Filleter, M.G. Kanatzidis, B. Chen, Z. Ning, E.H. Sargent, Improved charge extraction in inverted perovskite solar cells with dual-site-binding ligands, Science 384 (2024) 189–193, https://doi.org/10.1126/science.adm9474.
[39] S.D. Stranks, V.M. Burlakov, T. Leijtens, J.M. Ball, A. Goriely, H.J. Snaith, Recombination kinetics in organic-inorganic perovskites: excitons, free charge, and subgap states, PhysRevAppl 2 (2014) 034007, https://doi.org/10.1103/PhysRevApplied.2.034007.
[40] W.-J. Yin, J.-H. Yang, J. Kang, Y. Yan, S.-H. Wei, Halide perovskite materials for solar cells: a theoretical review, J. Mater. Chem. A 3 (2015) 8926–8942, https://doi.org/10.1039/C4TA05033A.
[41] K. Deepthi Jayan, V. Sebastian, Ab initio DFT determination of structural, mechanical, optoelectronic, thermoelectric and thermodynamic properties of RbGeI3 inorganic perovskite for different exchange-correlation functionals, Mater. Today Commun. 28 (2021) 102650, https://doi.org/10.1016/j.mtcomm.2021.102650.
[42] R.K. Ratnesh, M.K. Singh, J. Singh, Enhancing ZnO/Si heterojunction photodetector performance for ultra high responsivity across wide spectral range, J. Mater. Sci. Mater. Electron. 35 (2024) 756, https://doi.org/10.1007/s10854-024-12516-5.
[43] S. Bai, P. Da, C. Li, Z. Wang, Z. Yuan, F. Fu, M. Kawecki, X. Liu, N. Sakai, J.-T.-W. Wang, S. Huettner, S. Buecheler, M. Fahlman, F. Gao, H.J. Snaith, Planar perovskite solar cells with long-term stability using ionic liquid additives, Nature 571 (2019) 245–250, https://doi.org/10.1038/s41586-019-1357-2.
[44] D. Marongiu, M. Saba, F. Quochi, A. Mura, G. Bongiovanni, The role of excitons in 3D and 2D lead halide perovskites, J. Mater. Chem. C 7 (2019) 12006–12018, https://doi.org/10.1039/C9TC04292J.
[45] Z. Ku, Y. Rong, M. Xu, T. Liu, H. Han, Full printable processed mesoscopic CH3NH3PbI3/TiO2 heterojunction solar cells with carbon counter electrode, Sci. Rep. 3 (2013) 3132, https://doi.org/10.1038/srep03132.
[46] R.K. Ratnesh, M.K. Singh, V. Kumar, S. Singh, R. Chandra, M. Singh, J. Singh, Mango leaves (*Mangifera indica*)-derived highly florescent green graphene quantum dot nanoprobes for enhanced on–off dual detection of cholesterol and Fe^{2+} ions based on molecular logic operation, ACS Appl. Bio Mater. 7 (2024) 4417–4426, https://doi.org/10.1021/acsabm.4c00292.
[47] P.S. Whitfield, N. Herron, W.E. Guise, K. Page, Y.Q. Cheng, I. Milas, M. K. Crawford, Structures, phase transitions and tricritical behavior of the hybrid perovskite methyl ammonium lead iodide, Sci. Rep. 6 (2016) 35685, https://doi.org/10.1038/srep35685.
[48] P. Zheng, W. Zhou, Y. Mo, B. Zheng, M. Han, Q. Zhong, W. Yang, P. Gao, L. Yang, J. Liu, Multi boron-doping effects in hard carbon toward enhanced sodium ion storage, J. Energy Chem. (2024), https://doi.org/10.1016/j.jechem.2024.09.024.
[49] K. Yamamoto, T. Kuwabara, K. Takahashi, T. Taima, Study of planar heterojunction perovskite photovoltaic cells using compact titanium oxide by chemical bath deposition, Jpn. J. Appl. Phys. 54 (2015) 08KF02, https://doi.org/10.7567/JJAP.54.08KF02.
[50] P. Muralt, R.G. Polcawich, S. Trolier-McKinstry, Piezoelectric thin films for sensors, actuators, and energy harvesting, MRS Bull. 34 (2009) 658–664, https://doi.org/10.1557/mrs2009.177.
[51] T.S. Sherkar, C. Momblona, L. Gil-Escrig, J. Ávila, M. Sessolo, H.J. Bolink, L.J. A. Koster, Recombination in perovskite solar cells: significance of grain boundaries, interface traps, and defect ions, ACS Energy Lett. 2 (2017) 1214–1222, https://doi.org/10.1021/acsenergylett.7b00236.
[52] N. Li, S. Tao, Y. Chen, X. Niu, C.K. Onwudinanti, C. Hu, Z. Qiu, Z. Xu, G. Zheng, L. Wang, Y. Zhang, L. Li, H. Liu, Y. Lun, J. Hong, X. Wang, Y. Liu, H. Xie, Y. Gao, Y. Bai, S. Yang, G. Brocks, Q. Chen, H. Zhou, Cation and anion immobilization through chemical bonding enhancement with fluorides for stable halide perovskite solar cells, Nat. Energy 4 (2019) 408–415, https://doi.org/10.1038/s41560-019-0382-6.
[53] S. Gharibzadeh, B. Abdollahi Nejand, M. Jakoby, T. Abzieher, D. Hauschild, S. Moghadamzadeh, J.A. Schwenzer, P. Brenner, R. Schmager, A.A. Haghighirad, L. Weinhardt, U. Lemmer, B.S. Richards, I.A. Howard, U.W. Paetzold, Record open-circuit voltage wide-bandgap perovskite solar cells utilizing 2D/3D perovskite heterostructure, Adv. Energy Mater. 9 (2019) 1803699, https://doi.org/10.1002/aenm.201803699.
[54] M. Afsari, A. Boochani, M. Hantezadeh, Electronic, optical and elastic properties of cubic perovskite CsPbI3: using first principles study, Optik 127 (2016) 11433–11443, https://doi.org/10.1016/j.ijleo.2016.09.013.
[55] M.K. Shahzad, M.U. Farooq, R.A. Laghari, M.A. Khan, M.B. Tahir, W. Azeem, M. Mahmood Ali, V. Tirth, Investigation of structural, electronic, mechanical, & optical characteristics of Ra based-cubic hydrides RbRaX3 (X= F and cl) perovskite materials for solar cell applications: First principle study, Heliyon 9 (2023) e18407, https://doi.org/10.1016/j.heliyon.2023.e18407.
[56] P. Zhang, M. Li, W.-C. Chen, A perspective on perovskite solar cells: emergence, progress, and commercialization, Front. Chem. 10 (2022), https://doi.org/10.3389/fchem.2022.802890.
[57] J.-Y. Shao, Y.-W. Zhong, Design of small molecular hole-transporting materials for stable and high-performance perovskite solar cells, Chem. Phys. Rev. 2 (2021) 021302, https://doi.org/10.1063/5.0051254.
[58] Y. Chen, L. Zhang, Y. Zhang, H. Gao, H. Yan, Large-area perovskite solar cells – a review of recent progress and issues, RSC Adv. 8 (2018) 10489–10508, https://doi.org/10.1039/C8RA00384J.
[59] K.M. Anoop, T.N. Ahipa, Recent advancements in the hole transporting layers of perovskite solar cells, Sol. Energy 263 (2023) 111937, https://doi.org/10.1016/j.solener.2023.111937.
[60] H.S. Jung, N.-G. Park, Perovskite solar cells: from materials to devices, Small 11 (2015) 10–25, https://doi.org/10.1002/smll.201402767.
[61] A.A. Assi, W.R. Saleh, E. Mohajerani, Effect of metals (Au, Ag, and Ni) as cathode electrode on perovskite solar cells, IOP Conf. Ser.: Earth Environ. Sci 722 (2021) 012019, https://doi.org/10.1088/1755-1315/722/1/012019.
[62] S.A. Deepika, U.K. Verma, A. Tonk, Device structures of perovskite solar cells: a critical review, Phys. Status Solidi A 220 (2023) 2200736, https://doi.org/10.1002/pssa.202200736.
[63] Z. Shariatinia, Recent progress in development of diverse kinds of hole transport materials for the perovskite solar cells: a review, Renew. Sustain. Energy Rev. 119 (2020) 109608, https://doi.org/10.1016/j.rser.2019.109608.
[64] S. Liu, W. Huang, P. Liao, N. Pootrakulchote, H. Li, J. Lu, J. Li, F. Huang, X. Shai, X. Zhao, Y. Shen, Y.-B. Cheng, M. Wang, 17% efficient printable mesoscopic PIN metal oxide framework perovskite solar cells using cesium-containing triple cation perovskite, J. Mater. Chem. A 5 (2017) 22952–22958, https://doi.org/10.1039/C7TA07660F.
[65] M. Degani, Q. An, M. Albaladejo-Siguan, Y.J. Hofstetter, C. Cho, F. Paulus, G. Grancini, Y. Vaynzof, 23.7% Efficient inverted perovskite solar cells by dual interfacial modification, Sci. Adv. 7 (2021) eabj7930, https://doi.org/10.1126/sciadv.abj7930.
[66] D. Yang, X. Zhang, Y. Hou, K. Wang, T. Ye, J. Yoon, C. Wu, M. Sanghadasa, S. Liu, 28.3%-efficiency perovskite/silicon tandem solar cell by optimal transparent electrode for high efficient semitransparent top cell, Nano Energy 84 (2021) 105934, https://doi.org/10.1016/j.nanoen.2021.105934.
[67] A. Garg, R.K. Ratnesh, R.K. Chauhan, N. Mittal, H. Shankar, Current Advancement and Progress in BioFET: A Review. 2022 Int. Conf. Signal Inf. Process. IConSIP, IEEE, Pune, India, 2022, pp. 1–7.
[68] R. Wang, M. Mujahid, Y. Duan, Z.-K. Wang, J. Xue, Y. Yang, A review of perovskites solar cell stability, Adv. Funct. Mater. 29 (2019) 1808843, https://doi.org/10.1002/adfm.201808843.
[69] W. Chen, Y. Wu, J. Liu, C. Qin, X. Yang, A. Islam, Y.-B. Cheng, L. Han, Hybrid interfacial layer leads to solid performance improvement of inverted perovskite solar cells, Energ. Environ. Sci. 8 (2015) 629–640, https://doi.org/10.1039/C4EE02833C.
[70] E. Danladi, D. Dogo, S. Michael, F. Uloko, A. Salawu, Recent advances in modeling of perovskite solar cells using SCAPS-1D: effect of absorber and ETM thickness, East Eur. J. Phys. 2021 (5–17) (2021), https://doi.org/10.26565/2312-4334-2021-4-01.
[71] D. Ramirez, M. Alejandro Mejía Escobar, J.F. Montoya, F. Jaramillo, Understanding the role of the mesoporous layer in the thermal crystallization of a meso-superstructured perovskite solar cell, J. Phys. Chem. C 120 (2016) 8559–8567, https://doi.org/10.1021/acs.jpcc.6b02808.
[72] K.D. Jayan, Charting new horizons: unrivalled efficiency and stability in perovskite solar cells, Phys. Status Solidi A 221 (2024) 2300782, https://doi.org/10.1002/pssa.202300782.
[73] R. Kumar, R.K. Ratnesh, J. Singh, A. Kumar, R. Chandra, IoT-driven experimental framework for advancing electrical impedance tomography, ECS J. Solid State Sci. Technol. 13 (2024) 027002, https://doi.org/10.1149/2162-8777/ad2331.
[74] L.-H. Chou, X.-F. Wang, I. Osaka, C.-G. Wu, C.-L. Liu, Scalable ultrasonic spray-processing technique for manufacturing large-area CH3NH3PbI3 perovskite solar cells, ACS Appl. Mater. Interfaces 10 (2018) 38042–38050, https://doi.org/10.1021/acsami.8b12463.
[75] M. Cheng, C. Zuo, Y. Wu, Z. Li, B. Xu, Y. Hua, L. Ding, Charge-transport layer engineering in perovskite solar cells, Sci. Bull. 65 (2020) 1237–1241, https://doi.org/10.1016/j.scib.2020.04.021.
[76] T. Kim, J. Lim, S. Song, Recent progress and challenges of electron transport layers in organic–inorganic perovskite solar cells, Energies 13 (2020) 5572, https://doi.org/10.3390/en13215572.
[77] J. Chen, W.C.H. Choy, Efficient and stable all-inorganic perovskite solar cells, Sol. RRL 4 (2020) 2000408, https://doi.org/10.1002/solr.202000408.

[78] L. Lin, T.W. Jones, T.C.-J. Yang, N.W. Duffy, J. Li, L. Zhao, B. Chi, X. Wang, Wilson GJ. Inorganic Electron Transport Materials in Perovskite Solar Cells. Adv. Funct. Mater. 2021;31:2008300. 10.1002/adfm.202008300.

[79] Z. Yu, L. Sun, Inorganic hole-transporting materials for perovskite solar cells, Small Methods 2 (2018) 1700280, https://doi.org/10.1002/smtd.201700280.

[80] J. Lian, B. Lu, F. Niu, P. Zeng, X. Zhan, Electron-transport materials in perovskite solar cells, Small Methods 2 (2018) 1800082, https://doi.org/10.1002/smtd.201800082.

[81] E. Castro, O. Fernandez-Delgado, F. Arslan, G. Zavala, T. Yang, S. Seetharaman, F. D'Souza, L. Echegoyen, New thiophene-based C60 fullerene derivatives as efficient electron transporting materials for perovskite solar cells, New J. Chem. 42 (2018) 14551–14558, https://doi.org/10.1039/C8NJ03067G.

[82] S. Collavini, A. Cabrera-Espinoza, J.L. Delgado, Organic polymers as additives in perovskite solar cells, Macromolecules 54 (2021) 5451–5463, https://doi.org/10.1021/acs.macromol.1c00665.

[83] K. Mahmood, S. Sarwar, M.T. Mehran, Current status of electron transport layers in perovskite solar cells: materials and properties, RSC Adv. 7 (2017) 17044–17062, https://doi.org/10.1039/C7RA00002B.

[84] J. Urieta-Mora, I. García-Benito, A. Molina-Ontoria, N. Martín, Hole transporting materials for perovskite solar cells: a chemical approach, Chem. Soc. Rev. 47 (2018) 8541–8571, https://doi.org/10.1039/C8CS00262B.

[85] E. Raza, F. Aziz, Z. Ahmad, Stability of organometal halide perovskite solar cells and role of HTMs: recent developments and future directions, RSC Adv. 8 (2018) 20952–20967, https://doi.org/10.1039/C8RA03477J.

[86] Q.B. Ke, J.-R. Wu, C.-C. Lin, S.H. Chang, Understanding the PEDOT:PSS, PTAA and P3CT-X hole-transport-layer-based inverted perovskite solar cells, Polymers 14 (2022) 823, https://doi.org/10.3390/polym14040823.

[87] S.R. Raga, Y. Jiang, L.K. Ono, Y. Qi, Application of methylamine gas in fabricating organic–inorganic hybrid perovskite solar cells, Energy Technol. 5 (2017) 1750–1761, https://doi.org/10.1002/ente.201700423.

[88] Y. Chen, P. Lin, B. Cai, W. Zhang, Research progress of inorganic hole transport materials in perovskite solar cells, J. Inorg. Mater. 38 (991) (2023), https://doi.org/10.15541/jim20230105.

[89] M. Tountas, C. Polyzoidis, M. Loizos, K. Rogdakis, E. Kymakis, Improved performance of hole-transporting material-free perovskite solar cells using a low-temperature printed carbon paste, ACS Appl. Electron. Mater. 5 (2023) 6228–6235, https://doi.org/10.1021/acsaelm.3c01132.

[90] L. Zhou, J. Su, Z. Lin, X. Guo, J. Ma, T. Li, J. Zhang, J. Chang, Y. Hao, Synergistic interface layer optimization and surface passivation with fluorocarbon molecules toward efficient and stable inverted planar perovskite solar cells, Research 2021 (2021/9836752) (2021), https://doi.org/10.34133/2021/9836752.

[91] Q. Luo, H. Ma, Y. Zhang, X. Yin, Z. Yao, N. Wang, J. Li, S. Fan, K. Jiang, H. Lin, Cross-stacked superaligned carbon nanotube electrodes for efficient hole conductor-free perovskite solar cells, J. Mater. Chem. A 4 (2016) 5569–5577, https://doi.org/10.1039/C6TA01715K.

[92] Y. Yuan, Z. Xiao, B. Yang, J. Huang, Arising applications of ferroelectric materials in photovoltaic devices, J. Mater. Chem. A 2 (2014) 6027–6041, https://doi.org/10.1039/C3TA14188H.

[93] I. Kafedjiska, I. Levine, A. Musiienko, N. Maticiuc, T. Bertram, A. Al-Ashouri, C.A. Kaufmann, S. Albrecht, R. Schlatmann, I. Lauermann, Advanced characterization and optimization of NiO_x:Cu-SAM Hole-transporting bi-layer for 23.4% efficient monolithic Cu(In,Ga)Se_2-perovskite tandem solar cells. Adv. Funct. Mater. 2023; 33:2302924. 10.1002/adfm.202302924.

[94] R. Kumar, R.K. Ratnesh, J. Singh, R. Chandra, G. Singh, V. Vishnoi, Recent prospects of medical imaging and sensing technologies based on electrical impedance data acquisition system, J. Electrochem. Soc. 170 (2023) 117507, https://doi.org/10.1149/1945-7111/ad050f.

[95] Z. Li, Y. Wei, K. Zhou, X. Huang, X. Zhou, J. Xu, T. Kong, J. Lucas Bao, X. Dong, Y. Wang, A low redox potential and long life organic anode material for sodium-ion batteries, J. Energy Chem. 100 (2025) 557–564, https://doi.org/10.1016/j.jechem.2024.09.017.

[96] A. Ullah, K.H. Park, Y. Lee, S. Park, A.B. Faheem, H.D. Nguyen, Y. Siddique, K.-K. Lee, Y. Jo, C.-H. Han, S. Ahn, I. Jeong, S. Cho, B. Kim, Y.S. Park, S. Hong, Versatile hole selective molecules containing a series of heteroatoms as self-assembled monolayers for efficient p-i-n perovskite and organic solar cells, Adv. Funct. Mater. 32 (2022) 2208793, https://doi.org/10.1002/adfm.202208793.

[97] A. Farag, T. Feeney, I.M. Hossain, F. Schackmar, P. Fassl, K. Küster, R. Bäuerle, M. A. Ruiz-Preciado, M. Hentschel, D.B. Ritzer, A. Diercks, Y. Li, B.A. Nejand, F. Laufer, R. Singh, U. Starke, U.W. Paetzold, Evaporated self-assembled monolayer hole transport layers: lossless interfaces in p-i-n perovskite solar cells, Adv. Energy Mater. 13 (2023) 2203982, https://doi.org/10.1002/aenm.202203982.

[98] R. Chen, W. Zhang, X. Guan, H. Raza, S. Zhang, Y. Zhang, P.A. Troshin, S. A. Kuklin, Z. Liu, W. Chen, Rear electrode materials for perovskite solar cells, Adv. Funct. Mater. 32 (2022) 2200651, https://doi.org/10.1002/adfm.202200651.

[99] C.S. Ponseca, T.J. Savenije, M. Abdellah, K. Zheng, A. Yartsev, T. Pascher, T. Harlang, P. Chabera, T. Pullerits, A. Stepanov, J.-P. Wolf, V. Sundström, Organometal halide perovskite solar cell materials rationalized: ultrafast charge generation, high and microsecond-long balanced mobilities, and slow recombination, J. Am. Chem. Soc. 136 (2014) 5189–5192, https://doi.org/10.1021/ja412583t.

[100] E. Aydin, M. De Bastiani, X. Yang, M. Sajjad, F. Aljamaan, Y. Smirnov, M. N. Hedhili, W. Liu, T.G. Allen, L. Xu, E. Van Kerschaver, M. Morales-Masis, U. Schwingenschlögl, S. De Wolf, Zr-doped indium oxide (IZRO) transparent electrodes for perovskite-based tandem solar cells, Adv. Funct. Mater. 29 (2019) 1901741, https://doi.org/10.1002/adfm.201901741.

[101] M. Becker, M. Wark, Recent progress in the solution-based sequential deposition of planar perovskite solar cells, Cryst. Growth Des. 18 (2018) 4790–4806, https://doi.org/10.1021/acs.cgd.8b00686.

[102] N.J. Jeon, J.H. Noh, Y.C. Kim, W.S. Yang, S. Ryu, S.I. Seok, Solvent engineering for high-performance inorganic–organic hybrid perovskite solar cells, Nat. Mater. 13 (2014) 897–903, https://doi.org/10.1038/nmat4014.

[103] C. Xu, Y. Yao, G. Wang, J. Dong, G. Xu, Y. Zhong, D. Lu, X. Zhao, D. Liu, G. Zhou, X. Yang, P. Li, L. Chen, Q. Song, Self-woven monolayer polyionic mesh to achieve highly efficient and stable inverted perovskite solar cells, Chem. Eng. J. 428 (2022) 132074, https://doi.org/10.1016/j.cej.2021.132074.

[104] D. Bryant, P. Greenwood, J. Troughton, M. Wijdekop, M. Carnie, M. Davies, K. Wojciechowski, H.J. Snaith, T. Watson, D. Worsley, A transparent conductive adhesive laminate electrode for high-efficiency organic-inorganic lead halide perovskite solar cells, Adv. Mater. 26 (2014) 7499–7504, https://doi.org/10.1002/adma.201403939.

[105] J. Zhao, X. Zheng, Y. Deng, T. Li, Y. Shao, A. Gruverman, J. Shield, J. Huang, Is Cu a stable electrode material in hybrid perovskite solar cells for a 30-year lifetime? Energ. Environ. Sci. 9 (2016) 3650–3656, https://doi.org/10.1039/C6EE02980A.

[106] Z. Ku, X. Xia, H. Shen, N.H. Tiep, H.J. Fan, A mesoporous nickel counter electrode for printable and reusable perovskite solar cells, Nanoscale 7 (2015) 13363–13368, https://doi.org/10.1039/C5NR03610K.

[107] J.J. Yoo, G. Seo, M.R. Chua, T.G. Park, Y. Lu, F. Rotermund, Y.-K. Kim, C.S. Moon, N.J. Jeon, J.-P. Correa-Baena, V. Bulović, S.S. Shin, M.G. Bawendi, J. Seo, Efficient perovskite solar cells via improved carrier management, Nature 590 (2021) 587–593, https://doi.org/10.1038/s41586-021-03285-w.

[108] I. Jeong, H. Jin Kim, B.-S. Lee, H. Jung Son, J. Young Kim, D.-K. Lee, D.-E. Kim, J. Lee, M.J. Ko, Highly efficient perovskite solar cells based on mechanically durable molybdenum cathode, Nano Energy 17 (2015) 131–139, https://doi.org/10.1016/j.nanoen.2015.07.025.

[109] G. Grancini, C. Roldán-Carmona, I. Zimmermann, E. Mosconi, X. Lee, D. Martineau, S. Narbey, F. Oswald, F. De Angelis, M. Graetzel, M.K. Nazeeruddin, One-Year stable perovskite solar cells by 2D/3D interface engineering, Nat. Commun. 8 (2017) 15684, https://doi.org/10.1038/ncomms15684.

[110] J. Barichello, L. Vesce, F. Matteocci, E. Lamanna, A. Di Carlo, The effect of water in carbon-perovskite solar cells with optimized alumina spacer, Sol. Energy Mater. Sol. Cells 197 (2019) 76–83, https://doi.org/10.1016/j.solmat.2019.03.029.

[111] N. Bhati, M.K. Nazeeruddin, F. Maréchal, Critical analysis of decision variables for high-throughput experimentation (HTE) with perovskite solar cells, Sol. Energy 262 (2023) 111810, https://doi.org/10.1016/j.solener.2023.111810.

[112] A. Kumar, V.D. Ashwlayan, R.K. Ratnesh, J. Singh, M. Verma, Comparative assessment of anti-ulcer effects: Hydro-ethanolic extract from air-dried ray and disc florets vs essential oil of traditional Tagetes erecta (Asteraceae) in Swiss Albino rats, South Afr. J. Bot. 169 (2024) 197–209, https://doi.org/10.1016/j.sajb.2024.04.021.

[113] J. Zhao, M. Hou, Y. Wang, R. Wang, J. Zhang, H. Ren, G. Hou, Y. Ding, Y. Zhao, X. Zhang, Strategies for large-scale perovskite solar cells realization, Org. Electron. 122 (2023) 106892, https://doi.org/10.1016/j.orgel.2023.106892.

[114] Y. Rong, Y. Ming, W. Ji, D. Li, A. Mei, Y. Hu, H. Han, Toward industrial-scale production of perovskite solar cells: screen printing, slot-die coating, and emerging techniques, J. Phys. Chem. Lett. 9 (2018) 2707–2713, https://doi.org/10.1021/acs.jpclett.8b00912.

[115] R. Patidar, D. Burkitt, K. Hooper, D. Richards, T. Watson, Slot-die coating of perovskite solar cells: an overview, Mater. Today Commun. 22 (2020) 100808, https://doi.org/10.1016/j.mtcomm.2019.100808.

[116] I.A. Howard, T. Abzieher, I.M. Hossain, H. Eggers, F. Schackmar, S. Ternes, B. S. Richards, U. Lemmer, U.W. Paetzold, Coated and printed perovskites for photovoltaic applications, Adv. Mater. 31 (2019) 1806702, https://doi.org/10.1002/adma.201806702.

[117] C. Gong, S. Tong, K. Huang, H. Li, H. Huang, J. Zhang, J. Yang, Flexible planar heterojunction perovskite solar cells fabricated via sequential roll-to-roll microgravure printing and slot-die coating deposition, Sol. RRL 4 (2020) 1900204, https://doi.org/10.1002/solr.201900204.

[118] A.T. Barrows, A.J. Pearson, C.K. Kwak, A.D.F. Dunbar, A.R. Buckley, D.G. Lidzey, Efficient planar heterojunction mixed-halide perovskite solar cells deposited via spray-deposition, Energy Env Sci 7 (2014) 2944–2950, https://doi.org/10.1039/C4EE01546K.

[119] J.H. Heo, M.H. Lee, M.H. Jang, S.H. Im, Highly efficient $CH_3 NH_3 PbI_{3-x} Cl_x$ mixed halide perovskite solar cells prepared by re-dissolution and crystal grain growth via spray coating, J. Mater. Chem. A 4 (2016) 17636–17642, https://doi.org/10.1039/C6TA06718B.

[120] Z. Wei, H. Chen, K. Yan, S. Yang, Inkjet printing and instant chemical transformation of a $CH_3 NH_3 PbI_3$ /nanocarbon electrode and interface for planar perovskite solar cells, Angew. Chem. 126 (2014) 13455–13459, https://doi.org/10.1002/ange.201408638.

[121] S.-G. Li, K.-J. Jiang, M.-J. Su, X.-P. Cui, J.-H. Huang, Q.-Q. Zhang, X.-Q. Zhou, L.-M. Yang, Y.-L. Song, Inkjet printing of CH3NH3PbI3 on a mesoscopic TiO2 film for highly efficient perovskite solar cells, J. Mater. Chem. A 3 (2015) 9092–9097, https://doi.org/10.1039/C4TA05675B.

[122] P. Yang, H.J. Fan, Inkjet and extrusion printing for electrochemical energy storage: a minireview, Adv. Mater. Technol. 5 (2020) 2000217, https://doi.org/10.1002/admt.202000217.

[123] S.M. Rossnagel, Thin film deposition with physical vapor deposition and related technologies, J. Vac. Sci. Technol. A 21 (2003) S74–S87, https://doi.org/10.1116/1.1600450.
[124] M. Liu, M.B. Johnston, H.J. Snaith, Efficient planar heterojunction perovskite solar cells by vapour deposition, Nature 501 (2013) 395–398, https://doi.org/10.1038/nature12509.
[125] L.K. Ono, S. Wang, Y. Kato, S.R. Raga, Y. Qi, Fabrication of semi-transparent perovskite films with centimeter-scale superior uniformity by the hybrid deposition method, Energ. Environ. Sci. 7 (2014) 3989–3993, https://doi.org/10.1039/C4EE02539C.
[126] P. Fan, D. Gu, G.-X. Liang, J.-T. Luo, J.-L. Chen, Z.-H. Zheng, D.-P. Zhang, High-performance perovskite CH3NH3PbI3 thin films for solar cells prepared by single-source physical vapour deposition, Sci. Rep. 6 (2016) 29910, https://doi.org/10.1038/srep29910.
[127] A. Raj, M. Kumar, A. Anshul, Topical advances in fabrication technologies of perovskite solar cell heterostructures: performance and future perspective, Mater. Lett. 340 (2023) 134171, https://doi.org/10.1016/j.matlet.2023.134171.
[128] M.M. Tavakoli, L. Gu, Y. Gao, C. Reckmeier, J. He, A.L. Rogach, Y. Yao, Z. Fan, Fabrication of efficient planar perovskite solar cells using a one-step chemical vapor deposition method, Sci. Rep. 5 (2015) 14083, https://doi.org/10.1038/srep14083.
[129] G. Tong, X. Geng, Y. Yu, L. Yu, J. Xu, Y. Jiang, Y. Sheng, Y. Shi, K. Chen, Rapid, stable and self-powered perovskite detectors via a fast chemical vapor deposition process, RSC Adv. 7 (2017) 18224–18230, https://doi.org/10.1039/C7RA01430A.
[130] T. Yokoyama, D.H. Cao, C.C. Stoumpos, T.-B. Song, Y. Sato, S. Aramaki, M. G. Kanatzidis, Overcoming short-circuit in lead-free CH3NH3SnI3 perovskite solar cells via kinetically controlled gas–solid reaction film fabrication process, J. Phys. Chem. Lett. 7 (2016) 776–782, https://doi.org/10.1021/acs.jpclett.6b00118.
[131] J. Burschka, N. Pellet, S.-J. Moon, R. Humphry-Baker, P. Gao, M.K. Nazeeruddin, M. Grätzel, Sequential deposition as a route to high-performance perovskite-sensitized solar cells, Nature 499 (2013) 316–319, https://doi.org/10.1038/nature12340.
[132] D. Navas, S. Fuentes, A. Castro-Alvarez, E. Chavez-Angel, Review on sol-gel synthesis of perovskite and oxide nanomaterials, Gels 7 (2021) 275, https://doi.org/10.3390/gels7040275.
[133] H. Chen, Z. Wei, X. Zheng, S. Yang, A scalable electrodeposition route to the low-cost, versatile and controllable fabrication of perovskite solar cells, Nano Energy 15 (2015) 216–226, https://doi.org/10.1016/j.nanoen.2015.04.025.
[134] M. Al-Katrib, L. Perrin, L. Flandin, E. Planes, Electrodeposition in perovskite solar cells: a critical review, new insights, and promising paths to future industrial applications, Adv. Mater. Technol. 8 (2023) 2300964, https://doi.org/10.1002/admt.202300964.
[135] L.A. Castriotta, M. Zendehdel, N. Yaghoobi Nia, E. Leonardi, M. Löffler, B. Paci, A. Generosi, B. Rellinghaus, A. Di Carlo, Reducing losses in perovskite large area solar technology: laser design optimization for highly efficient modules and minipanels, Adv. Energy Mater. 12 (2022) 2103420, https://doi.org/10.1002/aenm.202103420.
[136] X. Lu, X. Fan, H. Zhang, Q. Xu, M. Ijaz, Review on preparation of perovskite solar cells by pulsed laser deposition, Inorganics 12 (2024) 128, https://doi.org/10.3390/inorganics12050128.
[137] H. Zhang, M.K. Nazeeruddin, W.C.H. Choy, Perovskite photovoltaics: the significant role of ligands in film formation, passivation, and stability, Adv. Mater. 31 (2019) 1805702, https://doi.org/10.1002/adma.201805702.
[138] M. Zhou, J.S. Sarmiento, C. Fei, X. Zhang, H. Wang, Effect of composition on the spin relaxation of lead halide perovskites, J. Phys. Chem. Lett. 11 (2020) 1502–1507, https://doi.org/10.1021/acs.jpclett.0c00004.
[139] A. Jindal, K.A. Mainuddin, R.K. Ratnesh, J. Singh, Nanotechnology driven lipid and metalloid based formulations targeting blood–brain barrier (3B) for brain tumor, Indian J. Microbiol. (2024), https://doi.org/10.1007/s12088-024-01330-6.
[140] Z. Wang, X. Zhu, S. Zuo, M. Chen, C. Zhang, C. Wang, X. Ren, Z. Yang, Z. Liu, X. Xu, Q. Chang, S. Yang, F. Meng, Z. Liu, N. Yuan, J. Ding, S. Liu, 27%-efficiency four-terminal perovskite/silicon tandem solar cells by sandwiched gold nanomesh, Adv. Funct. Mater. 30 (2020) 1908298, https://doi.org/10.1002/adfm.201908298.
[141] X. Shai, J. Wang, P. Sun, W. Huang, P. Liao, F. Cheng, B. Zhu, S.-Y. Chang, E.-P. Yao, Y. Shen, L. Miao, Y. Yang, M. Wang, Achieving ordered and stable binary metal perovskite *via* strain engineering, Nano Energy 48 (2018) 117–127, https://doi.org/10.1016/j.nanoen.2018.03.047.
[142] Z. Li, Y. Zhao, X. Wang, Y. Sun, Z. Zhao, Y. Li, H. Zhou, Q. Chen, Cost analysis of perovskite tandem photovoltaics, Joule 2 (2018) 1559–1572, https://doi.org/10.1016/j.joule.2018.05.001.
[143] A.J. Barker, A. Sadhanala, F. Deschler, M. Gandini, S.P. Senanayak, P.M. Pearce, E. Mosconi, A.J. Pearson, Y. Wu, A.R. Srimath Kandada, T. Leijtens, F. De Angelis, S.E. Dutton, A. Petrozza, R.H. Friend, Defect-assisted photoinduced halide segregation in mixed-halide perovskite thin films, ACS Energy Lett. 2 (2017) 1416–1424, https://doi.org/10.1021/acsenergylett.7b00282.
[144] Y.-M. Xie, Q. Xue, H.-L. Yip, Metal-halide perovskite crystallization kinetics: a review of experimental and theoretical studies, Adv. Energy Mater. 11 (2021) 2100784, https://doi.org/10.1002/aenm.202100784.
[145] I.L. Braly, R.J. Stoddard, A. Rajagopal, A.R. Uhl, J.K. Katahara, A.-K.-Y. Jen, H. W. Hillhouse, Current-induced phase segregation in mixed halide hybrid perovskites and its impact on two-terminal tandem solar cell design, ACS Energy Lett. 2 (2017) 1841–1847, https://doi.org/10.1021/acsenergylett.7b00525.
[146] E.T. Hoke, D.J. Slotcavage, E.R. Dohner, A.R. Bowring, H.I. Karunadasa, M. D. McGehee, Reversible photo-induced trap formation in mixed-halide hybrid perovskites for photovoltaics, Chem. Sci. 6 (2015) 613–617, https://doi.org/10.1039/c4sc03141e.
[147] Y. Li, D. Song, J. Meng, J. Dong, Y. Lu, X. Huo, A. Maqsood, Y. Song, S. Zhao, B. Qiao, Z. Xu, Solvent modification to suppress halide segregation in mixed halide perovskite solar cells, J. Mater. Sci. 55 (2020) 9787–9794, https://doi.org/10.1007/s10853-020-04697-1.
[148] M.I. Saidaminov, J. Kim, A. Jain, R. Quintero-Bermudez, H. Tan, G. Long, F. Tan, A. Johnston, Y. Zhao, O. Voznyy, E.H. Sargent, Suppression of atomic vacancies via incorporation of isovalent small ions to increase the stability of halide perovskite solar cells in ambient air, Nat. Energy 3 (2018) 648–654, https://doi.org/10.1038/s41560-018-0192-2.
[149] Z.J. Yu, J.V. Carpenter, Z.C. Holman, Techno-economic viability of silicon-based tandem photovoltaic modules in the United States, Nat. Energy 3 (2018) 747–753, https://doi.org/10.1038/s41560-018-0201-5.
[150] K.A. Bush, K. Frohna, R. Prasanna, R.E. Beal, T. Leijtens, S.A. Swifter, M. D. McGehee, Compositional engineering for efficient wide band gap perovskites with improved stability to photoinduced phase segregation, ACS Energy Lett. 3 (2018) 428–435, https://doi.org/10.1021/acsenergylett.7b01255.
[151] M. Wang, W. Wang, B. Ma, W. Shen, L. Liu, K. Cao, S. Chen, W. Huang, Lead-free perovskite materials for solar cells, Nano-Micro Lett 13 (2021) 62, https://doi.org/10.1007/s40820-020-00578-z.
[152] E.L. Unger, L. Kegelmann, K. Suchan, D. Sörell, L. Korte, S. Albrecht, Roadmap and roadblocks for the band gap tunability of metal halide perovskites, J. Mater. Chem. A 5 (2017) 11401–11409, https://doi.org/10.1039/C7TA00404D.
[153] V.D. Ashwlayan, R.K. Ratnesh, D. Sharma, A. Sharma, A. Sangal, A. Saifi, J. Singh, A comprehensive review on plant-based medications and chemical approaches for autism spectrum disorders (ASDs) psychopharmacotherapy, Indian J. Microbiol. (2024), https://doi.org/10.1007/s12088-024-01265-y.
[154] W. Ke, M.G. Kanatzidis, Prospects for low-toxicity lead-free perovskite solar cells, Nat. Commun. 10 (2019) 965, https://doi.org/10.1038/s41467-019-08918-3.
[155] J. Lee, W. Lee, K. Kang, T. Lee, S.K. Lee, Layer-by-layer structural identification of 2D ruddlesden–popper hybrid lead iodide perovskites by solid-state NMR spectroscopy, Chem. Mater. 33 (2021) 370–377, https://doi.org/10.1021/acs.chemmater.0c04078.
[156] X. Jiang, Z. Zang, Y. Zhou, H. Li, Q. Wei, Z. Ning, Tin halide perovskite solar cells: an emerging thin-film photovoltaic technology, Acc. Mater. Res. 2 (2021) 210–219, https://doi.org/10.1021/accountsmr.0c00111.
[157] A.K. Baranwal, H. Masutani, H. Sugita, H. Kanda, S. Kanaya, N. Shibayama, Y. Sanehira, M. Ikegami, Y. Numata, K. Yamada, T. Miyasaka, T. Umeyama, H. Imahori, S. Ito, Lead-free perovskite solar cells using Sb and Bi-based A3B2X9 and A3BX6 crystals with normal and inverse cell structures, Nano Converg. 4 (2017) 26, https://doi.org/10.1186/s40580-017-0120-3.
[158] S.M. Jain, T. Edvinsson, J.R. Durrant, Green fabrication of stable lead-free bismuth based perovskite solar cells using a non-toxic solvent, Commun. Chem. 2 (2019) 91, https://doi.org/10.1038/s42004-019-0195-3.
[159] Z. Zhang, Q. Sun, Y. Lu, F. Lu, X. Mu, S.-H. Wei, M. Sui, Hydrogenated Cs2AgBiBr6 for significantly improved efficiency of lead-free inorganic double perovskite solar cell, Nat. Commun. 13 (2022) 3397, https://doi.org/10.1038/s41467-022-31016-w.
[160] H.M. Ghaithan, Z.A. Alahmed, S.M.H. Qaid, M. Hezam, A.S. Aldwayyan, Density functional study of cubic, tetragonal, and orthorhombic $CsPbBr_3$ perovskite, ACS Omega 5 (2020) 7468–7480, https://doi.org/10.1021/acsomega.0c00197.
[161] K.J. Savill, A.M. Ulatowski, L.M. Herz, Optoelectronic properties of tin–lead halide perovskites, ACS Energy Lett. 6 (2021) 2413–2426, https://doi.org/10.1021/acsenergylett.1c00776.
[162] N.-G. Park, M. Grätzel, T. Miyasaka, editors. Organic-Inorganic Halide Perovskite Photovoltaics. Cham: Springer International Publishing; 2016. 10.1007/978-3-319-35114-8.
[163] A. Castro-Chong, A.J. Riquelme, T. Aernouts, L.J. Bennett, G. Richardson, G. Oskam, J.A. Anta, Illumination intensity dependence of the recombination mechanism in mixed perovskite solar cells, ChemPlusChem 86 (2021) 1347–1356, https://doi.org/10.1002/cplu.202100233.
[164] J. Lim, M. Kober-Czerny, Y.-H. Lin, J.M. Ball, N. Sakai, E.A. Duijnstee, M.J. Hong, J.G. Labram, B. Wenger, H.J. Snaith, Long-range charge carrier mobility in metal halide perovskite thin-films and single crystals via transient photo-conductivity, Nat. Commun. 13 (2022) 4201, https://doi.org/10.1038/s41467-022-31569-w.
[165] A. Bou, H. Aboliņš, A. Ashoka, H. Cruanyes, A. Guerrero, F. Deschler, J. Bisquert, Extracting *in situ* charge carrier diffusion parameters in perovskite solar cells with light modulated techniques, ACS Energy Lett. 6 (2021) 2248–2255, https://doi.org/10.1021/acsenergylett.1c00871.
[166] W. Li, Y.-Y. Sun, L. Li, Z. Zhou, J. Tang, O.V. Prezhdo, Control of charge recombination in perovskites by oxidation state of halide vacancy, J. Am. Chem. Soc. 140 (2018) 15753–15763, https://doi.org/10.1021/jacs.8b08448.
[167] D.B. Ritzer, T. Abzieher, A. Basibüyük, T. Feeney, F. Laufer, S. Ternes, B. S. Richards, S. Bergfeld, U.W. Paetzold, Upscaling of perovskite solar modules: the synergy of fully evaporated layer fabrication and all-laser-scribed interconnections, Prog. Photovolt. Res. Appl. 30 (2022) 360–373, https://doi.org/10.1002/pip.3489.
[168] G. Giuliano, A. Bonasera, M. Scopelliti, D. Chillura Martino, T. Fiore, B. Pignataro, Boosting the performance of one-step solution-processed perovskite solar cells using a natural monoterpene alcohol as a green solvent additive, ACS Appl. Electron. Mater. 3 (2021) 1813–1825, https://doi.org/10.1021/acsaelm.1c00084.

[169] I. Mohanty, S. Mangal, U.P. Singh, Defect optimization of CZTS/MASnI3 heterojunction solar cell yielding 30.8% efficiency, J. Electron. Mater. 52 (2023) 2587–2595, https://doi.org/10.1007/s11664-023-10221-3.
[170] J.-H. Im, H.-S. Kim, N.-G. Park, Morphology-photovoltaic property correlation in perovskite solar cells: one-step versus two-step deposition of CH3NH3PbI3, APL Mater. 2 (2014) 081510, https://doi.org/10.1063/1.4891275.
[171] M. Li, X. Yan, Z. Kang, X. Liao, Y. Li, X. Zheng, P. Lin, J. Meng, Y. Zhang, Enhanced efficiency and stability of perovskite solar cells via anti-solvent treatment in two-step deposition method, ACS Appl. Mater. Interfaces 9 (2017) 7224–7231, https://doi.org/10.1021/acsami.7b01136.
[172] Y.M. Lee, I. Maeng, J. Park, M. Song, J.-H. Yun, M.-C. Jung, M. Nakamura, Comprehensive understanding and controlling the defect structures: an effective approach for organic-inorganic hybrid perovskite-based solar-cell application, Front. Energy Res. 6 (2018) 128, https://doi.org/10.3389/fenrg.2018.00128.
[173] G. Kieslich, S. Sun, A.K. Cheetham, Solid-state principles applied to organic–inorganic perovskites: new tricks for an old dog, Chem. Sci. 5 (2014) 4712–4715, https://doi.org/10.1039/C4SC02211D.
[174] T.I. Alanazi, Current spray-coating approaches to manufacture perovskite solar cells, Results Phys. 44 (2023) 106144, https://doi.org/10.1016/j.rinp.2022.106144.
[175] N. Singh, R.K. Ratnesh, A. Kumar, P. Sharma, Aryan. Low refractive index photonic crystal fiber-based surface plasmon resonance sensor. 2024 IEEE Reg. 10 Symp. TENSYMP, New Delhi, India: IEEE; 2024, p. 1–7. 10.1109/TENSYMP61132.2024.10752178.
[176] C. Yadav, S. Kumar, Review on perovskite solar cells via vacuum and non-vacuum solution based methods, Results Surf. Interfaces 14 (2024) 100210, https://doi.org/10.1016/j.rsurfi.2024.100210.
[177] J. Lee, B.S. Kim, J. Park, J. Lee, K. Kim, Opportunities and challenges for perovskite solar cells based on vacuum thermal evaporation, Adv. Mater. Technol. 8 (2023) 2200928, https://doi.org/10.1002/admt.202200928.
[178] Y. Liao, H. Liu, W. Zhou, D. Yang, Y. Shang, Z. Shi, B. Li, X. Jiang, L. Zhang, L. N. Quan, R. Quintero-Bermudez, B.R. Sutherland, Q. Mi, E.H. Sargent, Z. Ning, Highly oriented low-dimensional tin halide perovskites with enhanced stability and photovoltaic performance, J. Am. Chem. Soc. 139 (2017) 6693–6699, https://doi.org/10.1021/jacs.7b01815.
[179] L.K. Ono, Y. Qi, S. Liu, Progress toward stable lead halide perovskite solar cells, Joule 2 (2018) 1961–1990, https://doi.org/10.1016/j.joule.2018.07.007.
[180] J. Werner, C.-H. Weng, A. Walter, L. Fesquet, J.P. Seif, S. De Wolf, B. Niesen, C. Ballif, Efficient monolithic perovskite/silicon tandem solar cell with cell area >1 cm^2, J. Phys. Chem. Lett. 7 (2016) 161–166, https://doi.org/10.1021/acs.jpclett.5b02686.
[181] R.E. Beal, D.J. Slotcavage, T. Leijtens, A.R. Bowring, R.A. Belisle, W.H. Nguyen, G. F. Burkhard, E.T. Hoke, M.D. McGehee, cesium lead halide perovskites with improved stability for tandem solar cells, J. Phys. Chem. Lett. 7 (2016) 746–751, https://doi.org/10.1021/acs.jpclett.6b00002.
[182] H. Baig, H. Kanda, A.M. Asiri, M.K. Nazeeruddin, T. Mallick, Increasing efficiency of perovskite solar cells using low concentrating photovoltaic systems, Sustain. Energy Fuels 4 (2020) 528–537, https://doi.org/10.1039/C9SE00550A.
[183] R. Brenes, M. Laitz, J. Jean, D.W. deQuilettes, V. Bulović, Benefit from photon recycling at the maximum-power point of state-of-the-art perovskite solar cells, PhysRevAppl 12 (2019) 014017, https://doi.org/10.1103/PhysRevApplied.12.014017.
[184] Q. Luo, C. Zhang, X. Deng, H. Zhu, Z. Li, Z. Wang, X. Chen, S. Huang, Plasmonic effects of metallic nanoparticles on enhancing performance of perovskite solar cells, ACS Appl. Mater. Interfaces 9 (2017) 34821–34832, https://doi.org/10.1021/acsami.7b08489.
[185] J. Chen, M.E. Messing, K. Zheng, T. Pullerits, Cation-dependent hot carrier cooling in halide perovskite nanocrystals, J. Am. Chem. Soc. 141 (2019) 3532–3540, https://doi.org/10.1021/jacs.8b11867.
[186] S. Cheng, H. Mai, I.H.H. Lin, Research of technical approach for improving the stability of perovskite solar cells, Highlights Sci. Eng. Technol. 73 (157–64) (2023), https://doi.org/10.54097/hset.v73i.12856.
[187] S. Baumann, G.E. Eperon, A. Virtuani, Q. Jeangros, D.B. Kern, D. Barrit, J. Schall, W. Nie, G. Oreski, M. Khenkin, C. Ulbrich, R. Peibst, J.S. Stein, M. Köntges, Stability and reliability of perovskite containing solar cells and modules: degradation mechanisms and mitigation strategies, Energ. Environ. Sci. (2024), https://doi.org/10.1039/D4EE01898B.
[188] J. Qin, Z. Che, Y. Kang, C. Liu, D. Wu, H. Yang, X. Hu, Y. Zhan, Towards operation-stabilizing perovskite solar cells: fundamental materials, device designs, and commercial applications, InfoMat 6 (2024) e12522, https://doi.org/10.1002/inf2.12522.
[189] M. Khalid, T.K. Mallick, Stability and performance enhancement of perovskite solar cells: a review, Energies 16 (2023) 4031, https://doi.org/10.3390/en16104031.
[190] B. Park, S.I. Seok, Intrinsic instability of inorganic–organic hybrid halide perovskite materials, Adv. Mater. 31 (2019) 1805337, https://doi.org/10.1002/adma.201805337.
[191] K.O. Brinkmann, J. Zhao, N. Pourdavoud, T. Becker, T. Hu, S. Olthof, K. Meerholz, L. Hoffmann, T. Gahlmann, R. Heiderhoff, M.F. Oszajca, N.A. Luechinger, D. Rogalla, Y. Chen, B. Cheng, T. Riedl, Suppressed decomposition of organometal halide perovskites by impermeable electron-extraction layers in inverted solar cells, Nat. Commun. 8 (2017) 13938, https://doi.org/10.1038/ncomms13938.
[192] S.P. Dunfield, L. Bliss, F. Zhang, J.M. Luther, K. Zhu, M.F.A.M. Van Hest, M. O. Reese, J.J. Berry, From defects to degradation: a mechanistic understanding of degradation in perovskite solar cell devices and modules, Adv. Energy Mater. 10 (2020) 1904054, https://doi.org/10.1002/aenm.201904054.
[193] G. Verkhogliadov, R. Haroldson, D. Gets, A.A. Zakhidov, S.V. Makarov, Temperature dependence of photoinduced phase segregation in bromide-rich mixed halide perovskites, J. Phys. Chem. C 127 (2023) 24339–24349, https://doi.org/10.1021/acs.jpcc.3c04887.
[194] G. Schileo, G. Grancini, Halide perovskites: current issues and new strategies to push material and device stability, J. Phys. Energy 2 (2020) 021005, https://doi.org/10.1088/2515-7655/ab6cc4.
[195] M. Chen, M.-G. Ju, H.F. Garces, A.D. Carl, L.K. Ono, Z. Hawash, Y. Zhang, T. Shen, Y. Qi, R.L. Grimm, D. Pacifici, X.C. Zeng, Y. Zhou, N.P. Padture, Highly stable and efficient all-inorganic lead-free perovskite solar cells with native-oxide passivation, Nat. Commun. 10 (2019) 16, https://doi.org/10.1038/s41467-018-07951-y.
[196] C.R. Osterwald, T.J. McMahon, History of accelerated and qualification testing of terrestrial photovoltaic modules: a literature review, Prog. Photovolt. Res. Appl. 17 (2009) 11–33, https://doi.org/10.1002/pip.861.
[197] K.D. Jayan, V. Sebastian, An overview of the first principles DFT exploration of various properties of the individual layers of perovskite solar cells, Adv. Asp. Eng. Res. 12 (2021) 1–12, https://doi.org/10.9734/bpi/aaer/v12/8864D.
[198] B. Li, W. Zhang, Improving the stability of inverted perovskite solar cells towards commercialization, Commun. Mater. 3 (2022) 1–13, https://doi.org/10.1038/s43246-022-00291-x.
[199] X. Wu, X. Ke, M. Sui, Recent progress on advanced transmission electron microscopy characterization for halide perovskite semiconductors, J. Semicond. 43 (2022) 041106, https://doi.org/10.1088/1674-4926/43/4/041106.
[200] J. Wei, Y. Zhao, H. Li, G. Li, J. Pan, D. Xu, Q. Zhao, D. Yu, Hysteresis analysis based on the ferroelectric effect in hybrid perovskite solar cells, J. Phys. Chem. Lett. 5 (2014) 3937–3945, https://doi.org/10.1021/jz502111u.
[201] S.R. Kothiyal, R.K. Ratnesh, A.K. Shukla, Enhancing sensing with surface plasmons resonance: theoretical insights and design strategies in photonic crystal fiber. Artif. Intell. Inf. Technol. 1st ed., London: CRC Press; 2024, p. 279–85. 10.1201/9781003510833-46.
[202] S. Miao, S. Yuan, D. Zhu, Q. Cai, H.-Y. Wang, Y. Wang, Y. Qin, X.-C. Ai, Mesoporous TiO_2 layer suppresses ion accumulation in perovskite solar cells, PCCP 24 (2022) 20689–20693, https://doi.org/10.1039/d2cp02037h.
[203] N.U. Rahman, W.U. Khan, W. Li, S. Khan, J. Khan, S. Zheng, T. Su, J. Zhao, M. P. Aldred, Z. Chi, Simultaneous enhancement in performance and UV-light stability of organic–inorganic perovskite solar cells using a samarium-based down conversion material, J. Mater. Chem. A 7 (2018) 322–329, https://doi.org/10.1039/C8TA09362H.
[204] N. Arora, M.I. Dar, S. Akin, R. Uchida, T. Baumeler, Y. Liu, S.M. Zakeeruddin, M. Grätzel, Low-cost and highly efficient carbon-based perovskite solar cells exhibiting excellent long-term operational and UV stability, Small 15 (2019) 1904746, https://doi.org/10.1002/smll.201904746.
[205] B. Li, W. Zhang, Improving the stability of inverted perovskite solar cells towards commercialization, Commun. Mater. 3 (2022) 65, https://doi.org/10.1038/s43246-022-00291-x.
[206] Y. Rong, Y. Hu, A. Mei, H. Tan, M.I. Saidaminov, S.I. Seok, M.D. McGehee, E. H. Sargent, H. Han, Challenges for commercializing perovskite solar cells, Science 361 (2018) eaat8235, https://doi.org/10.1126/science.aat8235.
[207] M. Dailey, Y. Li, A.D. Printz, Residual film stresses in perovskite solar cells: origins, effects, and mitigation strategies, ACS Omega 6 (2021) 30214–30223, https://doi.org/10.1021/acsomega.1c04814.
[208] K. Cooper, Scalable nanomanufacturing—a review, Micromachines 8 (2017) 20, https://doi.org/10.3390/mi8010020.
[209] F. Valipour, E. Yazdi, N. Torabi, B.F. Mirjalili, A. Behjat, Improvement of the stability of perovskite solar cells in terms of humidity/heat via compositional engineering, J. Phys. Appl. Phys. 53 (2020) 285501, https://doi.org/10.1088/1361-6463/ab8511.
[210] Y. Dong, W. Li, X. Zhang, Q. Xu, Q. Liu, C. Li, Z. Bo, Highly efficient planar perovskite solar cells via interfacial modification with fullerene derivatives, Small 12 (2016) 1098–1104, https://doi.org/10.1002/smll.201503361.
[211] S. Tan, I. Yavuz, N. De Marco, T. Huang, S.-J. Lee, C.S. Choi, M. Wang, S. Nuryyeva, R. Wang, Y. Zhao, H.-C. Wang, T.-H. Han, B. Dunn, Y. Huang, J.-W. Lee, Y. Yang, Steric impediment of ion migration contributes to improved operational stability of perovskite solar cells, Adv Mater Deerfield Beach Fla 32 (2020) e1906995, https://doi.org/10.1002/adma.201906995.
[212] Q. Wali, F.J. Iftikhar, N.K. Elumalai, Y. Iqbal, S. Yousaf, S. Iqbal, R. Jose, Advances in stable and flexible perovskite solar cells, Curr. Appl Phys. 20 (2020) 720–737, https://doi.org/10.1016/j.cap.2020.03.007.
[213] G. Haidari, Comparative 1D optoelectrical simulation of the perovskite solar cell, AIP Adv. 9 (2019) 085028, https://doi.org/10.1063/1.5110495.
[214] J. Peng, F. Kremer, D. Walter, Y. Wu, Y. Ji, J. Xiang, W. Liu, T. Duong, H. Shen, T. Lu, F. Brink, D. Zhong, L. Li, O. Lee Cheong Lem, Y. Liu, K.J. Weber, T.P. White, K.R. Catchpole, Centimetre-scale perovskite solar cells with fill factors of more than 86 per cent, Nature 601 (2022) 573–578, https://doi.org/10.1038/s41586-021-04216-5.
[215] B. Li, Y. Zhang, L. Fu, T. Yu, S. Zhou, L. Zhang, L. Yin, Surface passivation engineering strategy to fully-inorganic cubic CsPbI3 perovskites for high-performance solar cells, Nat. Commun. 9 (2018) 1076, https://doi.org/10.1038/s41467-018-03169-0.
[216] D. Bi, X. Li, J.V. Milić, D.J. Kubicki, N. Pellet, J. Luo, T. LaGrange, P. Mettraux, L. Emsley, S.M. Zakeeruddin, M. Grätzel, Multifunctional molecular modulators for perovskite solar cells with over 20% efficiency and high operational stability, Nat. Commun. 9 (2018) 4482, https://doi.org/10.1038/s41467-018-06709-w.

[217] S. Chen, A. Solanki, J. Pan, T.C. Sum, Compositional and morphological changes in water-induced early-stage degradation in lead halide perovskites, Coatings 9 (2019) 535, https://doi.org/10.3390/coatings9090535.
[218] M. Li, X. Yan, Z. Kang, Y. Huan, Y. Li, R. Zhang, Y. Zhang, Hydrophobic polystyrene passivation layer for simultaneously improved efficiency and stability in perovskite solar cells, ACS Appl. Mater. Interfaces 10 (2018) 18787–18795, https://doi.org/10.1021/acsami.8b04776.
[219] F. Zhang, X. Yang, H. Wang, M. Cheng, J. Zhao, L. Sun, Structure engineering of hole–conductor free perovskite-based solar cells with low-temperature-processed commercial carbon paste as cathode, ACS Appl. Mater. Interfaces 6 (2014) 16140–16146, https://doi.org/10.1021/am504175x.
[220] Q. Wali, F.J. Iftikhar, M.E. Khan, A. Ullah, Y. Iqbal, R. Jose, Advances in stability of perovskite solar cells, Org. Electron. 78 (2020) 105590, https://doi.org/10.1016/j.orgel.2019.105590.
[221] J.J. Yoo, S. Wieghold, M.C. Sponseller, M.R. Chua, S.N. Bertram, N.T.P. Hartono, J.S. Tresback, E.C. Hansen, J.-P. Correa-Baena, V. Bulović, T. Buonassisi, S. S. Shin, M.G. Bawendi, An interface stabilized perovskite solar cell with high stabilized efficiency and low voltage loss, Energ. Environ. Sci. 12 (2019) 2192–2199, https://doi.org/10.1039/C9EE00751B.
[222] K. Yan, Z. Wei, J. Li, H. Chen, Y. Yi, X. Zheng, X. Long, Z. Wang, J. Wang, J. Xu, S. Yang, High-performance graphene-based hole conductor-free perovskite solar cells: schottky junction enhanced hole extraction and electron blocking, Small 11 (2015) 2269–2274, https://doi.org/10.1002/smll.201403348.
[223] H. Xie, X. Yin, Y. Guo, D. Liu, T. Liang, G. Wang, W. Que, Hole transport free flexible perovskite solar cells with cost-effective carbon electrodes, Nanotechnology 32 (2021) 105205, https://doi.org/10.1088/1361-6528/abcf70.
[224] W. Jiang, X. Chen, Light absorption enhancement in ultrathin perovskite solar cells using plasmonic light trapping and bionic anti-reflection coating, AIP Adv. 12 (2022) 065106, https://doi.org/10.1063/5.0092059.
[225] M. Stolterfoht, P. Caprioglio, C.M. Wolff, J.A. Márquez, J. Nordmann, S. Zhang, D. Rothhardt, U. Hörmann, A. Redinger, L. Kegelmann, S. Albrecht, T. Kirchartz, M. Saliba, T. Unold, D. Neher, The perovskite/transport layer interfaces dominate non-radiative recombination in efficient perovskite solar cells, Energ. Environ. Sci. 12 (2019) 2778–2788, https://doi.org/10.1039/c9ee02020a.
[226] Y. Zhao, X. Yin, P. Li, Z. Ren, Z. Gu, Y. Zhang, Y. Song, Multifunctional perovskite photodetectors: from molecular-scale crystal structure design to micro/nano-scale morphology manipulation, Nano-Micro Lett 15 (2023) 187, https://doi.org/10.1007/s40820-023-01161-y.
[227] F. Cappelluti, G. Ghione, M. Gioannini, G. Bauhuis, P. Mulder, J. Schermer, M. Cimino, G. Gervasio, G. Bissels, E. Katsia, T. Aho, T. Niemi, M. Guina, D. Kim, J. Wu, H. Liu, Novel concepts for high-efficiency lightweight space solar cells, E3S Web Conf 16 (2017) 03007, https://doi.org/10.1051/e3sconf/20171603007.